Machining Chip-Breaking Prediction
with Grooved Inserts in Steel Turning

by

Li Zhou

A Ph.D. Research Proposal

Submitted to the faculty of the

WORCESTER POLYTECHNIC INSTITUTE

in partial fulfillment of the requirements for the

Degree of Doctor of Philosophy

in

Manufacturing Engineering

by

_____

December 2001

Committee members:

_____

Professor Yiming Rong, Major Advisor

_____

Professor Christopher A. Brown, MFE Program Director

Professor Richard D. Sisson, Member

Professor Mustapha S. Fofana, Member

Professor Ning Fang, Member

Abstract

Prediction of chip-breaking in machining is an important task for automated manufacturing. There are chip-breaking limits in maching chip-breaking processes, which determine the chip-breaking range. This paper presents a study of chip-breaking limits with grooved cutting tools, and a web-based machining chip-breaking prediction system. Based on the chip-breaking curve, the critical feed rate is modeled through an analysis of up-curl chip formation, and the critical depth of cut is formulated through a discussion of side-curl dominant chip-formation processes. Factors affecting chip-breaking limits are also discussed.

In order to predict chip-breaking limits, semi-empirical models are established. Although the coefficients that occur in the model are estimated through machining tests, the models are applicable to a broad range of machining conditions. The model parameters include machining conditions, tool geometry, and workpiece material properties. A new web-based machining chip-breaking prediction system is introduced with examples of industrial applications.

Nomenclature

f Feed rate

d Depth of cut

V Cutting speed

f_{cr} The critical feed rate

d_{cr} The critical depth of cut

f_0 The standard critical feed rate under pre-defined standard cutting condition

d_0 The standard critical depth of cut under pre-defined standard cutting condition

C_h Cutting ratio (the ratio of the undeformed chip thickness and the chip thickness)

ψ_λ Chip flow angle

h_{ch} Chip thickness

αh_{ch} Distance from neutral axial plane of the chip to the chip surface

r_ε Insert Nose radius

W_n Insert chip-breaking groove width

κ_γ Cutting edge angle

γ_0 Insert rake angle

γ_n Insert rake angle in normal direction

γ_{01} Insert land rake angle

λ_s Insert inclination angle

$b_{\gamma1}$ Insert/chip restricted contact length

h Insert backwall height

δ Chip scroll angle in side-curl

ε_B Chip-breaking strain (workpiece fracture strain)

θ Chip flow angle

η Chip back flow angle

K_{fm} Modification coefficient of the workpiece material effect on the critical feed rate

K_{fV} Modification coefficient of the cutting speed effect on the critical feed rate

K_{fT} Modification coefficient of the cutting tool (insert) effect on the critical feed rate

$K_{fr\varepsilon}$ Modification coefficient of the cutting tool (insert) nose radius effect on the critical feed rate

K_{fWn} Modification coefficient of the cutting tool (insert) chip-breaking groove width effect on the critical feed rate

K_{fk_r} Modification coefficient of the cutting edge angle effect on the critical feed rate

$K_{f\gamma_0}$ Modification coefficient of the cutting tool (insert) rake angle effect on the critical feed rate

$K_{fb_{r1}}$ Modification coefficient of the cutting tool (insert) land length effect on the critical feed rate

$K_{f\gamma_{01}}$ Modification coefficient of the cutting tool (insert) land rake angle effect on the critical feed rate

K_{fh} Modification coefficient of the cutting tool (insert) backwall height effect on the critical feed rate

K_{dm} Modification coefficient of the workpiece material effect on the critical depth of cut

K_{dV} Modification coefficient of the cutting speed effect on the critical depth of cut

K_{dT} Modification coefficient of the cutting tool (insert) effect on the critical depth of cut

$K_{dr\varepsilon}$ Modification coefficient of the cutting tool (insert) nose radius effect on

the critical depth of cut

K_{dWn} Modification coefficient of the cutting tool (insert) chip-breaking groove width effect on the critical depth of cut

K_{dk_r} Modification coefficient of the cutting edge angle effect on the critical depth of cut

$K_{d\gamma_0}$ Modification coefficient of the cutting tool (insert) rake angle effect on the critical depth of cut

$K_{db_{r1}}$ Modification coefficient of the cutting tool (insert) land length effect on the critical depth of cut

$K_{d\gamma_{01}}$ Modification coefficient of the cutting tool (insert) land rake angle effect on the critical depth of cut

K_{dh} Modification coefficient of the cutting tool (insert) backwall height effect on the critical depth of cut

K_R Coefficient related to the chip radius breaking

l_c Chip / tool contact length

M Bending moment

P_T Chip gravity force

P_W Friction force between chip and workpiece

R_C Chip up-curl radius

ρ Chip side-curl radius

R_L Chip-breaking radius

Table of Contents

List of Figures

List of Tables

1 **Introduction**

This chapter gives an overview of the chip-control in machining, followed by a description of the chip-breaking groove / cutting tool classification.

1.1 Overview of Machining Chip Formation

Manufacturing processes can be classified into three categories, material joining, forming, and removal processes (Trent, 2000). Machining process is a material removal process. Conventionally, the concept of machining is described as removing metal by mechanically forcing a cutting edge through a workpiece. It includes processes such as turning, milling, boring, drilling, facing, and broaching, which are all chip-forming operations. In the last few decades, some entirely new machining processes have been developed, such as the ultrasonic machining, thermal metal removal processes, electrochemical material removal processes, laser machining processes etc., which are very different from the conventional machining processes. However, the conventional metal cutting operations are still the most widely used fabrication processes, a \$60billion /per year business. It is still essential to develop a more fundamental understanding of metal cutting processes.

Although conventional metal cutting processes are chip-forming processes, chip-control has been overlooked in manufacturing process control for a long time.

However, with the automation of manufacturing processes, machining chip-control becomes an essential issue in machining operations in order to carry out the manufacturing processes efficiently and smoothly, especially in today's unmanned machining systems.

After material is removed from the workpiece, it flows out in the form of chips. After flowing out, the chip curls either naturally or through contact with obstacles. If the material strain exceeds the material breaking strain, the chip will break. Chip flow, chip curl, and chip-breaking are three main areas of chip-control research.

The most logical approach in developing cutting models for machining with chip-breaking is to investigate and understand the absolute direction of chip flow, since chip curling and the subsequent chip-breaking processes depend very heavily on the nature of chip flow and its direction.

Chips have two flow types:

- Chip side flow - Chip flow on the tool face.

- Chip back flow - Chip flow viewed in a plane perpendicular to the cutting edge. This type of flow indicates the amount of chip leaning toward the secondary face (or the tool groove profile) of the tool in machining with grooved tools as well as tools with complex tool face geometries.

The combined effects of these two chip flow types make a three-dimensional chip flow, subsequently leading to three-dimensional chip curl and breaking.

For chip flow study, the most important objective is to establish the model of the

chip side-flow angle, which in most research is called the chip flow angle. Figure 1-1 shows chip side flow and chip back flow.

Chip side flow (Jawahir 1993)   Chip back flow (Johnson, 1962)

Figure 1-1 Chip Flow

Naturally a chip will curl after it flows out. Contact with the chip-breaking groove or chip breaker or other obstacles will also make a chip curl. There are three basic forms of chip curl, and all shapes of free chips can be constructed by combinations of these three basic shapes or straight chip:

- Chip up-curl

- Chip side-curl

- Chip lateral-curl. The chip lateral-curl was found in recent studies (Fang, N. 2001).

The most important work for chip curl study is to establish models for the chip up-curl radius and the chip side-curl radius, both of which have a very significant influence on chip-breaking. Figure 1-2 shows chip up-curl and chip side-curl.

Chip side-curl   Chip up-curl

Figure 1-2 Chip Side-curl and Chip Up-curl (Jawahir 1993)

Machining chips vary greatly in shape and length. In machining, short broken chips are desired because unexpected long chips may damage the finished work-piece surface; may break the inserts, or even hurt the operator. Therefore the study of chip-breaking is very important for optimizing the machining process. Efficient chip-control will contributes to higher reliability of the machining process, a better-finished surface, and increased productivity.

Chip-breaking is a cyclic process. In each cycle a chip first flows out with some initial curling. A chip will keep on flowing out until it comes into contact with and is blocked by obstacles like the work-piece surface or the cutting tool. The chip curl radius will then become smaller and smaller with the chip continuously flowing out. When the chip curls tightly enough to make the chip deformation exceed the chip material breaking strain, the old chip will break, and new chips will form, grow, and flow out.

The chip-breaking research problem includes many issues. Figure 1-3 shows the main scope of chip-breaking study. The main goals of chip-breaking research is to establish a chip-breaking prediction model for chip-breaking prediction, machining process design, tool selection, and tool design.
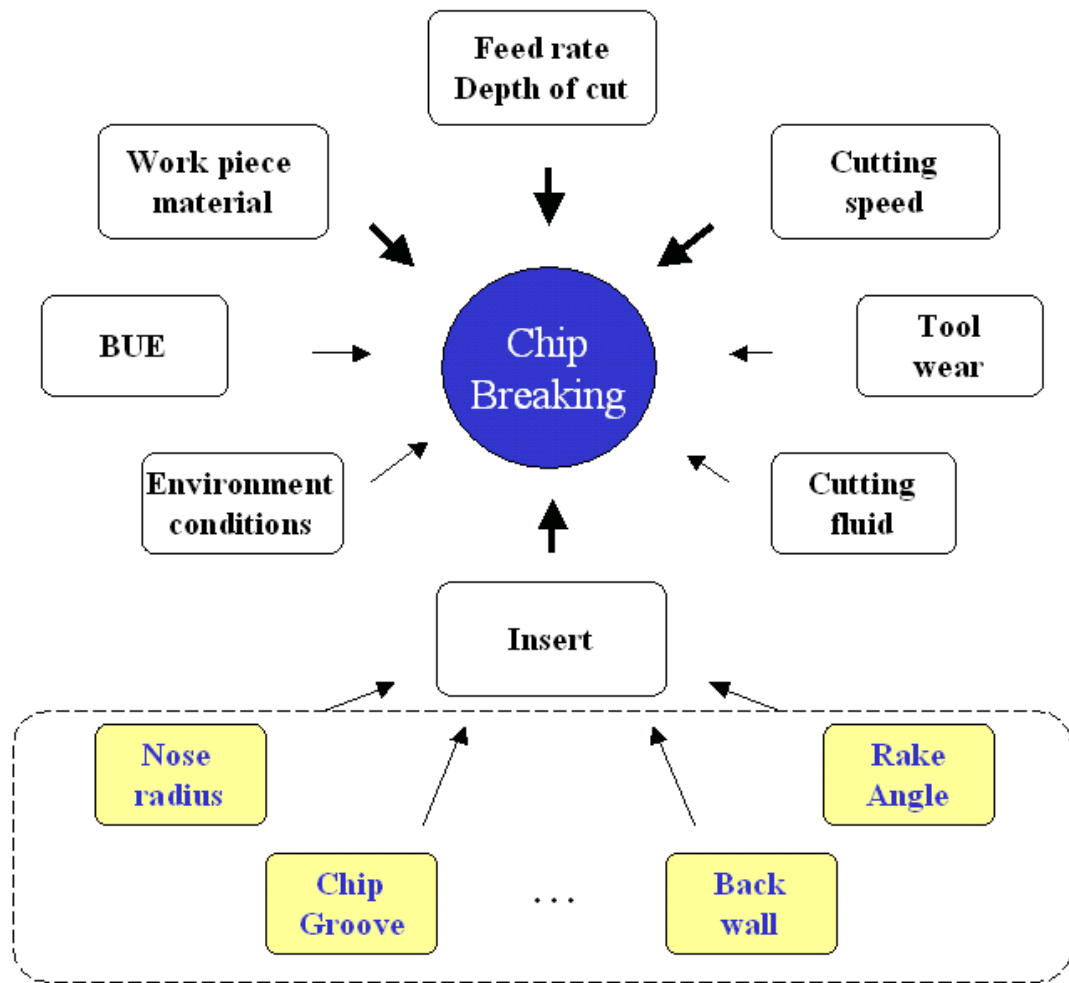
Figure 1-3 Research Fields of Chip-Control

There are two main chip-breaking modes— chip-breaking by chip/work-surface contact or chip-breaking by chip/tool flank-surface contact. In the first mode, a chip may

break by contact with the surface to be machined, which caused by chip side-curl; a chip may, instead, break by contact with the machined surface, which is caused by chip up-curl. The second breaking mode is three-dimensional chip-breaking caused by chip side-curl.

There are three ways to break a chip:

- Change cutting conditions

- Change cutting a tool geometric features

- Design and use a chip breaker or chip-breaking groove

Increasing the depth of cut or the feed rate can significantly improve chip breakability. However usually in industry this is not practical way due to the limitations of the machining process. Therefore, optimizing the design of the cutting tool geometric features and the chip breaker / chip-breaking groove is the most possible and efficient way to break the chip.

Chip curl is limited in nature so that is difficult for breaking. In industry cutting tools are usually grooved to help chip break. The chip-breaking groove can help a chip curl more tightly to make the chip easier to break; and under particular conditions, the chip-breaking groove can also reduce friction on a tool rake-face to reduce the power consumption of the metal cutting process. The next section will discuss the chip-breaking groove and the cutting tool classification.

1.2 Chip-Breaking Groove & Cutting Tool Classification

Corresponding to different applications, chip-breaking grooves vary greatly. To investigate the chip-breaking groove's effects on metal cutting, the chip-breaking groove needs to be classified first. In this thesis, different chip-breaking models are developed for cutting tools with different types of chip-breaking grooves, based on the chip-breaking groove classification introduced in this section.

The cutting tool can be classified into five categories: flat rake face tools, tools with block type chip breaker, tools with two-dimensional chip-breaking groove, tools with three-dimensional chip-breaking groove, and tools with complicated geometry modifications. Figure 1-4 illustrates the five kinds of cutting tools.

Commercial tools with complicated geometric modifications may include pimples and dimples on the rake face, and waviness on the cutting edge. Such tools may also contain combination of the above elements. In this thesis chip-breaking models are developed for two-dimensional grooved cutting tools and for three-dimensional grooved cutting tools.
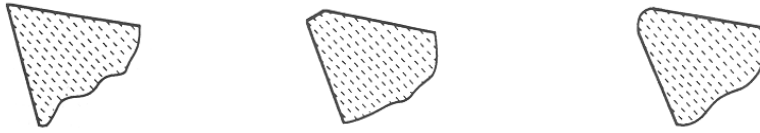
(i) Straight Cutting Edge   (ii) Chamfered Cutting Edge   (iii) Rounded Cutting Edge

(a) Flat Rake Face Tool (Jawahir, 1993)

(b) Tool with Block Type Chip Breaker

(c) Tool with Two-Dimensional Chip-Breaking Groove

(d) Tools with Three-Dimensional Chip-Breaking Groove

(e) Tools with Complicated Geometry Modifications

Figure 1-4 Classification of Chip Breaker / Chip-Breaking Groove

1.3 Chip-Breaking Limits

Chip-breaking limits are defined as the critical feed rate and the critical depth of cut. When feed rate is larger than the critical feed rate, and depth of cut is larger than the critical depth of cut, the chip will always break, otherwise the chip will not break. Figure 1-5 shows a chip-breaking chart.
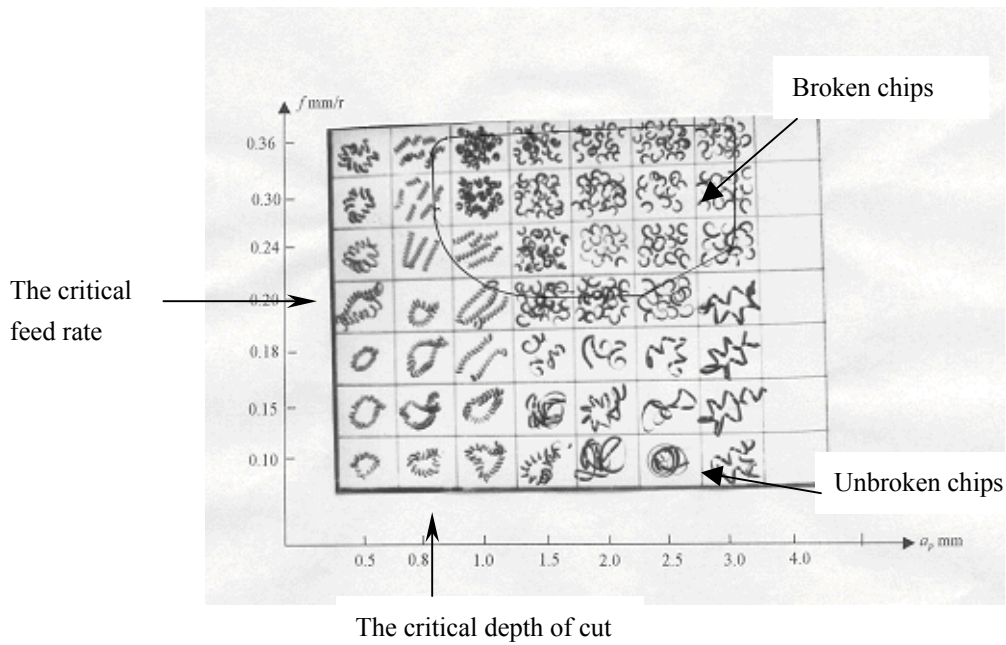
Figure 1-5 A Sample Chip-Breaking Chart

Figure 1-6 illustrates a typical chip-breaking chart. Generally the chip-breaking curve can be divided into three typical parts: up-curl dominated chip-breaking region AB, side-curl dominated chip-breaking region CD, and transitional region BC.
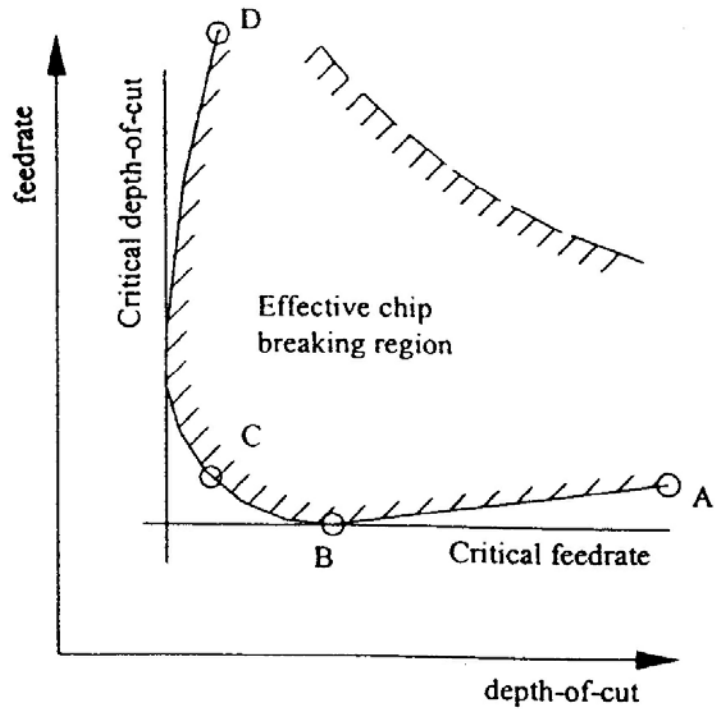
Figure 1-6 Typical Chip-Breaking Chart (Li, Z. 1990)

- *Up-curl Dominant Part AB and the Critical Feed Rate*

    In the part AB of the chip-breaking limit curve, shown above, the lowest point B

is the minimum feed rate. This part is primarily a straight line with a slope and can be

regarded as a two-dimensional chip-curling region. On each side of this part, the broken

area primarily consists of up-curled C-type chips, while the unbroken area primarily

consists of snarling chips. The objective of the theoretical analysis is to seek a formula

for estimating the minimum feed rate, which is defined as the **Critical Feed Rate** (f_{cr}) (Li,

Z. 1990). In machining, cutting tools with line-arc grooves and line-arc-line grooves are

often used.

- *Side-curl dominant Part CD and the Critical Depth of Cut*

    The part CD of the chip-breaking limit curve involves side-curl dominated

chip-breaking processes. This part shows a complex three-dimensional chip curling (see Figure 1-6). On each side of this part, the broken area is mainly composed of side-curled spiral type continuous chips. Oblique-curl spiral continuous chips are also found in the larger feed rate area. The minimum point in the horizontal coordinate corresponds to the **Critical Depth of Cut** (d_{cr}) (Li, Z. 1990). When the depth of cut is smaller than this value, the chip usually does not break. The key is to seek the critical depth of cut. In this case, side-curl ε type chips are usually generated.

- *Transitional Part BC*

This part shows a more complex three-dimensional chip curling. On both sides of this part are oblique curling spiral chips. When the number of chip rolls is few, the chips are similar to C-type chips, otherwise they are ε or snarling-type chips.

The critical feed rate and the critical depth of cut are the two chip-breaking limits. There is a chip-breaking condition: *The chip will always break when the depth of cut is greater than the critical depth of cut and the feed rate is greater than the critical feed rate. Otherwise the chip will not break.*

If the critical feed rate and the critical depth of cut could be predicted, chip-breaking could then be predicted. This would greatly simplify chip-breaking prediction research. The chip-breaking limits theory is the basis of the research conducted in this dissertation.

2 The State of the Art

This chapter reviews earlier efforts in chip-control research. For chip-control research, two questions should be presented: How does a chip form and move in space? And how does a chip break? In this chapter, previous investigations on chip flow, chip curl, and chip-breaking are first reviewed, which are relevant to the first question. Next, previous attempts to develop chip-breaking criteria are presented, which bear on the second question. The Nakayama's chip-breaking criterion, and Li's work on chip-breaking limits are reviewed in detail. This is particularly important because the chip-breaking predictive models developed in this dissertation are based on chip-breaking limits theory and Nakayama's work. Finally, existing problems in chip-control research are reviewed.

2.1 Chip Flow

Chip-breaking modes depend on the nature of chip flow and its direction. Understanding the chip flow mechanism is important for chip-control. Chip flow is determined by many factors and is usually described with the chip flow angle ψ_λ. The chip-flow angle is the angle between the chip-flow direction on the cutting tool rake-face and the normal line of the cutting edge (see Figure 2-1). Establishing the model of the chip flow angle is the main objective of chip flow research. Due to the extreme

complexity of the chip formation process, only limited success has been achieved in chip-flow research, especially for three-dimensional conditions (three-dimensional groove, and three-dimensional cutting).
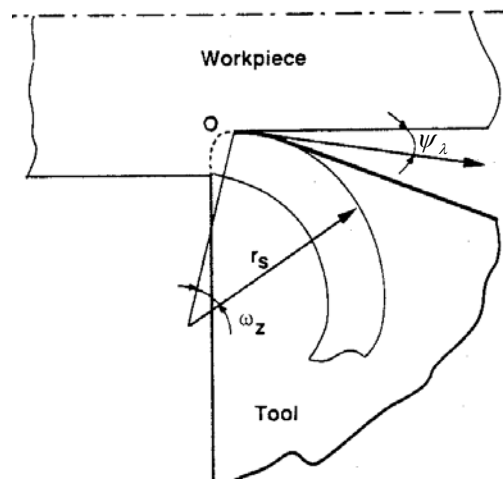
Figure 2-1 Chip Flow Angle (Jawahir, 1993)

A lot of work has been done on chip-flow angle research during the last few decades, and there are many methods for calculating the chip-flow angle.

The investigation of chip flow began with modeling over plane rake face tools. Merchant, Shaffer and Lee used the plasticity theory to attempt to obtain a unique relationship between the chip shear plane angle, the tool rake angle and the friction angle between the chip and the tool (Merchant, 1945; Lee, 1951). Shaw (1953) proposed a modification to the model presented by Lee and Shaffer. Palmer (1959) presented the shear zone theory by allowing for variation in the flow stress for a work-hardening material. van Turkovich (1967) investigated the significance of work material properties and the cyclic nature of the chip-formation process in metal cutting. Slip-Line Field

Theory is widely applied in chip-formation research and some slip-line field models are presented (Usui, 1963; Johnson, 1970; Fang, N. 2001). Being computationally successful, Slip Line Field models do not agree well with experiment results due to lack of knowledge of the high strain rate and temperature flow properties of the chip material.

Through studying the chip flow in free oblique cutting, Stabler presented a famous "Stabler Rule" (Stabler, 1951):

$$\psi_\lambda = k\lambda_s \qquad\qquad (2\text{-}1)$$

where the ψ_λ is the chip flow angle, the λ_s is the cutting-tool inclination angle, and c is a material constant. This rule is applicable for free oblique cutting.

Another chip-flow model is presented with the assumption that the chip flow is perpendicular to the major axis of the projected area of cut. This model uses empirical substitutions to consider the effect of cutting forces (Colwell, 1954). That is:

$$\psi_\lambda = \arctan\left[\frac{1}{d}\left(r_\varepsilon \tan\frac{\kappa_\gamma}{2} + \frac{f}{2} + d\cdot\arctan\kappa_\gamma\right)\right] - \psi_\gamma \qquad (2\text{-}2)$$

where d is the depth of cut, f is the feed rate, κ_γ is the cutting edge angle, r_ε is the nose radius, and ψ_γ is the minor cutting edge angle. Since Colwell's equation does not consider the effect of the work-piece material, this model therefore will result in significant error under particular conditions.

Okushima considered that chip flow is invariant with cutting speed and chip flow should be the summation of elemental flow angles over the entire length of the cutting edge (Okushima, 1959).

A chip flow model was presented by Young in 1987, assuming Stabler's flow rule, with validity for infinitesimal chip width, and the directions of elemental friction forces summed up to obtain the direction of chip flow (Young 1987).

The above chip-flow studies are all for chip side-flow angle ψ_λ. Jawahir found that a chip also has another form of flow — back flow and presented a chip back-flow angle model (Jawahir 1988-a).

Chip flow is only a part of chip space movement. To understand the chip movement mechanism, it is necessary to study chip curl.

2.2 Chip Curl

Chip curl has two basic modes: up-curl and side-curl. Recently the third chip curl mode – lateral curl – was found (Fang, N. 2001). The different material flow speed in different directions along the chip, results in different modes of chip curl. The chip up-curl is much simpler than the other two kinds of chip curl; therefore the greatest achievements have been in chip up-curl modeling. Chip side-curl is much more difficult than up-curl and presently there are no applicable models of the chip side-curl. Study on the lateral curl has only began recently.

2.2.1. Chip Up-Curl

Chip up-curl is the chip curl in the chip depth direction. The axis of chip up-curl approximately parallels the chip / cutting tool rake-face detachment line. The up-curl level is described with chip up-curl radius R_C. In metal cutting, the material flow speed in the chip bottom is generally greater than the material flow speed in the chip top surface,

which therefore results in chip up-curl. For the flat rake-face tool, Nakayama considered that when there is a build-up edge on the cutting tool, the part of the chip that flows over the build-up edge will come in contact with the tool rake-face, which brings a bent moment to the chip (Nakayama, 1962-b). For the grooved tool, the chip-breaking groove could help chip curl (see Figure 2-2).
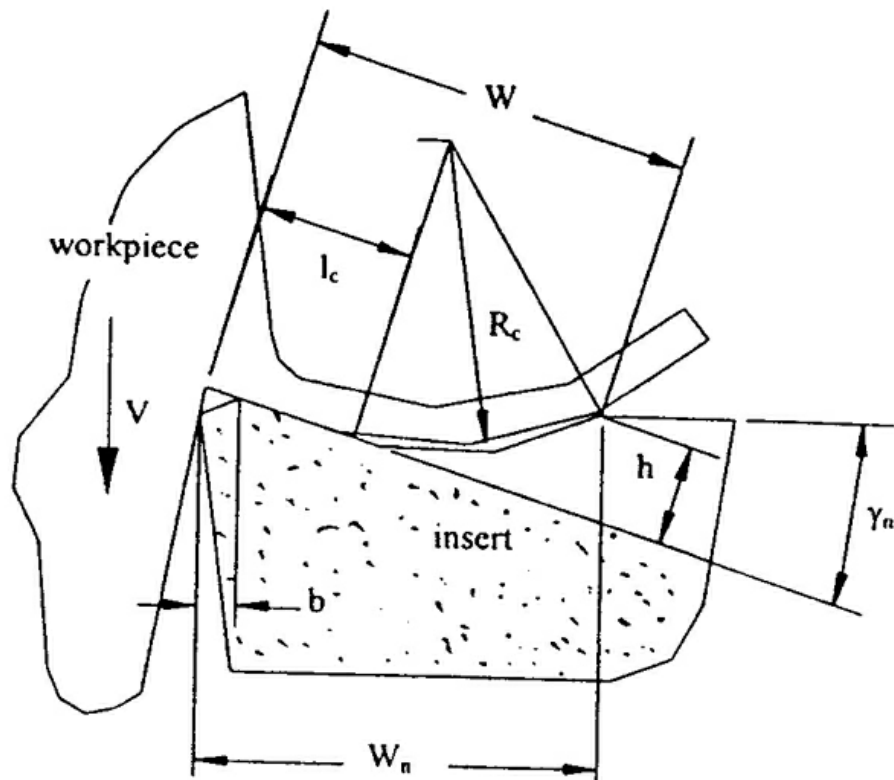
Figure 2-2 Chip Up-Curl Process with Grooved Cutting Tool (Li, Z. 1990)

The chip up-curl radius has a critical influence on up-curl-dominated chip-breaking. The main objective of chip up-curl research is to establish the model of the chip up-curl radius.

It has been found that when chip flow angle ψ_λ is big enough, a chip will flow through the whole chip-breaking groove (Jawahir, 1988-e). In this case the chip up-curl radius is:

$$R_C = R \tag{2-3}$$

where R is the chip-breaking groove radius. When ψ_λ is small, a chip does not flow through the whole chip-breaking groove. In this case, the chip up-curl radius is:

$$R_C = K_{ch} \frac{B}{2\sin\psi_\lambda} \tag{2-4}$$

where B is the chip-breaking groove width, K_{ch} is a constant determined by the chip material (Jawahir, 1988-e).

Based on chip/cutting tool geometric analysis, Li presented a chip up-curl radius equation as:

$$R_C = \frac{W_n}{2\sin\gamma_n}\left(1 - 2\frac{l_c}{W_n}\cos\gamma_n + \frac{l_c^2}{W_n^2}\right) \tag{2-5}$$

Li's work will be reviewed in detail later.

2.2.2. Chip Side-Curl

Chip side-curl is the chip curl in the direction of chip width. The side-curl axis is generally perpendicular to the chip bottom surface. The chip side-curl can be described with chip side-curl radius R_o. The chip side-curl is caused by differences in the material

flow speed along the chip width direction on the chip bottom surface (see Figure 2.3).

Figure 2-3 Mechanism of Chip Side-Curl

The chip side-curl radius has a critical influence on side-curl-dominated chip-breaking. The main objective of chip side-curl research is to establish the model of the chip side-curl radius.

Nakayama considered that the chip material had side flow, which leads to chip side-curl. He also considered that the thicker the chip, the greater the chip material side flow, therefore the greater the chip side-curl. He proposed following side-curl radius equation, where b_{ch} is the chip width and h_{ch} is the chip thickness (Nakayama 1990):

$$\frac{1}{R_0} = \frac{0.75}{b_{ch}} - \frac{0.09}{h_{ch}}$$

(2-6)

2.2.3. Chip Lateral-Curl and Combination Chip Curl

Study on the screwing curl has begun recently. In real cases, the chip curl form is

a combination of the three basic curl forms: up-curl, side-curl, and lateral curl.

2.3 Chip-Breaking

As discussed in Chapter 1, chip-breaking has two basic modes: chip-breaking by chip/work surface contact or chip-breaking by chip/tool flank surface contact. For chip-breaking research, we need to set up the chip-breaking criteria; for industry application, we need to find efficient ways to break chips.

The following is a summary of the two approaches of chip-breaking research:

1. Material stress analysis – to find the chip-breaking strain ε_B.

Research work by this approach includes:

- Chip curl analysis (Nakayama, 1962; Z. Li, Z. 1990)

- FEA (Kiamecki, 1973; Lajczok, 1980; Strenkowski, 1985; etc.)

2. Experiment-based work

This approach uses the machining database to do chip-breaking prediction. Fang and Jawahir have done a lot of work in establishing a database system based on fuzzy mathematical model for chip breakability assessments (Fang, X. 1990-a, Jawahir, 1989). This approach requires lots of time, money, and labor to establish the chip breaking prediction database. With new work-piece materials, new cutting tools / lathe, and new machining methods constantly coming out, it is difficult to establish and maintain a chip-breaking database for chip-breaking prediction.

Tool designers optimize their tool design based on many cutting tests. In industry machining process, some special devices such as rotating knife, a high-pressure gas/fluid

jet, and a vibrating cutting tool are also designed to break the chip. However, the most efficient and most common way to break the chip is to use the chip-breaking groove / chip breaker and optimize geometric features of the cutting tool.

Presently, there has been only limited success in the chip-breaking criterion study. The theoretical achievements fall behind industry reality and requirements.

Equation (2-8) is the common chip-breaking criterion for up-curl-dominated chip-breaking, presented by Nakayama (Nakayama, 1962-b). This work will be reviewed in detail in Section 2.4.

$$\begin{cases} \varepsilon > \varepsilon_B \\ \varepsilon = \alpha h_c (1/R_c - 1/R_L) \end{cases} \qquad (2\text{-}7)$$

where, ε is the chip maximum fracture strain, ε_B is the chip material breaking strain, h_c is the chip thickness, αh_c is the distance from chip surface to its neutral layer, R_C is the chip flow radius, and R_L is the chip-breaking radius

Presently most research on chip-breaking critera are for two-dimensional chip-breaking. The chip-breaking criterion for three-dimensional chip-breaking needs further investigation. three-dimensional chip-breaking criteria could not be established without a reasonable two-dimensional chip-breaking model.

The finite element method has been applied in chip-breaking process analysis for plane rake-face tools for orthogonal machining, and most recently for three-dimensional machining (Kiamecki, 1973; Lajczok, 1980; Strenkowski, 1985, 1990). These analyses are computationally successful, but their predictions do not agree with the experiments.

One reason could be the lack of knowledge of the high strain rate and temperature flow properties of the chip material (Jawahir, 1993).

2.4 Nakayama's Chip-Breaking Criterion

Nakayama's chip-breaking criterion (Equation 2-8) is the common chip-breaking criterion in such research; therefore it is reviewed in detail here.

Nakayama considers that when the actual chip fracture strain (ε) is bigger than the tensile strain on the chip (ε_B), the chip will break. It is noted that the ε is proportional to the ratio of chip thickness and chip curl radius. That is:

$$\varepsilon \propto \frac{h_{ch}}{R_C} \quad \text{(Li, Z. 1990)} \tag{2-8}$$

where h_{ch} is the chip thickness, R_C is the chip up-curl radius.

Nakayama considers that a chip flows out with up-curl radius R_C, and then is blocked by the work-piece surface or the cutting tool. With the chip material continuously flowing out, the chip curl radius will be increasing continuously. When chip reaches up-curl radius R_L, whether it will break or not is determined by whether the chip maximum fracture strain ε is greater than the chip material breaking strain ε_B.

Assuming chip cross-section shape is rectangle, we can calculate ε by the following equation:

$$\varepsilon = \frac{h_{ch}}{2}\left(\frac{1}{R_C} - \frac{1}{R_L}\right) \quad \text{(Li, Z. 1990)} \tag{2-9}$$

If the cross-section shape is not rectangular, the above equation can be written as:

$$\varepsilon = \alpha h_{ch} \left(\frac{1}{R_C} - \frac{1}{R_L} \right) \quad \text{(Li, Z. 1990)} \tag{2-10}$$

where α is cross-section shape coefficient; and αh_{ch} is the distance from neutral axis of the chip cross section to the chip surface. Therefore we establish the chip-breaking criterion:

$$\alpha h_{ch} \left(\frac{1}{R_C} - \frac{1}{R_L} \right) \geq \varepsilon_B \quad \text{(Li, Z. 1990)} \tag{2-11}$$

2.5 Li's Work on Chip-Breaking

Developing a reasonable chip-breaking criterion is the prerequisite for establishing an applicable chip-breaking predictive model. However the extreme complexity of the chip-breaking process makes the theoretical analysis and modeling of chip-breaking very difficult. Based on Nakayama's work and chip-breaking limits theory, through chip curl analysis, Li (1990) presented a new semi-empirical chip-breaking model. Since it is the basis of the chip-breaking models developed in this research, it will be reviewed in detail in the following part.

2.5.1. Theoretical Analysis of f_{cr} and d_{cr}

In the last chapter we reviewed the following chip-breaking condition based on chip-breaking limits theory:

The chip will always break when the depth of cut is greater than the critical depth of cut (d_{cr}), and the feed rate is greater than the critical feed rate (f_{cr}). Otherwise, the chip will not break.

In Nakayama's model, for up-curl dominated chip-breaking region, the h_{ch} can be

calculated as:

$$h_{ch} = \frac{f \sin \kappa_\gamma}{C_h}$$
(2-12)

where κ_γ is the cutting edge angle, and C_h is the cutting ratio.

Substituting h_c into Equation (2-8) we get:

$$f_{cr} = \frac{\varepsilon}{\left(\alpha (1/R_c - 1/R_L) \dfrac{\sin \kappa_\gamma}{C_h} \right)}$$
(2-13)

When $f > f_{cr}$, the chip will break. When $f \le f_{cr}$, the chip will break.

f_{cr} is defined as the **critical feed rate**. From Figure 2-2 the f_{cr} equation for up-curl dominated chips with two-dimensional grooved inserts can be obtained as follows (Li, Z. 1990):

$$f_{cr} = \frac{\varepsilon_B}{2\alpha} \cdot \frac{C_h W_n K_R}{\sin \kappa_r \sin \gamma_n} \cdot (1 - 2 \frac{l_f}{W_n} \cos \gamma_n)$$
(2-14)

where W_n is the width of chip-breaking groove, K_R is the coefficient related to the chip radius breaking:

$$K_R = R_L / (R_L - R_C)$$
(2-15)

l_c is the chip / tool contact length, κ_γ is the cutting edge angle, and γ_n is the rake angle in normal direction.

As with f_{cr}, a **critical depth of cut** (d_{cr}) can be defined for the side-curl-dominated chip-breaking region (Figure 2.4 and 2.5). The equation of d_{cr} for two-dimensional grooved inserts is as follows (Li, Z. 1990):

$$\begin{cases} d_{cr} = \dfrac{\varepsilon_B \rho \cos \delta}{\alpha} - (\dfrac{\pi}{2} - 1)r_\varepsilon \,, \text{ for } \ d \ge r_\varepsilon & \text{(2-16)} \\[4mm] d_{cr} = (\cos \dfrac{57.3\varepsilon_B \rho \cos \delta}{\alpha r_\varepsilon}) - r_\varepsilon \,, \text{ for } \ d < r_\varepsilon & \text{(2-17)} \end{cases}$$

where ρ is the radius of side-curl chips, and δ is a chip cross section related parameter.

Figure 2-4 Chip Flow of Side-Curl Dominated ε-Type Chips (Li, Z. 1990)
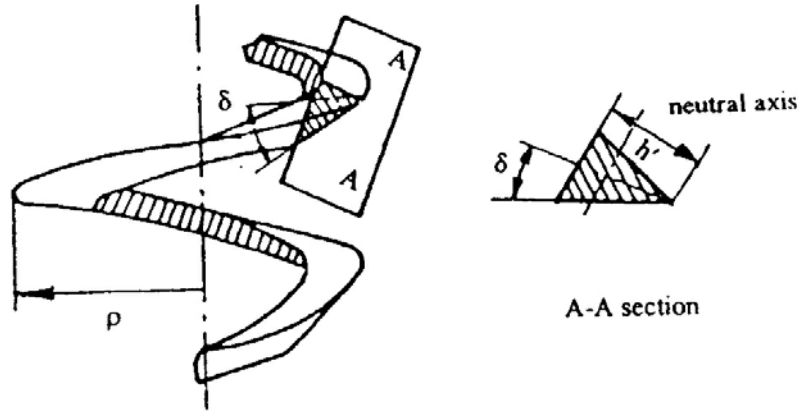
Figure 2-5 A Segment of ε-Type Chip and Its Cross Section (Li, Z. 1990)

2.5.2. Semi-Empirical Chip-Breaking Predictive Model

The theoretical equations of d_{cr} and f_{cr}, shown above, cannot be used directly to predict chip-breaking limits because not all parameters in the equation can be calculated directly. Therefore a semi-empirical chip-breaking predictive model based on theoretical equations of d_{cr} and f_{cr} is presented (Li, Z. 1990) for industry application.

The chip-breaking limits are influenced by a lot of factors but are mainly determined by the work-piece material, cutting speed, and insert geometric features (Figure 2-6).

Applying the single-factor modeling method, Li presented the following chip-breaking predictive model:

$$\begin{cases} f_{cr} = f_0 K_{fT} K_{fv} K_{fm} \\ d_{cr} = d_0 K_{dT} K_{dv} K_{dm} \end{cases} \tag{2-18}$$
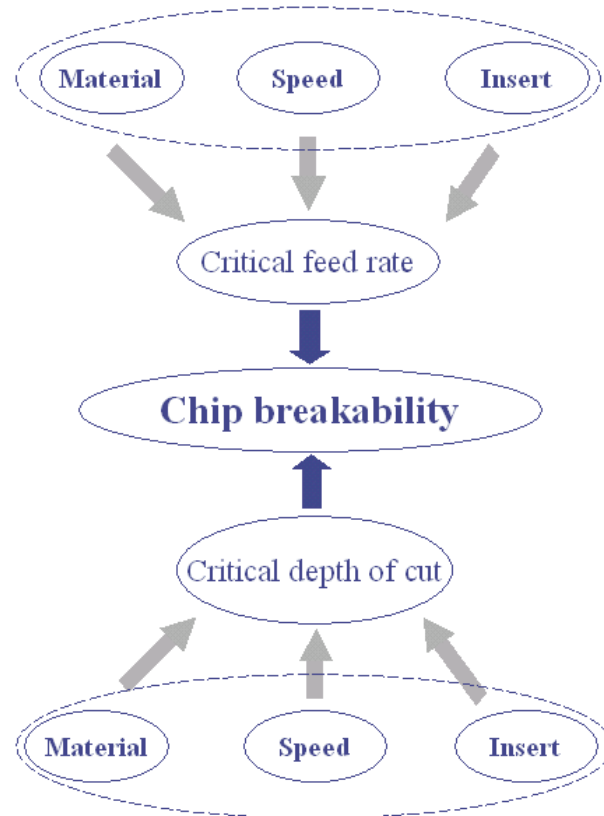
Figure 2-6 Factors Influence Chip Breakability

where f_0 and d_0 is the standard critical feed rate and the standard critical depth of cut under a predefined standard cutting condition. The predefined standard cutting condition can be any cutting condition. K_{fT} and K_{dT} are the cutting tool (inserts) effect coefficient; K_{fV} and K_{dV} are the cutting speed effect coefficient; and K_{fm} and K_{dm} are the work-piece material effect coefficient. K_{dV} and K_{fV} are functions of cutting speed; K_{dm} and K_{fm} are functions of workpiece material; and K_{dT} and K_{fT} are functions of cutting tool.

The empirical coefficients K_{dm}, K_{dV}, K_{dT}, K_{fm}, K_{fV}, and K_{fT} are developed through cutting tests. Once the empirical equations of K_{dm}, K_{dV}, K_{dT}, K_{fm}, K_{fV}, and K_{fT} have been set up, they can be calculated when the cutting condition is specified. Then the f_{cr} and d_{cr} can be figured out under any conditions by multiplying the f_0 and d_0 with K_{dm}, K_{dV}, K_{dT},

K_{fm}, K_{fV}, and K_{fT}, respectively. Therefore the chip-breaking can be predicted under any given cutting condition.

Work-piece material coefficients K_{dm} and K_{fm}

Use Equation 2-21 to get the work-piece material constants. First, conduct a group of cutting tests under predefined conditions with the given work-piece material, then we can get a group of d_{cr} and f_{cr}; dividing them by the d_0 and f_0, we can then get the coefficients K_{dm} and K_{fm}. Collecting all K_{dm} and K_{fm} for different work-piece materials, we then can set up a work-piece material coefficients database.

$$\begin{cases} K_{fm} = f_{cr} / f_0 \\ K_{dm} = d_{cr} / d_0 \end{cases} \tag{2-19}$$

When the predefined standard condition is changed, the above K_{dm} and K_{fm} should multiply by a constant respectively. e.g. under condition 1, the chip breaking limits got from cutting tests are f_{01} and d_{01}, and under condition 2, the chip breaking limits got from cutting tests are f_{02} and d_{02}. Then when using condition 1 as predefined standard cutting condition, we have $K_{fm} = f_{cr} / f_{01}$ and $K_{fm} = f_{cr} / f_{01}$; and when using condition 2 as predefined standard cutting condition, we have $K_{fm}' = f_{cr} / f_{02}$ and

$K_{fm}' = f_{cr} / f_{02}$

Cutting speed coefficients K_{dV} and K_{fV}

Use Equation 2-22 to set up the cutting speed empirical equations. First, conduct several groups of cutting tests under predefined conditions, except changing the cutting speed for several levels. Then we can get several groups of d_{cr} and f_{cr}; dividing them by

the d_0 and f_0, we can then get several K_{dV} and K_{fV}. Then we can use curve-fit to develop

the general empirical equations for the K_{dV} and K_{fV}. After the empirical equations are

established we can figure out K_{dV} and K_{fV} for any cutting speed without conducting any

extra cutting tests.

$$\begin{cases} K_{fV} = f_{cr} / f_0 = a_f V + b_f \\ K_{dV} = d_{cr} / d_0 = a_d V + b_d \end{cases} \qquad (2\text{-}20)$$

If the predefined standard condition is different, the above equations of the K_{dV}

and K_{fV} should multiply by a constant respectively.

Insert geometric coefficients K_{dT} and K_{fT}

Li (1990) set up the K_{dT} and K_{fT} models for two-dimensional grooved inserts as

follows. The predefined standard condition is still the same as before. The K_{dT} and K_{fT} are

developed as functions of the insert nose radius r_ε, the chip-breaking groove width W_n

and the cutting edge angle k_r.

$$K_{fT} = K_{fr\varepsilon} \times K_{fk_r} \times K_{fWn} \qquad (2\text{-}21)$$

where $K_{fr\varepsilon}$ is the nose radius effect coefficient, K_{fk_r} is the cutting edge angle effect

coefficient, and K_{fWn} is the width of the chip-breaking groove effect coefficient.

$$K_{dT} = K_{dr\varepsilon} \times K_{dk_r} \times K_{dWn} \qquad (2\text{-}22)$$

where $K_{dr\varepsilon}$ is the nose radius effect coefficient, K_{dk_r} is the cutting edge angle effect

coefficient, and K_{dWn} is the width of the chip-breaking groove effect coefficient.

In this research, an improved model based on Li's model will be developed along

with the experimental study, which will be described in Chapter 4.

2.6 Existing Problems

For today's unmanned manufacturing systems, chip-control needs to be considered as important as tool wear, cutting forces, surface finish, and machining accuracy. It is essential to develop an efficient chip-breaking prediction tool to optimize the machining processes. Presently, a big gap still exists between analytical work and practical requirements in the chip-control field. Three main problems exist in the chip-breaking prediction research:

1. The chip-breaking prediction model for two-dimensional grooved inserts is not complete.

Li's semi-empirical model provides a solid base for chip-breaking prediction for two-dimensional grooved inserts. However some important insert geometric features (e.g., the rake angle), which have significant influence on chip-breaking, are not included in the model.

2. Lack of chip-breaking prediction model for three-dimensional grooved inserts.

Three-dimensional grooved inserts are the most popular inserts in finish cutting in industry. It is crucial for chip-control to establish an efficient chip-breaking prediction model for three-dimensional grooved inserts.

3. Current industry solutions are very costly.

Currently research in the practical application of chip-control is a very time-money-labor-consuming job. An easy-to-maintain chip-breaking prediction system, which does not require a huge number of cutting tests, is required by the machining

industry. For online chip-control, the system should be accessible through the Internet.

3 Objectives and Scope of Work

3.1 Approach

To optimize the machining process, chip-control is very important. Developing an efficient chip-breaking predictive tool is essential to the machining industry. The tool should fulfill the following industry requirements:

1. Predict whether a chip breaks under given cutting conditions when the cutting tool is specified.

2. Optimize cutting-tool design and cutting condition design to make chip break.

Presently, there is a big gap between the theoretical research and the above stated industry requirements. Most industry cutting processes employ oblique cutting with three-dimensional grooved cutting tools, while most successful analytical models are for orthogonal cutting with simple grooved tools. For oblique cutting with three-dimensional grooved cutting tools, there is a lack of fully reasonable chip-breaking criterion. Therefore presently database-based systems are used for chip-breaking prediction and a "try and see" method is used for tool design / selection in industry applications. Both methods are very costly.

The semi-empirical chip-breaking model approach (Li, Z. 1990), shown in the

Chapter 1, is a practical way to bridge the gap, with great advantages:

1. It concentrates on the chip curl process instead of the chip formation process so that it avoids the extremely complicated chip flow issue.

2. Supported by the chip-breaking limits theory, it only needs to consider the up-curl dominated chip-breaking process and the side-curl dominated chip-breaking process for chip-breaking prediction. Therefore the problem is greatly simplified.

3. It does not fully rely on theoretical analysis. Instead, it uses limited cutting tests to develop the semi-empirical equations of chip-breaking limits. The number of cutting tests needed to develop the semi-empirical models is greatly reduced in comparison with present industry chip-breaking databases.

4. The semi-empirical chip-breaking model is intended for oblique cutting with grooved cutting tools, so that is an appealing solution for industry application.

Given these advantages, the semi-empirical model approach is applied in this research.

3.2 Objectives

The objective of this research is to develop a semi-empirical chip-breaking predictive system for oblique steel turning with grooved cutting tools. It contains three parts:

1. Extending Li's semi-empirical chip-breaking predictive model for two-dimensional grooved inserts to include important geometric features of cutting tools.

The effects of the cutting tool's rake angle, land length, land rake angle, and backwall height, which are important for chip-breaking but are not considered in Li's model, are studied and included in the expanding model.

2. Developing a semi-empirical chip-breaking predictive model for three-dimensional grooved inserts.

The chip-breaking problems mainly exist in the finish cutting, where the depth of cut is small. More than 70% of the industry inserts used in finish cutting are three-dimensional grooved inserts. The particular significance of this work is that it presents an applicable predictive tool for three-dimensional grooved inserts.

3. Developing a web-based semi-empirical chip-breaking predictive system.

For online chip-breaking prediction and tool /cutting condition design in industry applications, it is important to develop a web-based chip-breaking predictive system based on a reasonable chip-breaking predictive model.

3.3 Outline of the Dissertation

This section provides an overview of how the rest of the dissertation is organized.

▪ Chapter 4 is the extended study on chip-breaking limits for two-dimensional grooved inserts. Through chip / insert geometric analysis, the original model of the chip-breaking limits are extended to include the insert rake angle, land length, land rake angle and backwall height effects. New equations of the critical feed rate and the critical depth of cut are presented in this chapter. Li's semi-empirical chip-breaking model is then

extended to include those features. Experiments are conducted to develop the empirical equations for the modification coefficients of the insert geometric features.

- Chapter 5 presents the semi-empirical chip-breaking predictive models for three-dimensional grooved inserts. The definition of the three-dimensional grooved inserts is given first. The chip-breaking limits are then described as functions of the insert geometric feature parameters. The semi-empirical chip-breaking model for three-dimensional grooved inserts are then established. Cutting tests are conducted to develop the semi-empirical equations. The experiment-based approach is also used for developing an experimental based chip-breaking prediction model.

- Chapter 6 presents a web-based chip-breaking predictive system. The system is a powerful chip-control tool that is accessible through the Internet. This chapter introduces the system structure and the system user interface.

- Chapter 7 summarizes all work in this dissertation and describes the possible future directions in developing chip-breaking predictive models.

4 Extended Study on Chip-Breaking Limits for Two-Dimensional Grooved Inserts

This chapter discusses chip-breaking for two-dimensional grooved inserts. The definition of the two-dimensional grooved insert is given first. Then an improved semi-empirical model of the chip-breaking limits is developed in this part.

4.1 Geometry of Two-Dimensional Grooved Inserts

The cutting tool classification has been defined in Chapter 1. For two-dimensional grooved inserts, the groove width along the cutting edge is the same, except the two ends of the groove. Figure 4.1-1 shows the geometry of two-dimensional grooved inserts.
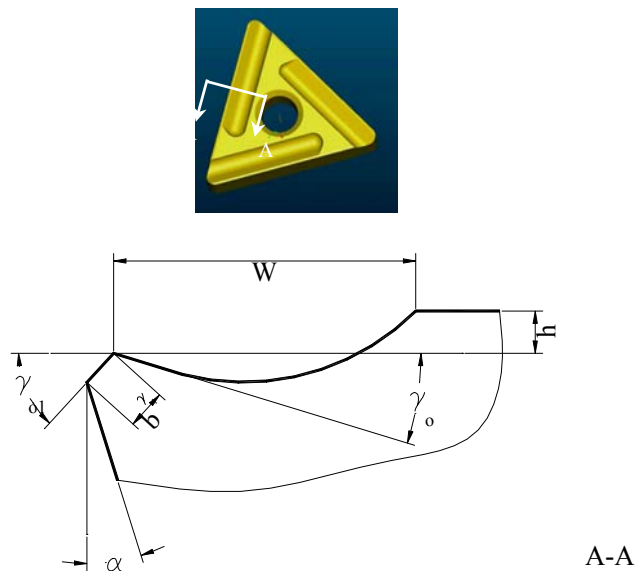
Figure 4-1 Geometry of Two-Dimensional Grooved Inserts

4.2 The Critical Feed Rate (f_{cr})

In this section, theoretical analysis is conducted to get the improved equation of the critical feed rate, which contains four more geometric parameters than Li's equation of the critical feed rate (see Equation (2-15)).

The equation of the f_{cr} developed by Li is:

$$f_{cr} = \frac{\varepsilon_b c_h k_r}{2\sin\kappa_r} R_c \tag{4-1}$$

To get the theoretical equation of f_{cr}, the equation of the chip up-curl radius R_c should be calculated first.

4.2.1. Equation of the Chip Up-curl Radius R_C

Figure 4-2 shows the geometric parameters of the insert, where l_c is the chip-tool rake-face contact length, h is the backwall height, γ_0 is the rake angle, and W is the chip-breaking groove width, measured along the tool rake face. Then the R_c can be presented as:

$$
\begin{aligned}
R_c &= \frac{[(W\cos\gamma_0 - h\sin\gamma_0) - l_c]^2 + (W\sin\gamma_0 + h\cos\gamma_0)^2}{2(W\sin\gamma_0 + h\cos\gamma_0)} \\
&= \frac{W^2 + h^2 + l_c^2 + 2l_c(-W\cos\gamma_0 + h\sin\gamma_0)}{2(W\sin\gamma_0 + h\cos\gamma_0)}
\end{aligned}
\tag{4-2}
$$
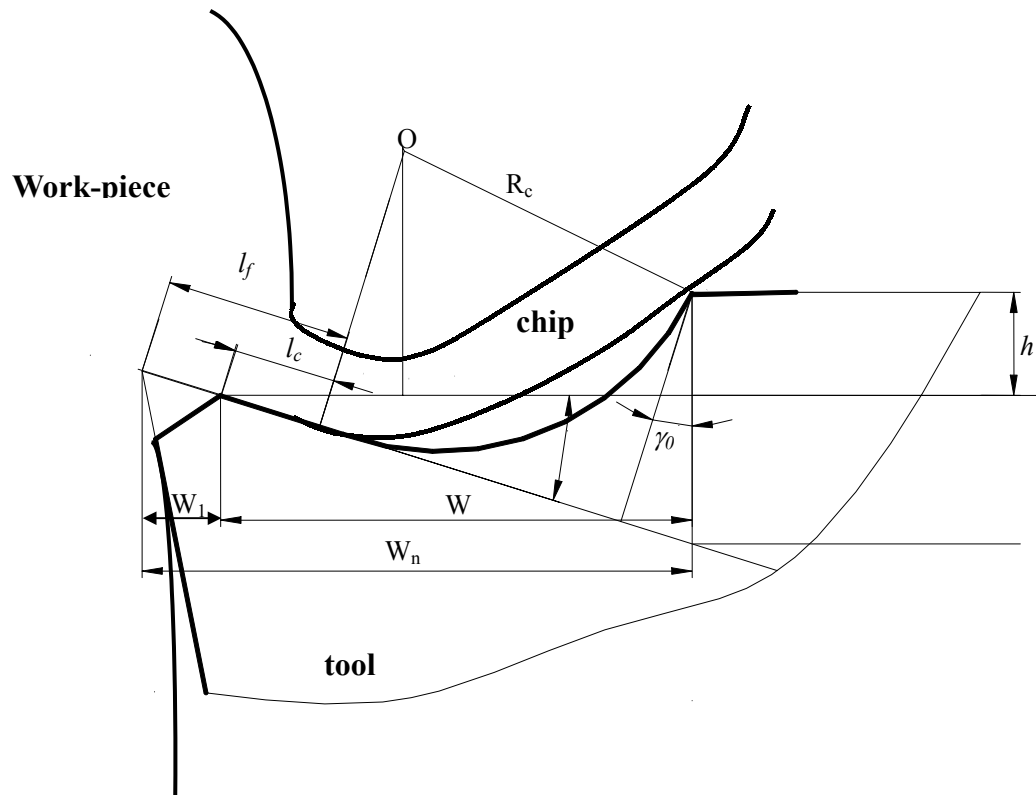
Figure 4-2 The Geometric Parameters of Two-Dimensional Grooved Insert (1)

As shown in Figure 4-2, because $W_n = W + W_1$ $\qquad$ (4-3)

And $l_f = l + l_c$ $\qquad$ (4-4)

Just as in Li's work, the parameter l_f can be calculated as:

$$l_f = \beta' W_n \qquad (4\text{-}5)$$

where β' is a coefficient estimated experimentally to be equal to 0.2 for carbon steel machining (Li, Z. 1990).

As shown in Figure 4-3, by substituting Equation (4-5) into Equation (4-4), the l_c becomes:

$$l_c = \beta'W + b_{r1}\frac{\cos(\gamma_{01}-\alpha)}{\cos(\gamma_0+\alpha)}(\beta\cos\gamma_0 - 1) \tag{4-6}$$
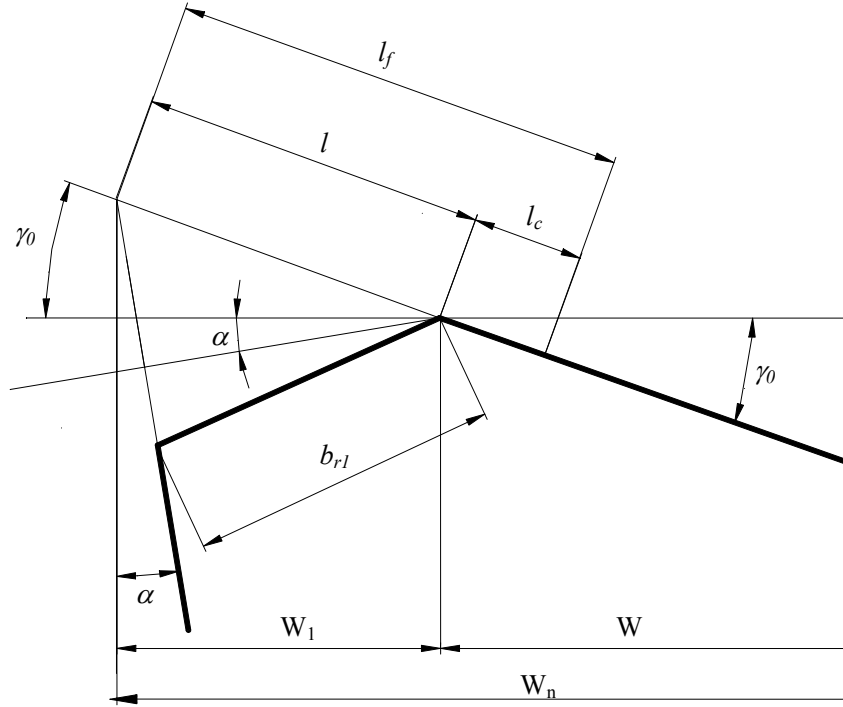
Figure 4-3 The Geometric Parameters of Two-Dimensional Grooved Insert (2)

Then the R_c can be calculated as:

$$R_c = \frac{W^2 + h^2 + l_f^2 - 2l_f\left(W\cos\gamma_0 - h\sin\gamma_0 + b_{r1}\frac{\cos(\gamma_{01}-\alpha)}{\cos(\gamma_0+\alpha)}\right)}{2(W\sin\gamma_0 + h\cos\gamma_0)} +$$
$$\frac{2b_{r1}\frac{\cos(\gamma_{01}-\alpha)}{\cos(\gamma_0+\alpha)}(W\cos\gamma_0 - h\sin\gamma_0) + b_{r1}^2\frac{\cos(\gamma_{01}-\alpha)^2}{\cos(\gamma_0+\alpha)^2}}{2(W\sin\gamma_0 + h\cos\gamma_0)} \tag{4-7}$$

4.2.2. Equation of the Critical Feed Rate f_{cr}

By substituting Equation (4-7) to Equation (4-1), the new theoretical model of f_{cr} can be established as:

$$f_{cr} = \frac{\varepsilon_b c_h k_r}{2\sin\kappa_r} \cdot \left(\frac{W^2 + h^2 + l_f^2 - 2l_f(W\cos\gamma_0 - h\sin\gamma_0 + b_{r1}\frac{\cos(\gamma_{01} - \alpha)}{\cos(\gamma_0 + \alpha)})}{2(W\sin\gamma_0 + h\cos\gamma_0)} + \frac{2b_{r1}\frac{\cos(\gamma_{01} - \alpha)}{\cos(\gamma_0 + \alpha)}(W\cos\gamma_0 - h\sin\gamma_0) + b_{r1}^2\frac{\cos(\gamma_{01} - \alpha)^2}{\cos(\gamma_0 + \alpha)^2}}{2(W\sin\gamma_0 + h\cos\gamma_0)} \right) \qquad (4\text{-}8)$$

The above equation shows f_{cr} is the equation of the insert geometric parameters, cutting speed and work-piece material. It can be used to analyze the effect of the insert geometric parameter on chip-breaking.

4.3 The Critical Depth of Cut

The critical depth of cut determines the chip-breaking range in the side-curl-dominated chip-breaking region. Applying Nakayama's chip-breaking criterion:

$$\varepsilon_B = \alpha h_{ch}\left(\frac{1}{R_0} - \frac{1}{R_L}\right) \qquad (4\text{-}9)$$

where αh_{ch} is equal to the distance from neutral axial plane of the chip to the chip surface (Li, Z. 1990). It can be calculated as (Li, Z. 1990) Equation 4-10.

$$\alpha h_{ch} = \frac{b_{ch} + c}{3} \qquad (4\text{-}10)$$

where b_{ch} is the chip width.

$$\because \quad \frac{1}{R_L} \to 0$$

$$\therefore \quad \varepsilon_B = \frac{\alpha h_{ch}}{R_0} \tag{4-11}$$

Applying the chip side-curl radius equation 4-11 (Li, Z. 1990):

$$\frac{1}{R_0} = \left(\frac{0.75}{\xi_1 b} - \frac{0.09}{\xi_2 a} \right) \frac{1}{k} \tag{4-12}$$

where the ξ_1 is the chip-width distortion coefficient and ξ_2 is the chip thickness distortion coefficient. That is,

$$b_{ch} = \xi_1 b \qquad t_{ch} = \xi_2 a \tag{4-13}$$

where k is a modification coefficient to the chip side-curl radius. t_{ch} is the chip thickness. a, b, and c are chip cross-section geometric parameters and are shown in Figure 4-4.

Substituting Equation 4-12 to 4-11, ε_B can be calculated as:

$$\varepsilon_B = \frac{\xi_1 b + c}{3} \left(\frac{0.75}{\xi_1 b} - \frac{0.09}{\xi_2 a} \right) \frac{1}{k} \tag{4-14}$$

Calculating Equation (4-14) as an equation of variable b, we have,

$$b = \frac{1}{0.06 \xi_1} \left(-p \pm \sqrt{p^2 + 0.12q} \right) \tag{4-15}$$

where

$$\begin{cases} p = (\varepsilon_B k - 0.25) \xi_2 a + 0.03c \\ q = 0.25 \xi_2 ac \end{cases} \tag{4-16}$$
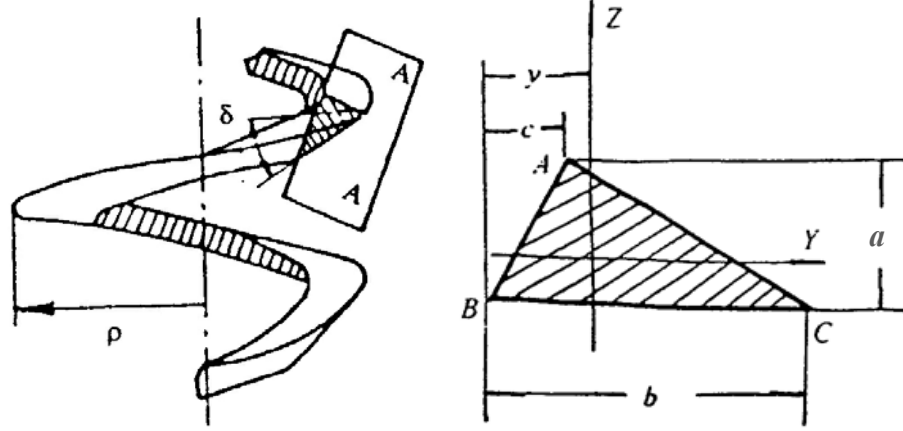
Figure 4-4   A Segment of a ε-Type Chip and Its Cross Section (Li, Z. 1990)

From Figure 4-5, a and b can be calculated as a function of the chip flow angle

ψ_λ, (Li, Z. 1990)

$$c = f \cos(\kappa_r - \Psi_\lambda) \qquad (4\text{-}17)$$

When $d \leq r_\varepsilon(1 - \cos\kappa_r), f \leq 2r_\varepsilon$

$$a = r_\varepsilon(1 - \cos\psi_\lambda) + f \sin(\kappa_r - \psi_\lambda)$$
$$b = 2r_\varepsilon \sin\psi_\lambda$$
$$\psi_\lambda = \frac{1}{2}\left(\arccos\frac{r_\varepsilon - d_{cr}}{r_\varepsilon} + \arcsin\frac{f}{2r_\varepsilon}\right) \qquad (4\text{-}18)$$

When $d \geq r_\varepsilon(1 - \cos\kappa_r), f \leq 2r_\varepsilon$

$$a = r_\varepsilon\left[1 - \frac{\sin(\beta - \Psi_\lambda)}{\sin\beta}\right] + f \sin(\kappa_r - \Psi_\lambda)$$
$$b = \frac{\sqrt{r_\varepsilon^2 - \dfrac{f^2}{4}} + d - r_\varepsilon}{\sin(\kappa_r - \Psi_\lambda)}$$
$$\beta = \angle BAO = \arctan\frac{r_\varepsilon \sin\kappa_r}{d - r_\varepsilon(1 - \cos\kappa_r)} \qquad (4\text{-}19)$$
$$\psi_\lambda = \kappa_r - \text{arccot}\left(\cot\kappa_r + \frac{r_\varepsilon}{d_{cr}}\tan\frac{\kappa_r}{2} + \frac{f}{2d_{cr}}\right)$$

41

Figure 4-5 Depth of Cut and Cutting Flow Angle (Li, Z. 1990)

Substituting a, b and c to Equation 4-14, the d_{cr} can be got as,

When $d \leq r_\varepsilon(1 - \cos\kappa_r), f \leq 2r_\varepsilon$

$$d_{cr} = r_\varepsilon - r_\varepsilon \cos\left(2\arcsin\frac{-p + \sqrt{p^2 + 0.12q}}{0.12\xi_1 r_\varepsilon} - \arcsin\frac{f}{2r_\varepsilon}\right) \qquad (4\text{-}20)$$

When $d \geq r_\varepsilon(1 - \cos\kappa_r), f \leq 2r_\varepsilon$

$$d_{cr} = r_\varepsilon - \sqrt{r_\varepsilon^2 - \frac{f^2}{4}} + \frac{1}{0.06\xi_1}\left(-p + \sqrt{p^2 + 0.12q}\right)\sin(\kappa_r - \Psi_\lambda) \qquad (4\text{-}21)$$

Equation (4-8) cannot be used to calculate f_{cr} directly, since a few variables in the equation cannot be predicted, for example, the cutting ratio C_h and the l_f. Also both sides of the Equation 4-20 and 4-21 contains d_{cr} so that they can not be used to calculate d_{cr} directly too. To apply the theoretical model in industry, a semi-empirical model has to be developed; this is illustrated by Equation (2-19). Cutting tests have been conducted to develop the model.

4.4 Semi-Empirical Chip-Breaking Model

for Two-Dimensional-Grooved Inserts

Recalling the semi-empirical model of f_{cr} and d_{cr}:

$$f_{cr} = f_0 K_{fT} K_{fv} K_{fm}$$
$$d_{cr} = d_0 K_{dT} K_{dv} K_{dm}$$

where

$$K_{fT} = K_{fr\varepsilon} \cdot K_{fk_r} \cdot K_{fWn}$$
$$K_{dT} = K_{dr\varepsilon} \cdot K_{dk_r} \cdot K_{dWn}$$

To take the rake angle, back-wall height, land length, and land rake angle's

effects into account, the equation of K_{fT} and K_{dT} are modified as follows:

$$K_{fT} = K_{fr_\varepsilon} \cdot K_{fW_n} \cdot K_{f\gamma_0} \cdot K_{f\gamma_{01}} \cdot K_{fh} \cdot K_{fb_{\gamma 1}}$$
$$K_{dT} = K_{dr_\varepsilon} \cdot K_{dW_n} \cdot K_{d\gamma_0} \cdot K_{d\gamma_{01}} \cdot K_{dh} \cdot K_{db_{\gamma 1}}$$

(4-22)

The modification coefficients $K_{f\gamma_0}$, $K_{fb_{r1}}$, $K_{f\gamma_{01}}$, K_{fh}, $K_{d\gamma_0}$, $K_{db_{r1}}$, $K_{d\gamma_{01}}$,

and K_{dh} have been added to the model. The semi-empirical chip-breaking model for

two-dimensional grooved inserts are then extended to the following form:

$$\begin{cases}
f_{cr} = f_0 K_{fT} K_{fV} K_{fm} \\[2ex]
K_{fT} = K_{fr_\varepsilon} \times K_{fW_n} \times K_{f\gamma_0} \times K_{f\gamma_{01}} \times K_{fh} \times K_{fb_{\gamma1}} \\[1.5ex]
K_{fV} = F_f(V) \\[1.5ex]
K_{fm} = F_f(m) \\[3ex]
d_{cr} = d_0 K_{dT} K_{dV} K_{dm} \\[2ex]
K_{dT} = K_{dr_\varepsilon} \times K_{dW_n} \times K_{d\gamma_0} \times K_{d\gamma_{01}} \times K_{dh} \times K_{db_{\gamma1}} \\[1.5ex]
K_{dV} = F_d(V) \\[1.5ex]
K_{dm} = F_d(m)
\end{cases} \qquad (4\text{-}23)$$

The original modification coefficients $K_{f\kappa_r}$, K_{fw_n}, K_{fr_ε}, $K_{d\kappa_r}$, K_{dw_n}, and

K_{dr_ε} have been developed as linear functions of the relative parameters (Li, Z. 1990).

The unknown coefficients $K_{f\gamma_0}$, $K_{fb_{r1}}$, $K_{f\gamma_{01}}$, K_{fh}, $K_{d\gamma_0}$, $K_{db_{r1}}$, $K_{d\gamma_{01}}$, and K_{dh}

will be developed in the same way. For example, the $K_{f\gamma_0}$ will be in the form of:

$$K_{f\gamma_0} = a\gamma_0 + b$$

where *a* and *b* are constants that will be got from experimental study.

Therefore the purpose of the experiments is to get the coefficients $K_{f\gamma_0}$, $K_{fb_{r1}}$,

$K_{f\gamma_{01}}$, K_{fh}, $K_{d\gamma_0}$, $K_{db_{r1}}$, $K_{d\gamma_{01}}$, and K_{dh}.

4.5 Experimental Work

This chapter introduces the experimental study done for the extended model of

the chip-breaking limits.

4.5.1. Design of the Experiments

To get the coefficients $K_{f\gamma_0}$, $K_{fb_{r1}}$, $K_{f\gamma_{01}}$, K_{fh}, $K_{d\gamma_0}$, $K_{db_{r1}}$, $K_{d\gamma_{01}}$, and

K_{dh}, eighteen inserts were designed to be used in the experiments. Their designed

geometric parameters are listed in Table 4-1. All inserts used here has a 1mm nose radius

Table 4-1 Insert Geometric Parameters Design

Insert Number	γ_0	$b_{\gamma 1}$	γ_{01}	h	Other Parameters
1	10 °	0.2 mm	-10 °	0 mm	
2	14 °	0.2 mm	-10 °	0 mm	
3	18 °	0.2 mm	-10 °	0 mm	
4	22 °	0.2 mm	-10 °	0 mm	
5	18 °	0.05mm	-10 °	0 mm	
6	18°	0.1 mm	-10 °	0 mm	$\kappa_\gamma = 90°$
7	18 °	0.2 mm	-10 °	0 mm	$\lambda_s = -6°$
8	18 °	0.3 mm	-10 °	0 mm	$\alpha_0 = 6°$
9	18 °	0.4 mm	-10 °	0 mm	$\kappa_\gamma' = 30°$
10	18 °	0.2 mm	0 °	0 mm	
11	18 °	0.2 mm	-5 °	0 mm	
12	18°	0.2 mm	-10 °	0 mm	
13	18°	0.2 mm	-15 °	0 mm	
14	18 °	0.2 mm	-20 °	0 mm	
15	18 °	0.2 mm	-10 °	0 mm	$\kappa_\gamma = 90°$
16	18 °	0.2 mm	-10 °	0.1 mm	$\lambda_s = -6°$
17	18 °	0.2 mm	-10 °	0.2 mm	$\alpha_0 = 6°$
18	18 °	0.2 mm	-10 °	0.4 mm	$\kappa_\gamma' = 30°$

Note: the shaded parameters are predefined standard inserts

The predefined standard cutting condition is listed below:

- Work-piece material: 1045 steel;

- Surface feeding speed: V_c= 100 m/min;

- Nose radius: 1mm

- Main cutting-edge angle: 90°

4.5.2. Experimental Results

The chip-breaking limits obtained from the cutting tests are listed in Table 4-2.

Table 4-2 Cutting Test Results

No.	γ_0 (Deg)	γ_{01} (Deg)	$b_{\gamma 1}$ (mm)	h (mm)	fcr (mm/rev)	dcr (mm)
1	10	-10	0.2	0	0.2	0.8
2	14	-10	0.2	0	0.18	0.8
3	18	-10	0.2	0	0.18	0.8
4	22	-10	0.2	0	0.15	0.8
5	18	-10	0.05	0	0.1	1
6	18	-10	0.1	0	0.15	1
7	18	-10	0.2	0	0.18	0.8
8	18	-10	0.3	0	0.18	1
9	18	-10	0.4	0	0.2	1
10	18	0	0.2	0	0.2	1
11	18	-5	0.2	0	0.2	1
12	18	-10	0.2	0	0.18	0.8
13	18	-15	0.2	0	0.2	1
14	18	-20	0.2	0	0.2	1
15	18	-10	0.2	0	0.18	0.8
16	18	-10	0.2	0.1	0.15	0.8
17	18	-10	0.2	0.2	0.1	0.8
18	18	-10	0.2	0.4	0.05	0.8

To make the experimental results as reliable as possible, all the tests are repeated three times under the same experimental conditions at different times. Furthermore, cutting tests around the breaking / non-breaking boundary of the chip-sample charts are repeated more times to make the values of f_{cr} and d_{cr} as accurate as possible. Part of the sample chip-breaking charts are listed in **Appendix I.**

4.5.3. Experimental Data Analysis

The following empirical equations of the modification coefficients had been developed from the experimental results:

$$K_{f\gamma 0} = 1.32 - 0.0208\gamma_0 \qquad (4\text{-}24)$$

$$K_{d\gamma 0} = 1 \qquad (4\text{-}25)$$

$$K_{fb_{\gamma 1}} = 0.696 + 1.52b_{\gamma 1} \qquad (4\text{-}26)$$

$$K_{db_{\gamma 1}} = 1 \qquad (4\text{-}27)$$

$$K_{f\gamma 01} = 1 \qquad (4\text{-}28)$$

$$K_{d\gamma 01} = 1 \qquad (4\text{-}29)$$

$$K_{fh} = 1 - 1.84h \qquad (4\text{-}30)$$

$$K_{dh} = 1 \qquad (4\text{-}31)$$

The predefined standard values are:

- Rake angle: 12°.
- Land Length: 0.2mm
- Land Rake Angle: -10°
- Raised backwall height: 0mm

Next the experimental results of the rake angle, back-wall height, land length, and land rake angle will be analyzed one by one through comparison with the calculation results of the theoretical equations developed in this chapter. Equation (4-8) is used to calculate theoretical predicting values of f_{cr}.

Both previous work (Li, Z. 1990) and our cutting tests show that for two-dimensional grooved inserts the critical depth of cut is mainly determined by the

insert nose radius. Other insert geometric features only have minor effects on the critical

depth of cut. That is to say:

$$d_{cr} \approx r_{\varepsilon} \quad \text{(for two-dimensional grooved inserts)} \tag{4-32}$$

Equation (4-32) is used to calculate theoretical predicting values of d_{cr}.

4.5.3.1.　Rake Angle

For grooved inserts, a larger rake angle means a larger groove depth W_n, which

could make the chip-curl tighter, so that the chip breakability improves. It is found that

the experimental values of the f_{cr} slightly decrease with the increase of the rake angle,

which matches the theoretical models well.

Equation (4-8) does not take effects of friction on the rake face into account,

which may explains the difference between the theoretical f_{cr} and the experimental results.

The friction can increase chip deformation to improve chip breakability, thus the test

results of f_{cr} will be smaller than the theoretical values of f_{cr}.

For d_{cr}, the rake angle only has slight influence. Therefore when changing the

rake angle, the d_{cr} remains the same value (0.8mm), which is close to the insert nose

radius (1.0mm).

Figure 4-6 shows the comparison of the theoretical values, empirical equation

predicting values, and the experimental results when changing the insert rake angle.

4.5.3.2.　Land Length

When the land length increases, the actual chip/rake face contact length and the

groove width will increase, too, so that the chip up-curl radius will increase, leading to a

larger f_{cr} . It should have minor influence on d_{cr} .

The calculation results show that the f_{cr} increases with the increase in the land length. The d_{cr} keeps close to the insert nose radius.

Figure 4-7 shows the comparison of the theoretical values, empirical equation predicting values, and the experimental results when changing the insert land length.

4.5.3.3. Land Rake Angle

In general, the land rake angle should have little influence on chip-breaking when it is not very great due to the effects of the chip-flow sticking region.

The calculation results clearly show that the land rake angle has very little influence on chip breakability. The critical feed rate and the critical depth of cut almost do not change with the change of the land rake angle.

Figure 4-8 shows the comparison of the theoretical values, empirical equation predicting values, and the experimental results when changing the insert land rake angle.

4.5.3.4. Raised Backwall Height

The increase of the back-wall height will force the chip to up-curl more tightly, which will improve the chip breakability. The calculation results clearly show that the critical feed rate will decrease with the increase of the back-wall height, which matches the theoretical prediction well. The critical depth of cut is still determined by the nose radius. The raised backwall height only has insignificant influence on d_{cr}.

Figure 4-9 shows the comparison of the theoretical values, empirical equation predicting values, and the experimental results when changing the insert backwall height.
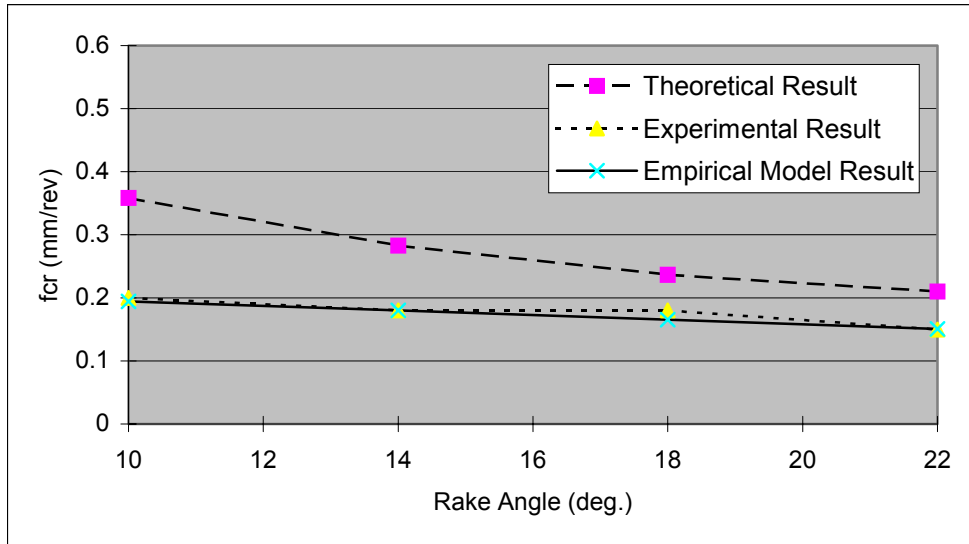
Theoretical / experimental / empirical model results of f_{cr}
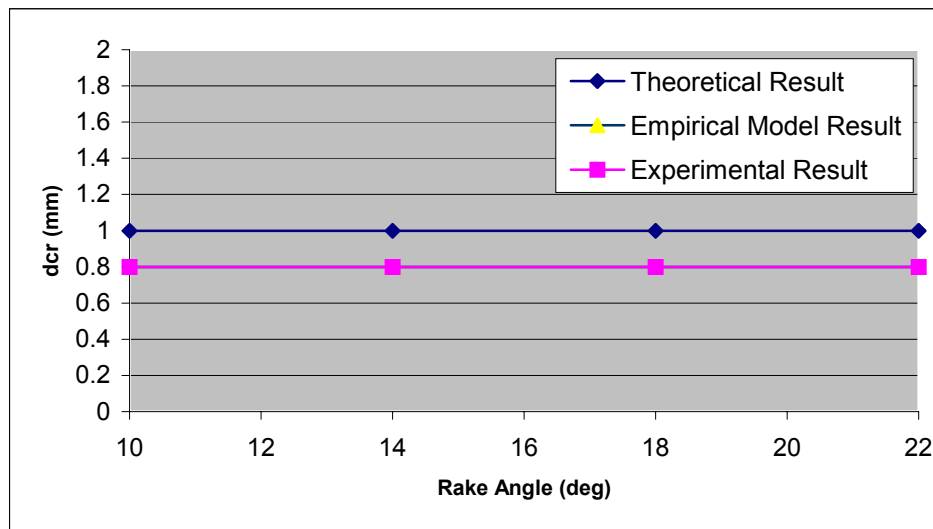
Theoretical / experimental / empirical model results of d_{cr}

Figure 4-6 Rake Angle and Chip-Breaking Limits

Theoretical / experimental / empirical model results of f_{cr}

Theoretical / experimental / empirical model results of d_{cr}

Figure 4-7 Land Length and Chip-Breaking Limits

Theoretical / experimental / empirical model results of f_{cr}

Theoretical / experimental / empirical model results of d_{cr}

Figure 4-8 Land Rake Angle and Chip-Breaking Limits
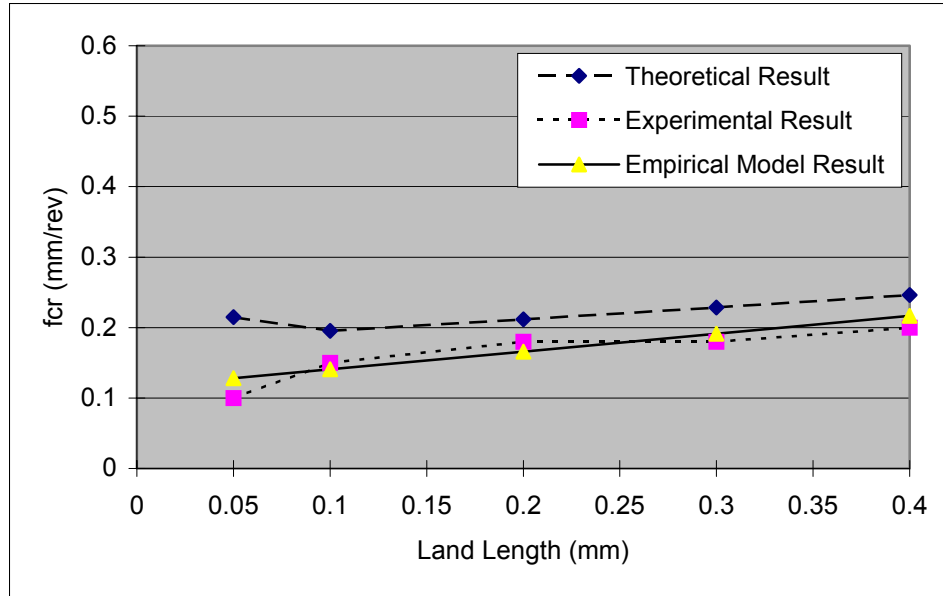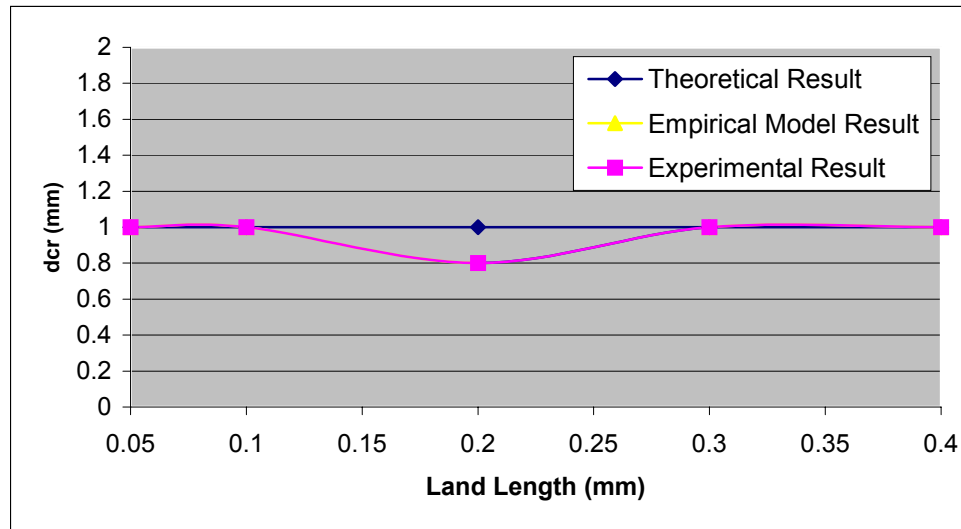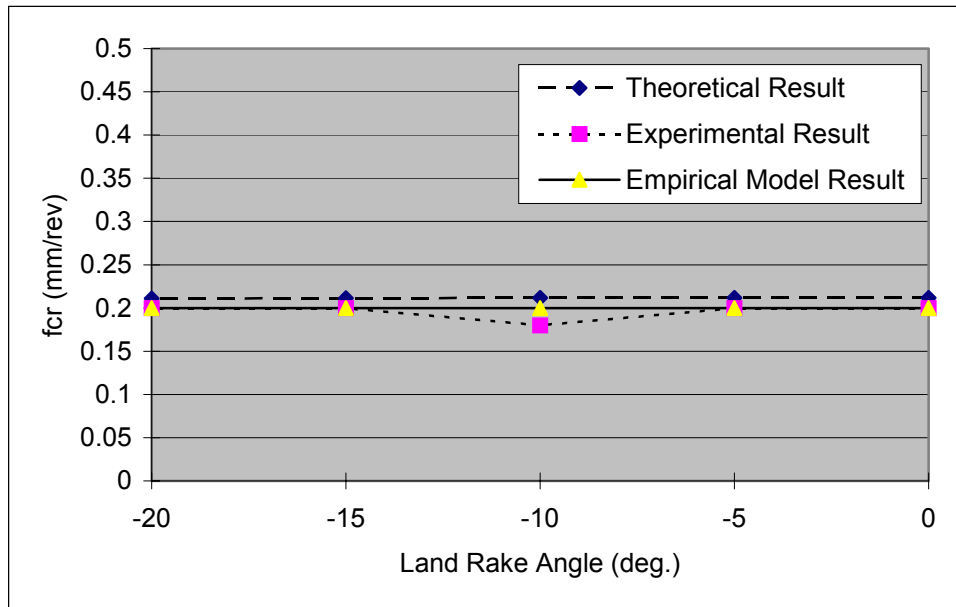
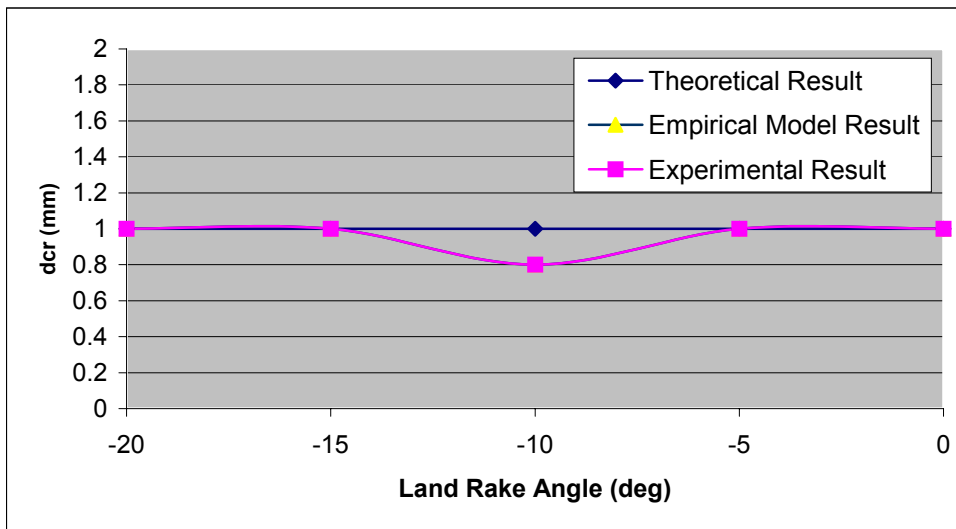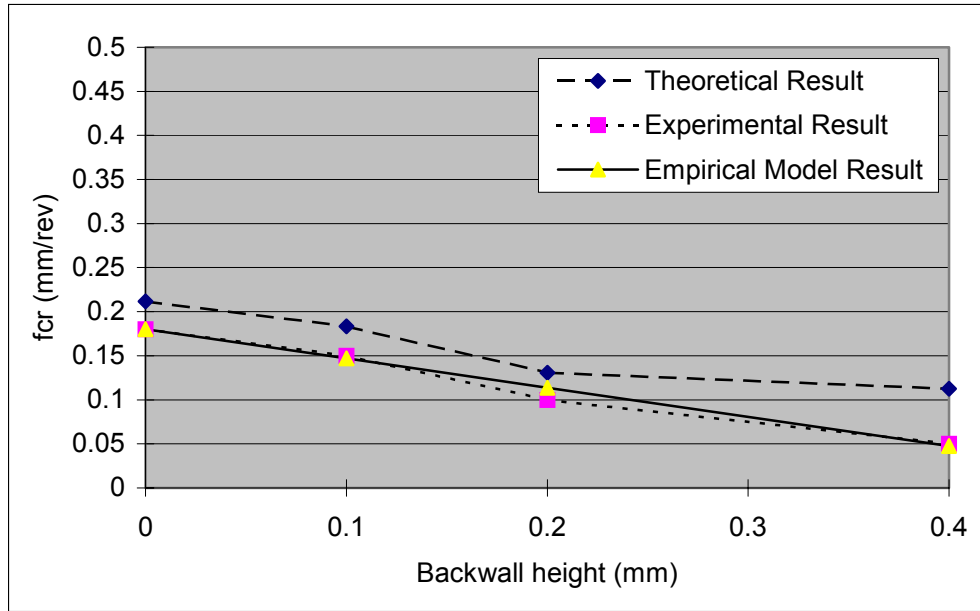Theoretical / experimental / empirical model results of f_{cr}
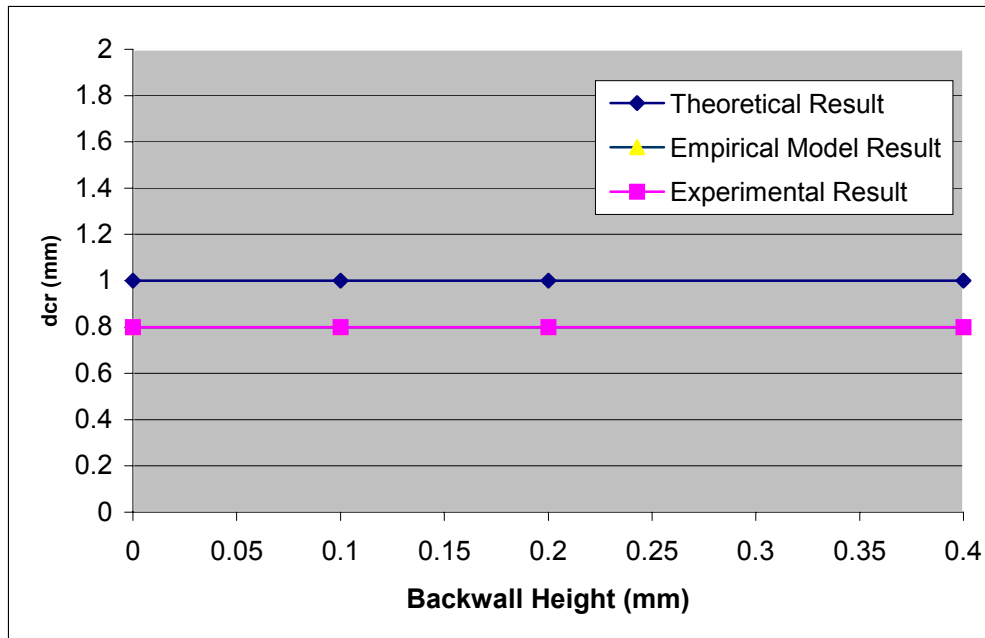
Theoretical / experimental / empirical model results of d_{cr}

Figure 4-9 Raised Backwall Height and Chip-Breaking Limits

4.6 Summary

In this chapter, the chip-breaking prediction for two-dimensional grooved inserts has been studied. The insert geometric parameters — the rake angle, the land length, the land rake angle, and the raised backwall height — are taken into consideration when developing the chip-breaking prediction model. Work done in this section includes three parts:

1. The theoretical equations of the chip-breaking limits are developed as:

$$f_{cr} = \frac{\varepsilon_b c_h k_r}{2\sin\kappa_r} \cdot \left(\frac{W^2 + h^2 + l_f^2 - 2l_f\left(W\cos\gamma_0 - h\sin\gamma_0 + b_{r1}\dfrac{\cos(\gamma_{01}-\alpha)}{\cos(\gamma_0+\alpha)}\right)}{2(W\sin\gamma_0 + h\cos\gamma_0)} + \frac{b_{r1}\dfrac{\cos(\gamma_{01}-\alpha)}{\cos(\gamma_0+\alpha)}(W\cos\gamma_0 - h\sin\gamma_0) + b_{r1}^2\dfrac{\cos(\gamma_{01}-\alpha)^2}{\cos(\gamma_0+\alpha)^2}}{2(W\sin\gamma_0 + h\cos\gamma_0)} \right)$$

and

When $d \le r_\varepsilon(1-\cos\kappa_r)$, $f \le 2r_\varepsilon$

$$d_{cr} = r_\varepsilon - r_\varepsilon \cos\left(2\arcsin\frac{-p+\sqrt{p^2+0.12q}}{0.12\xi_1 r_\varepsilon} - \arcsin\frac{f}{2r_\varepsilon}\right)$$

When $d \ge r_\varepsilon(1-\cos\kappa_r)$, $f \le 2r_\varepsilon$

$$d_{cr} = r_\varepsilon - \sqrt{r_\varepsilon^2 - \frac{f^2}{4}} + \frac{1}{0.06\xi_1}\left(-p+\sqrt{p^2+0.12q}\right)\sin(\kappa_r - \Psi_\lambda)$$

2. An extended semi-empirical chip-breaking prediction model is developed as:

$$f_{cr} = f_0 K_{fT} K_{fv} K_{fm}$$

$$K_{fT} = K_{fr_\varepsilon} \times K_{fW_n} \times K_{f\gamma_0} \times K_{f\gamma_{01}} \times K_{fh} \times K_{fb_{\gamma 1}}$$

$$K_{fV} = F_f(V)$$

$$K_{fm} = F_f(m)$$

$$d_{cr} = d_0 K_{dT} K_{dv} K_{dm}$$

$$K_{dT} = K_{dr_\varepsilon} \times K_{dW_n} \times K_{d\gamma_0} \times K_{d\gamma_{01}} \times K_{dh} \times K_{db_{\gamma 1}}$$

$$K_{dV} = F_d(V)$$

$$K_{dm} = F_d(m)$$

3. The modification coefficients for the rake angle, the land length, the land rake

angle, and the raised backwall height have been developed through experiments:

$$K_{f\gamma 0} = 1.32 - 0.0208\gamma_0 \qquad\qquad K_{d\gamma 0} = 1$$

$$K_{fb_{\gamma 1}} = 0.696 + 1.52 b_{\gamma 1} \qquad\qquad K_{db_{\gamma 1}} = 1$$

$$K_{f\gamma 01} = 1 \qquad\qquad K_{d\gamma 01} = 1$$

$$K_{fh} = 1 - 1.84h \qquad\qquad K_{dh} = 1$$

5 Chip-Breaking Predictive Model for Three-Dimensional Grooved Inserts

This chapter discusses chip-breaking for three-dimensional grooved inserts, which are the most popular type of inserts for medium / finish steel turning in industry. The definition of the three-dimensional grooved inserts will be given first. A few key geometric parameters are used to define the geometric features of three-dimensional grooved inserts. Their influence on chip-breaking will be analyzed. Cutting experiments are applied to prove their influence and to develop the semi-empirical chip-breaking predictive model for three-dimensional grooved inserts. Semi-empirical equations have been developed to calculate the chip-breaking limits and the cutting tool modification coefficients as linear functions of the insert feature parameters.

5.1 Definition of Three-Dimensional Grooved Inserts

The three-dimensional grooved insert are defined as inserts with non-straight chip-breaking grooves that are shown in Figure 5-1. The chip-breaking groove width of the three-dimensional grooved insert is not constant along the cutting edge. Figure 5-2 shows two examples of industry inserts with non-uniform chip grooves. A protrusion exists on the insert nose that can help chip-breaking more when the depth of cut is small. Generally, the protrusion is very close to the insert nose tip to improve the chip-breaking

when depth of cut is very small. three-dimensional grooved inserts are widely used in medium / fine steel cutting due to its good chip breakability. More than 70% of the industry inserts used in finish cutting can be categorized as three-dimensional grooved inserts.
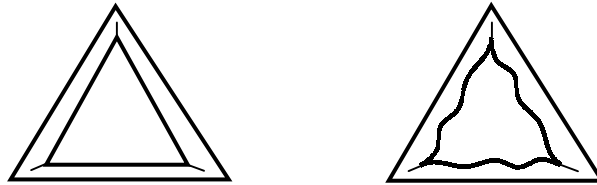
Figure 5-1 Three-Dimensional Grooved Insert

TNMP332K KC850   TNMG332MF 235

Figure 5-2 Two Examples of Commercial Three-Dimensional Grooved Insert

There are two reasons to work on chip-breaking prediction for the three-dimensional grooved insert:

1.   In steel cutting, the chip-breaking problem exists mostly in finish cutting processes, in which three-dimensional grooved inserts are widely applied. Solving the chip-breaking difficulty of three-dimensional grooved inserts means solving an important part of the whole chip-breaking problem. Furthermore it will help greatly to reduce the gap between the theoretical work of the chip-breaking and the industry reality.

2.   Chip-breaking has been studied extensively for flat rake face inserts and two-dimensional grooved inserts, and great progress has been achieved. However,

chip-breaking study is still far behind the industry requirements for inserts with a more complicated groove, due to the difficulty of studying chip-breaking for inserts with complicated three-dimensional groove. The three-dimensional grooved inserts do not have very complicated geometric features, so that they can be treated as an extension of two-dimensional grooved inserts, and more important, it is much easier to describe the geometric features of three-dimensional grooved inserts, which have fewer feature parameters than the inserts with complicated three-dimensional groove, Thus, it is much easier to study the chip-breaking limits for the simple three-dimensional grooved inserts than for the complicated grooved three-dimensional inserts.

The semi-empirical approach is still applied in the study to develop chip-breaking prediction model.

5.2 Insert feature parameters

Most three-dimensional grooved inserts have complicate geometric features, although not all of those features have significant influence on chip-breaking. As shown in Figure 5-3, nine geometric parameters that may have significant influence on chip-breaking are taken into consideration when developing the chip-breaking predictive model for three-dimensional grooved inserts. They are:

- Tool rake angle in normal direction γ_n Tool inclination angle λ_s

- Tool nose radius r_ε Length of the protrusion edge on the insert nose l_1

- Distance of the protrusion end point to the tool tip L

- Restricted contact length: $b_{\gamma 0}$

- Raised back-wall height h

- Groove width W_n

- Angle α of the protrusion

Insert geometric parameters:

$$\gamma_n, \quad \lambda_s, \quad r_\varepsilon,$$
$$l_1, \quad L, \quad b_{\gamma 0},$$
$$h, \quad W_n, \quad \alpha$$
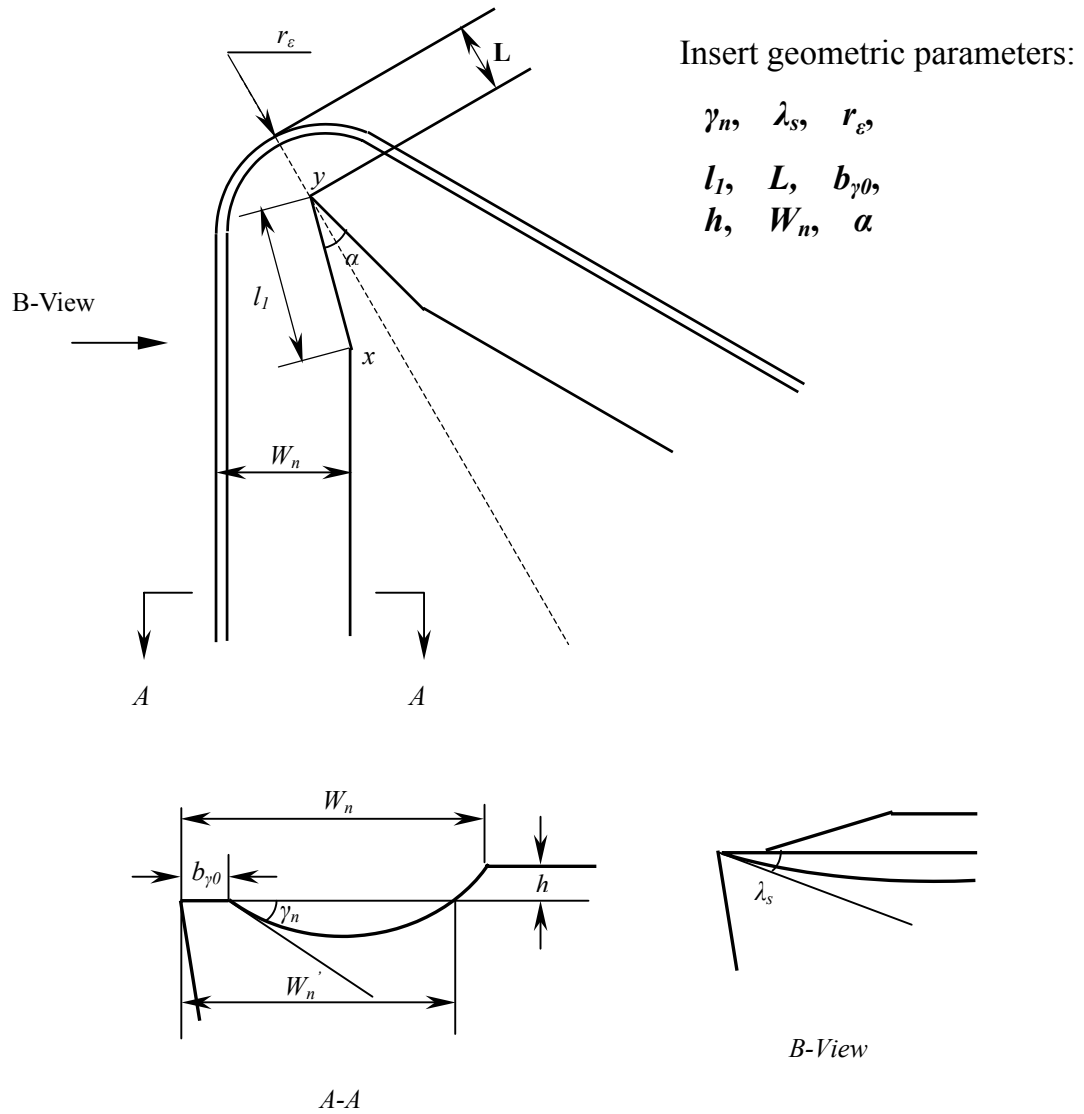
B-View

A-A

B-View

Figure 5-3 The Three-Dimensional Grooved Insert Geometric Features

5.3 Feature Parameters Based Predictive Model
of Chip-Breaking Limits

Suppose other cutting conditions are constant, the critical feed rate and the

critical depth of cut can be described by the equation:

$$f_{cr} = F_f(r_\varepsilon, L, l_1, \alpha, W_n, b_{\gamma 0}, \gamma, h, \lambda_s)$$
$$d_{cr} = F_d(r_\varepsilon, L, l_1, \alpha, W_n, b_{\gamma 0}, \gamma, h, \lambda_s)$$

(5-1)

The influence of the nose radius r_ε, the restricted contact length $b_{\gamma 0}$, the rake

angle γ_n, the backwall height h, and the inclination angle λ_s on the f_{cr} and d_{cr} have been

discussed in previous sections.

The three geometric features l_1, L, and α are actually not independent. When any

two of them are known, the third one is determined. Therefore two of them should be

chosen and put into the chip-breaking predictive model.

When the angle α becomes 60 degree, the three-dimensional grooved insert

becomes a two-dimensional grooved insert. Therefore two-dimensional grooved inserts

can be treated as a special case of the three-dimensional grooved inserts. For

two-dimensional grooved inserts, the α is 60 degree and the l_1 does not exist. Therefore in

order to include two-dimensional grooved inserts into the final chip-breaking predictive

model, the geometric features α and L will be used and the l_1 will be abandoned, which

makes two-dimensional grooved inserts become special cases of three-dimensional

grooved inserts..

An equivalent groove width W_E can be used when considering the influence of

the angle α and the distance of the groove end point to the tool tip L on chip-breaking for

three-dimensional grooved inserts (Li, Z. 1990). As shown in Figure 5-4, when we

increase the angle α, the groove width at any point along the line xy will decrease.

Therefore the equivalent groove width W_E will decrease, which will lead to better chip

breakability. Experimental data strongly supports this conclusion.

Figure 5-4 α and the Groove Width (Change α, Fix L)

As shown in Figure 5-5, increasing L means backing off the protrusion on the insert nose. The chip will have more freedom to flow, which leads to worse breakability. Changing L directly changes the distance of the region that no backwall exists to help the chip break, and this also changes the groove width along the line xy; therefore, it should also have great influence on the f_{cr} and d_{cr}. Experimental results also support this conclusion.
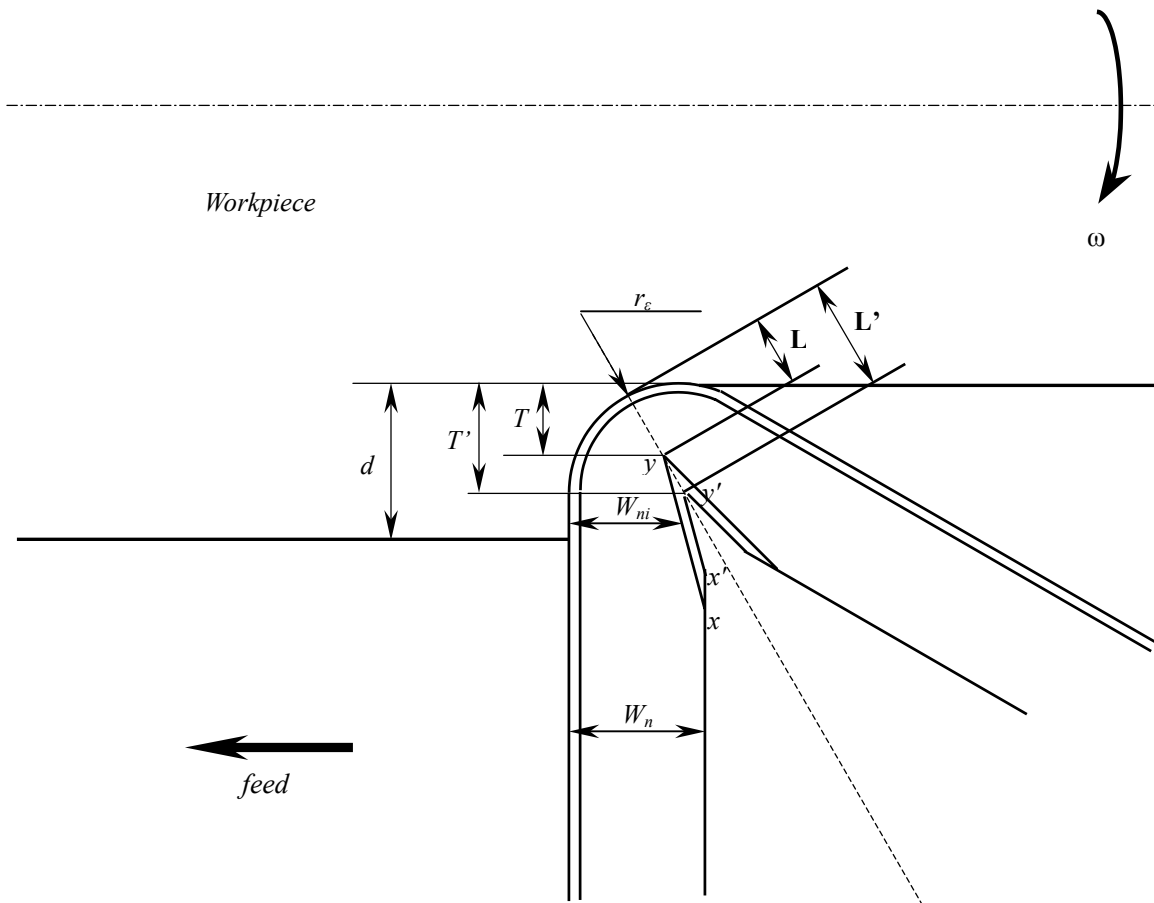

Figure 5-5 L and the Groove Width (Change L, Fix α)

In this research the experimental results show that the critical depth of cut for all three-dimensional inserts is smaller than the distance S (Figure 5-4). This makes sense, because the three-dimensional inserts are designed to use the protrusion on the nose to help chip-breaking when the depth of cut is small. Therefore only the insert nose part with the protrusion needs to be considered when analyzing chip-breaking limits. This fact simplifies the modeling work, because the groove width W_n does not take effects any more and can be removed from Equation 5-1. Equation 5-1 can then be rebuilt as:

$$f_{cr} = F_f(r_\varepsilon, L, \alpha, b_{\gamma 0}, \gamma, h, \lambda_s)$$
$$d_{cr} = F_d(r_\varepsilon, L, \alpha, b_{\gamma 0}, \gamma, h, \lambda_s)$$

(5-2)

5.4 Semi-empirical Chip-Breaking Prediction Model

Assuming a linear relationship exists between the features parameters and the chip-breaking limits, Equation 5-2 can be further described as:

$$f_{cr} = k_{f0} + k_{f1}r_\varepsilon + k_{f2}L + k_{f3}\alpha + k_{f4}b_{\gamma 0} + k_{f5}\gamma + k_{f6}h + k_{f7}\lambda_s$$
$$d_{cr} = k_{d0} + k_{d1}r_\varepsilon + k_{d2}L + k_{d3}\alpha + k_{d4}b_{\gamma 0} + k_{d5}\gamma + k_{d6}h + k_{d7}\lambda_s$$

(5-3)

Dividing both sides of Equation (5-3) by the pre-defined standard chip-breaking limits f_0 and d_0 respectively, the semi-empirical chip-breaking limits predictive model for three-dimensionalgrooved inserts can then be described as:

$$
\begin{cases}
f_{cr} = f_0 K_{fT} K_{fv} K_{fm} \\[2mm]
K_{fT} = k'_{f0} + k'_{f1} r_\varepsilon + k'_{f2} L + k'_{f3}\alpha + k'_{f4} b_{\gamma 0} + k'_{f5}\gamma + k'_{f6} h + k'_{f7}\lambda_s \\[2mm]
K_{fV} = F_f(V) \\[2mm]
K_{fm} = F_f(m) \\[4mm]
d_{cr} = d_0 K_{dT} K_{dv} K_{dm} \\[2mm]
K_{dT} = k'_{d0} + k'_{d1} r_\varepsilon + k'_{d2} L + k'_{d3}\alpha + k'_{d4} b_{\gamma 0} + k'_{d5}\gamma + k'_{d6} h + k'_{d7}\lambda_s \\[2mm]
K_{dV} = F_d(V) \\[2mm]
K_{dm} = F_d(m)
\end{cases}
\tag{5-4}
$$

The modification coefficients of the cutting speed and the workpiece material have been developed (Li, Z. 1990). The empirical equations of the cutting tool coefficients K_{fT} and K_{dT} are developed in this study.

5.5 Design of the Experiments

Cutting experiments are designed to develop the empirical equation of Equations (5-3) and (5-4).

The cutting experiments need three-dimensional grooved inserts with different feature parameter values. Since the geometric features of the three-dimensional grooved inserts are much more complicated than two-dimensional grooved inserts, it is not possible to make three-dimensional grooved inserts with customized feature parameters values, which have been done in chip breaking modeling for two-dimensional grooved

inserts (refer to Chapter 4). Therefore industry inserts have been chosen for use in the experiments, instead of making inserts ourselves. To make the experimental results more reliable, lots of three-dimensional grooved industry inserts have been used in the cutting tests.

There is a kind of industry insert that does not fully match the definition of the three-dimensional grooved inserts but, which can be treated as three-dimensional grooved inserts when the depth of cut is small. Figure 5-6 shows the geometric features of this kind of insert. The geometric difference between this inserts and standard three-dimensional grooved inserts is that the edge of the protrusion is not straight. The first part of the edge of protrusion is parallel to the main cutting edge. When applying this kind of insert in experiments of cutting 1010 steel at a surface feeding speed of 523sfpm, the experimental results show that the critical depths of cut are generally smaller than the distance S shown in the figure. Therefore when studying chip-breaking limits, this kind of insert can also be treated as three-dimensional grooved inserts. Its angle α is 60 degrees. To enlarge the sample space, that is to say, to make the available number of different inserts for cutting tests as many as possible, this kind of industry insert is also included in the cutting tests.
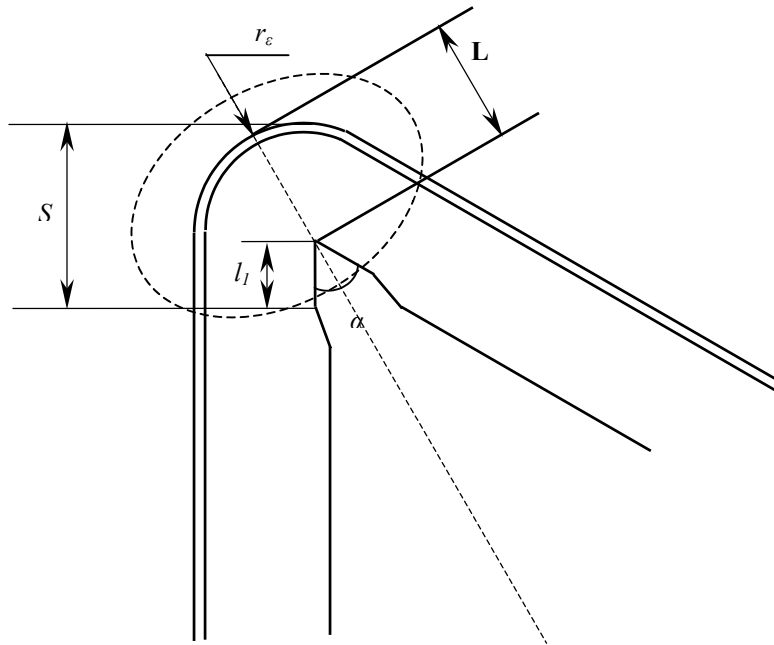
Figure 5-6 Geometry of a Special Kind of Industry Insert

Among all the seven feature parameters shown in Equation 5-2, only the value of the insert nose radius is available from the insert manufacturers. Therefore other parameters need to be measured first. To get the feature parameter values more accurately, equipment has been developed for the insert measuring. Also a software system is developed to read the raw measurement data and calculate the feature parameters. The software is written in C++. It has a user-friendly interface and is very easy to use. Figure 5-7 shows a screenshot of the software interface (nose radius measuring is shown in the picture). The measurement system is developed in cooperation with Harbin University of Science & Technology, Harbin, China.
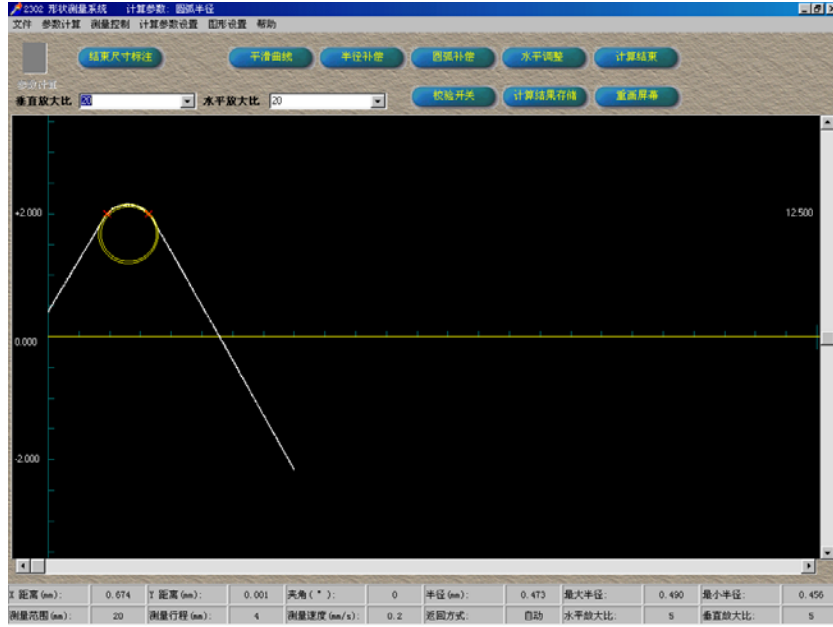
Figure 5-7 Screenshot of the Insert Geometry Measurement Software
(In cooperation with Harbin University of Science & Technology, Harbin, China, 2000)

The insert measurement results show that most three-dimensional grooved inserts have very close values of the inclination angle λ_s and the backwall height h. Only very few inserts have very different λ_s and h from the others. To make the results more reliable, only the inserts that have very close values of λ_s and h are applied in the cutting tests. The λ_s and h are then treated as constants in the experiments; therefore, they are not included in the final equations of chip-breaking limits, which are shown in Equation 5-4.

$$
\begin{aligned}
f_{cr} &= k_{f0} + k_{f1}r_\varepsilon + k_{f2}L + k_{f3}\alpha + k_{f4}b_{\gamma 0} + k_{f5}\gamma \\
d_{cr} &= k_{d0} + k_{d1}r_\varepsilon + k_{d2}L + k_{d3}\alpha + k_{d4}b_{\gamma 0} + k_{d5}\gamma
\end{aligned}
\tag{5-5}
$$

Then the equations of the cutting tool modification coefficients become:

$$
\begin{aligned}
K_{fT} &= k'_{f0} + k'_{f1}r_\varepsilon + k'_{f2}L + k'_{f3}\alpha + k'_{f4}b_{\gamma 0} + k'_{f5}\gamma \\
K_{dT} &= k'_{d0} + k'_{d1}r_\varepsilon + k'_{d2}L + k'_{d3}\alpha + k'_{d4}b_{\gamma 0} + k'_{d5}\gamma
\end{aligned}
\tag{5-6}
$$

Finally, five feature parameters are included in the equation of chip-breaking limits and the cutting tool modification coefficients. To develop Equation (5-5) and (5-6),

67

the cutting conditions, except the five insert feature parameters, need to be fixed. A standard cutting condition needs to be chosen for the cutting tests. The standard cutting condition chosen is as follows:

- Work-piece material: 1010 steel

- Cutting speed: 523sfpm

- Main cutting edge angle: 90 degree

- Insert: TNMP332K KC850

The process of the experiments can be summarized as shown in the flow chart:
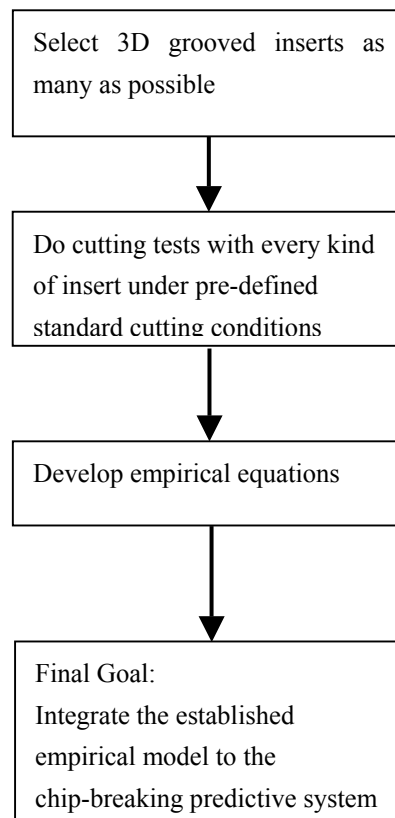
```
┌─────────────────────────────┐
│ Select 3D grooved inserts as│
│ many as possible            │
└─────────────────────────────┘
              │
              ▼
┌─────────────────────────────┐
│ Do cutting tests with every │
│ kind of insert under        │
│ pre-defined standard        │
│ cutting conditions          │
└─────────────────────────────┘
              │
              ▼
┌─────────────────────────────┐
│ Develop empirical equations │
└─────────────────────────────┘
              │
              ▼
┌─────────────────────────────┐
│ Final Goal:                 │
│ Integrate the established   │
│ empirical model to the      │
│ chip-breaking predictive    │
│ system                      │
└─────────────────────────────┘
```

Figure 5-8 Modeling Process for Three-Dimensional Grooved Inserts

5.6 Experimental Results

Thirty-three kinds of industry inserts had been measured by the insert measurement tool. The measurement results show that the geometric features of a few kinds of inserts do not match the definition of the three-dimensional grooved inserts. For example, the insert TNMG331-614025, TNMG332-614025 and TNMG333-614025 both have bumps in the chip-breaking groove; the inserts TNMG331K-KC9025, TNMG332K-KC9025, and TNMG333K-KC9025 have two small pimples on the insert nose. Those inserts had not been used in the cutting tests. Finally, twenty-two kinds of industry inserts with three-dimensional groove have been used in the cutting tests. The geometric parameters measurement results of those inserts are listed in Table 5-1. (The nose radius values are provided by the inserts manufacturers.) Part of the insert pictures and the chip-breaking charts are listed in **Appendix B**.

Table 5-1 Insert Measurement Results

No.	Insert Type	r_ε (in)	L *(in)*	α (radian)	$b_{\gamma 0}$ (in)	γ (radian)
1	TNMG 331 KC850	0.016	0.088	1.047	0.012	0.299
2	TNMG 332 KC850	0.031	0.078	1.047	0.012	0.261
3	TNMG 333 KC850	0.047	0.039	1.047	0.012	0.310
4	TNMG 432 KC850	0.031	0.044	1.047	0.014	0.344
5	TNMG MF 331 235	0.016	0.008	1.047	0.001	0.096
6	TNMG MF 332 235	0.031	0.008	1.047	0.001	0.193
7	TNMG MF 333 235	0.047	0.008	1.047	0.001	0.308
8	TNMG MF 334 4025	0.063	0.007	1.047	0.001	0.208
9	TNMG QF 331 4025	0.016	0.001	0.520	0.004	0.263
10	TNMG QF 332 4025	0.031	0.003	0.358	0.004	0.263
11	TNMG QF 333 4025	0.047	0.006	0.785	0.004	0.170
12	TNMG UF 331 KC9025	0.016	0.003	0.524	0.001	0.257
13	TNMG UF 332 KC9025	0.031	0.007	0.524	0.001	0.257
14	TNMS 431 KC850	0.016	0.012	0.785	0.001	0.301
15	TNMS 433 KC850	0.047	0.050	0.960	0.001	0.328
16	TNMG 332 23	0.031	0.041	1.047	0.010	0.282
17	TNMG 332 4025	0.031	0.044	1.047	0.010	0.266
18	TNMG 432 4025	0.031	0.034	1.047	0.016	0.246
19	TNMS 332 KC850	0.031	0.012	1.047	0.001	0.309
20	TNMP 331K KC850	0.016	0.079	1.047	0.001	0.161
21	TNMP 332K KC850	0.031	0.008	1.047	0.001	0.175
22	TNMP 333K KC850	0.047	0.066	1.047	0.001	0.175

Table 5-2 Cutting Test Results[*]

No.	Insert Type	The Critical Feed Rate (in/rev)	The Critical Depth of Cut (in)
1	TNMG 331 KC850	0.0029	0.05
2	TNMG 332 KC850	0.0065	0.06
3	TNMG 333 KC850	0.0082	0.07
4	TNMG 432 KC850	0.0056	0.05
5	TNMG MF 331 235	0.0017	0.02
6	TNMG MF 332 235	0.0020	0.03
7	TNMG MF 333 235	0.0029	0.04
8	TNMG MF 334 4025	0.0037	0.04
9	TNMG QF 331 4025	0.0025	0.03
10	TNMG QF 332 4025	0.0056	0.05
11	TNMG QF 333 4025	0.0065	0.06
12	TNMG UF 331 KC9025	0.0017	0.01
13	TNMG UF 332 KC9025	0.0037	0.05
14	TNMS 431 KC850	0.0029	0.04
15	TNMS 433 KC850	0.0082	0.05
16	TNMG 332 23	0.0065	0.05
17	TNMG 332 4025	0.0065	0.04
18	TNMG 432 4025	0.0065	0.05
19	TNMS 332 KC850	0.0029	0.05
20	TNMP 331K KC850	0.0029	0.04
21	TNMP 332K KC850	0.0029	0.03
22	TNMP 333K KC850	0.0037	0.05

[*]Note: standard cutting condition: workpiece: 1010 steel, cutting speed: 523sfpm,
main cutting edge angle: 90degree;

The insert measurement results with the cutting tests results further proved that the nose radius has great influence on chip-breaking. Generally, for every family of inserts, the type 331 has the best chip breakability, which has the smallest nose radius ($r_\varepsilon = 1/64$ in); when increasing the nose radius from 331 to 332 ($r_\varepsilon = 1/32$ in), 333 ($r_\varepsilon = 3/64$ in) etc., the chip breakability become worse. Figure 5-10 and Figure 5-11 clearly show that. The only exception is the insert family TNMP33xK-KC850: the TNMP332K-KC850 has smaller critical depth of cut than the TNMP331K-KC850. It could be ascribed to the different groove types of the TNMP33xK-KC850. Generally the inserts can be classified into insert families. The inserts in the same family have the same brand name, except for one digit that stand for the nose radius value. This digit is replaced as an 'x' in the insert family name here, e.g., TNMP33xK-KC850, TNMG33xK-KC9025. In most cases the inserts in the same family have the same chip-breaking groove type, similar other geometric features, and have a different nose radius, from 331 ($r_\varepsilon = 1/64$ in) to 334 ($r_\varepsilon = 1/16$ in). Therefore, for inserts in the same family, chip breakability decreases from 331 to 334 due to the increase of the nose radius. For different insert families, although the inserts may have the same nose radius, the chip breakability varies because the other geometric parameters, such as the L and α, are different. The insert family TNMP33xK-KC850 is an exception because the TNMP332K-KC850 has a different groove from TNMP331K-KC850 and TNMP333K-KC850, which are shown in Figure 5-9. It is very clear that the TNMP332K-KC850 is a standard three-dimensional grooved insert with a protrusion on

the insert nose, while the TNMP331K-KC850 and TNMP333K-KC850 are pure two-dimensional grooved inserts with the same groove type and without protrusion on the insert nose. Therefore, when the depth of cut is small, the protrusion on the TNMP332K-KC850 can help the chip curl more tightly, sequentially leading to a smaller d_{cr} than TNMP331K-KC850, although its nose radius is bigger. The TNMP331K-KC850 and the TNMP333K-KC850 have close feature parameters, except for different nose radius. Therefore, the TNMP331K-KC850 has smaller d_{cr} and f_{cr} than the TNMP333K-KC850. This example proved the influence of the feature parameter L.

TNMP331K-KC850   TNMP332K-KC850   TNMP333K-KC850
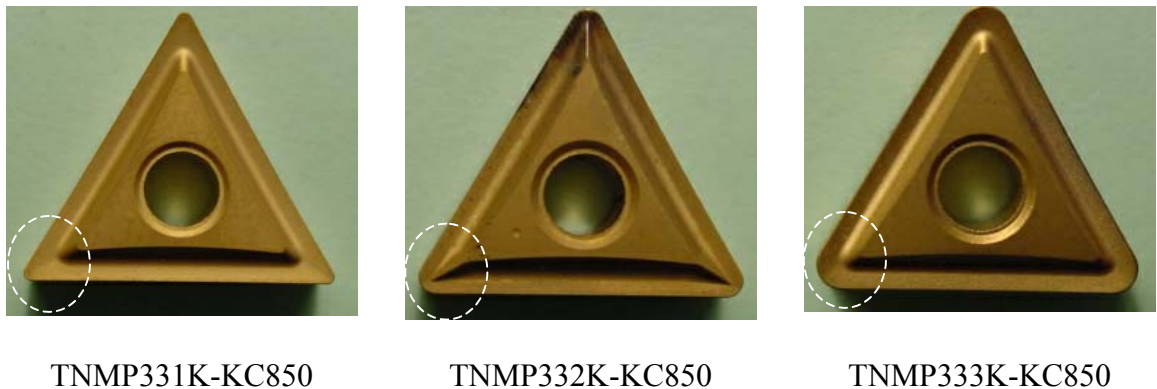
Figure 5-9 Insert TNMP33xK-KC850
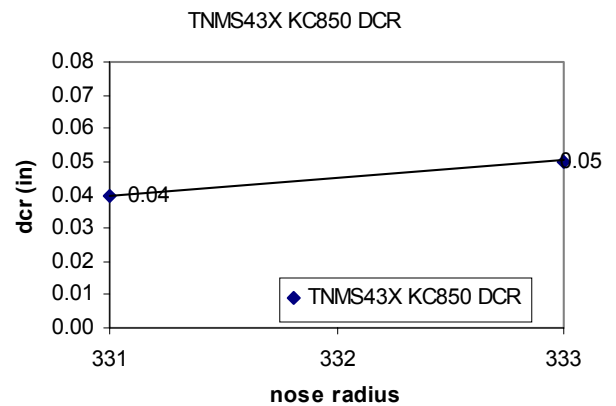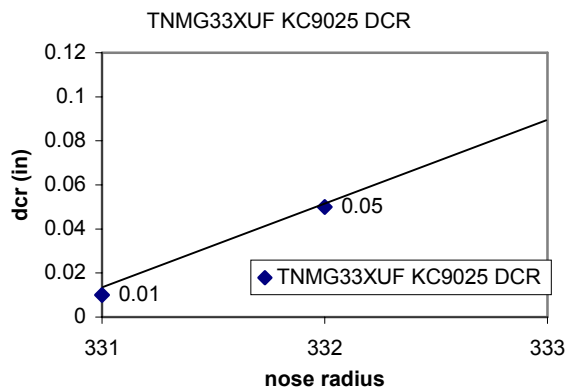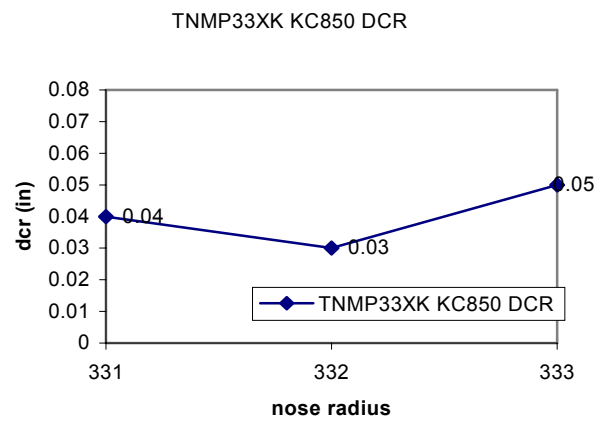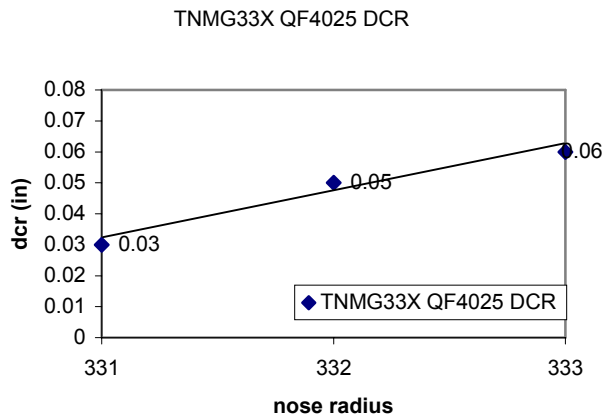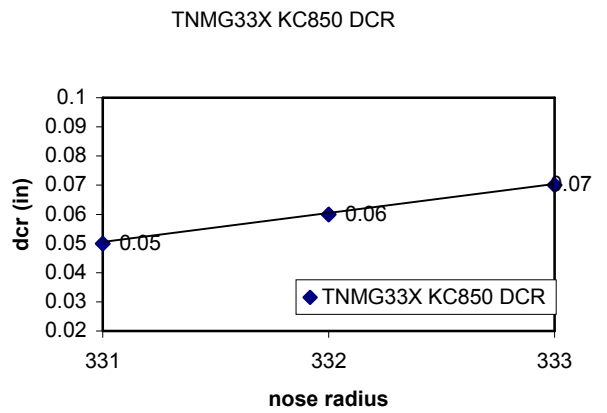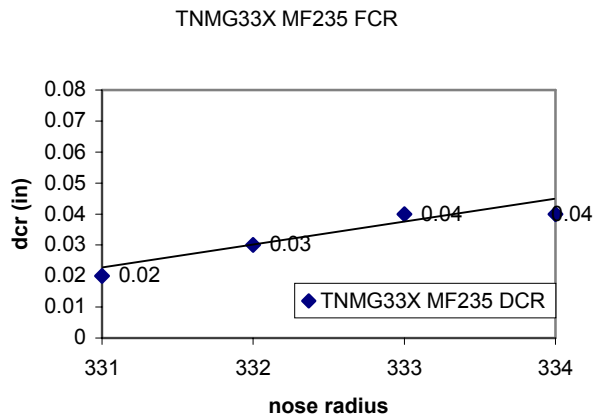
Figure 5-10 d_{cr} **VS** r_ε **for Different Insert Families**
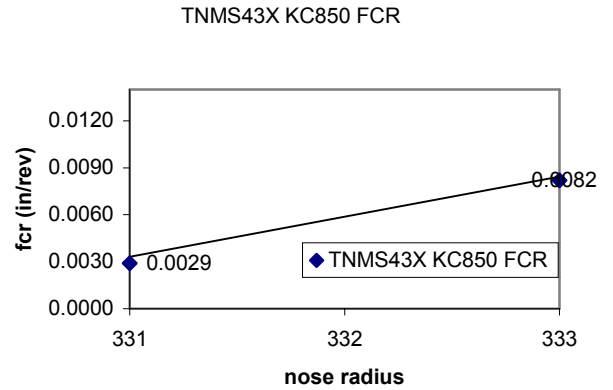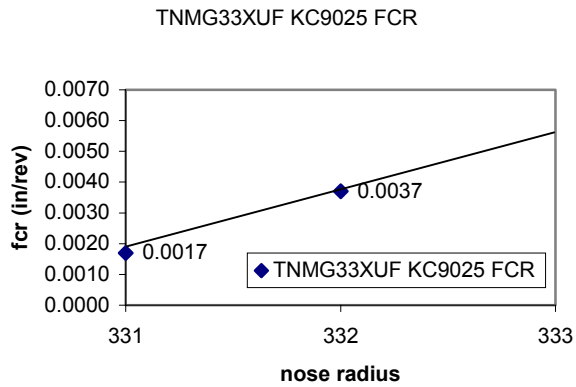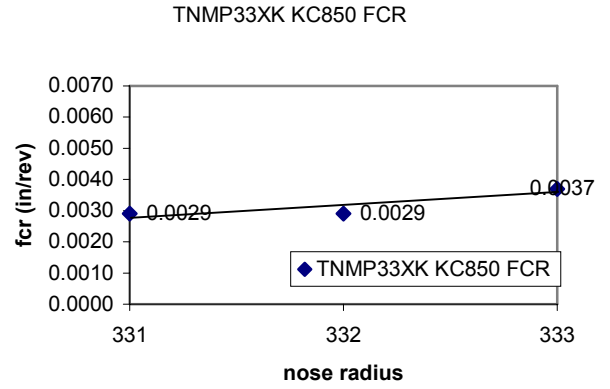
Figure 5-11 f_{cr} VS r_ε **for Different Insert Families**
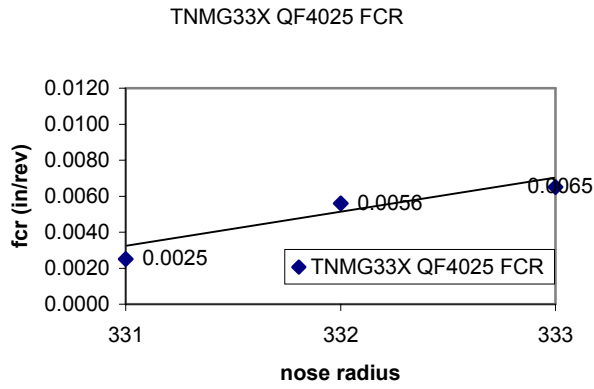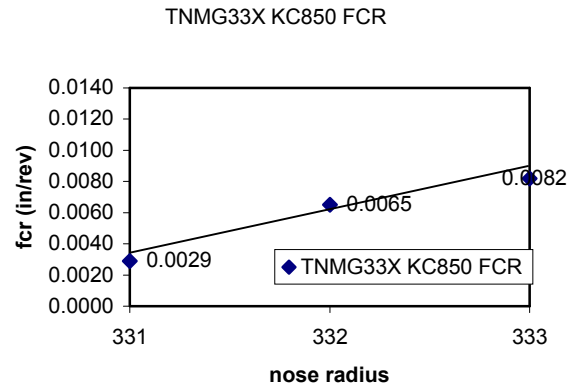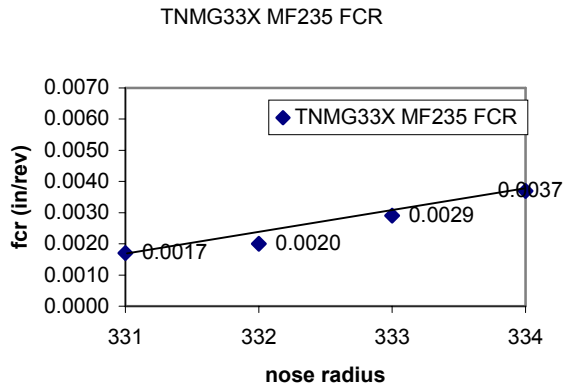
Processing the data shown in Table 5-1 and Table 5-2 by multi-elements linear curve-fit in Matlab, we can get the following equation:

$$\begin{cases} f_{cr} = 0.010 + 0.099r_{\varepsilon} + 0.0474L - 0.009\alpha + 0.304b_{\gamma0} - 0.014\gamma_n \\ d_{cr} = 0.064 + 1.17r_{\varepsilon} + 0.228L - 0.06\alpha + 0.753b_{\gamma0} - 0.033\gamma_n \end{cases} \tag{5-7}$$

The equations of the cutting tool modification coefficients can then be got as:

$$\begin{cases} K_{fT} = 3.45 + 34.13r_{\varepsilon} + 16.35L - 3.10\alpha + 104.8b_{\gamma0} - 4.82\gamma_n \\ K_{dT} = 2.13 + 39r_{\varepsilon} + 7.6L - 2\alpha + 25.1b_{\gamma0} - 1.1\gamma_n \end{cases} \tag{5-8}$$

And

$$f_{cr} = f_0 K_{fT} K_{fv} K_{fm}$$
$$d_{cr} = d_0 K_{dT} K_{dv} K_{dm}$$

The predefined chip-breaking limits here are gotten from cutting tests with insert TNMP332K KC850 at speed 523sfpm for cutting 1010 steel:

$$f_0 = 0.0029 in / rev$$
$$d_0 = 0.03 in$$

Figure 5-12 and Figure 5-13 show the comparison of the f_{cr} and d_{cr} taken from the cutting tests and the f_{cr} and d_{cr} calculated by Equation (5-7) and (5-8). The calculated values match the experimental results well. The predictive results of the d_{cr} are better than that of the f_{cr}. It should be ascribed to the different accuracy of the feed rate and the depth of cut of the lathe used in the cutting tests. The lathe used in the cutting tests is a DoAll turning machine, which can adjust the depth of cut freely but lacks the ability to adjust the feet rate freely. Therefore the experimental results are more accurate with the depth of cut than with the feed rate.

Equation (5-7) and (5-8) prove the insert nose radius influence on the chip

breakability: the f_{cr} and d_{cr} will decrease greatly with the decreasing of the nose radius.

Equation (5-7) and (5-8) also show chip breakability increases (the f_{cr} and d_{cr} decrease) with a decreasing of the L or increasing of the angle α. This also matches the analysis in the section 5.3.

Equation (5-7) and (5-8) also verified the influence of the restricted contact length on chip-breaking. During the cutting process, the existence of the restricted contact length make the chip flow back into the groove; then, by the obstruction action of the backwall, the chip curls away from the groove, acquiring a curvature (Jawahir, 1990). Previous work shows that when decreasing the restricted contact length, there is an increase in chip curvature, or, a decrease in chip curl radius, which therefore leads to better chip breakability. The relationship between the restricted contact length and chip-breaking limits shown in Equation 5-5 exactly matches this analysis.

The influence of the rake angle shown in Equation (5-7) and (5-8) matches the discussion of the rake angle influence on chip breakability in Chapter 5.

Applying Equation (5-8), chip-breaking limits can be predicted once the insert feature parameters are known, consequently chip-breaking can be predicted with Equation (5-8).

The equation can be used not only for chip-breaking prediction but also be useful for insert design. It discloses the relationship between the insert /chip-breaking groove geometric features and the chip-breaking limits, which can guide the design of insert geometric features for achieving better chip breakability of the insert.
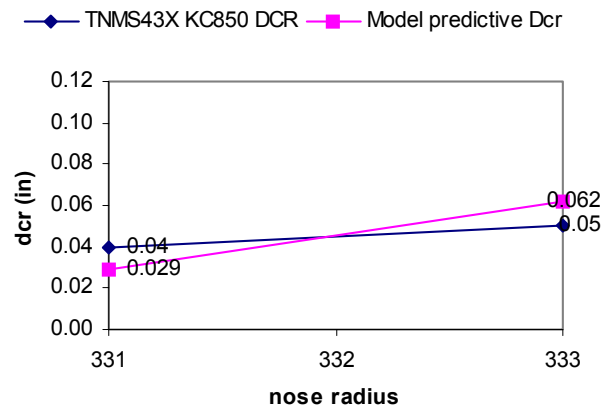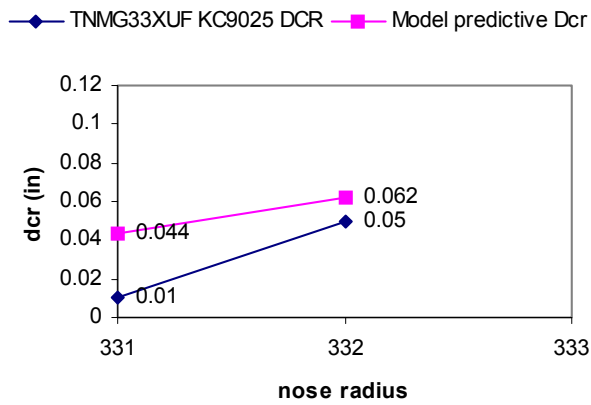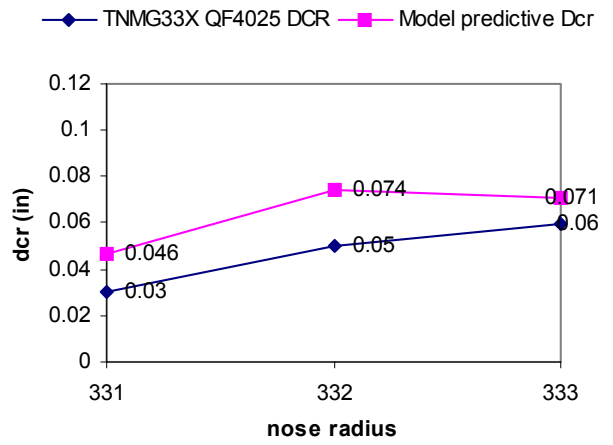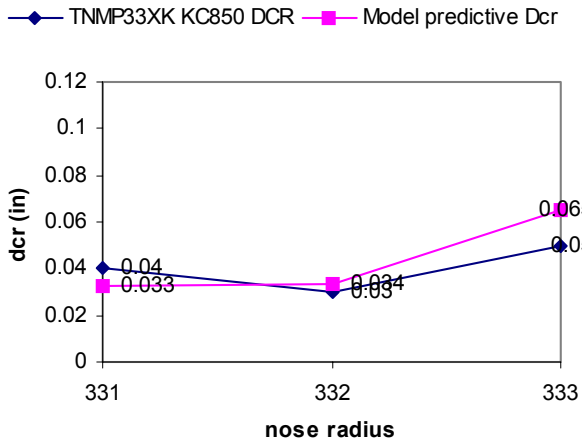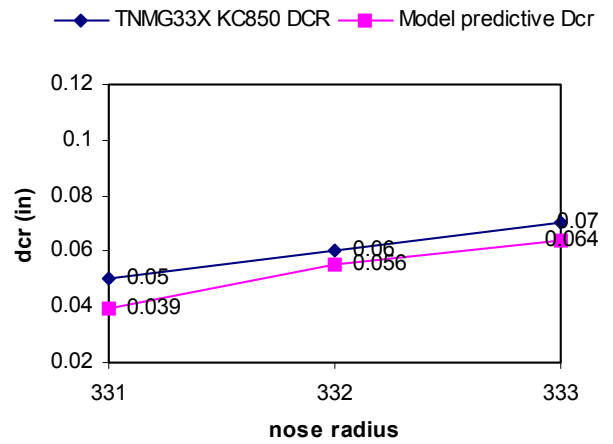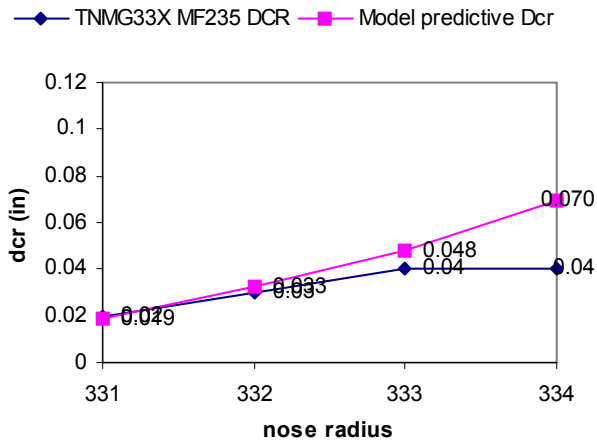
Figure 5-12 d_{cr}: Experimental Results VS Model Predictive Results

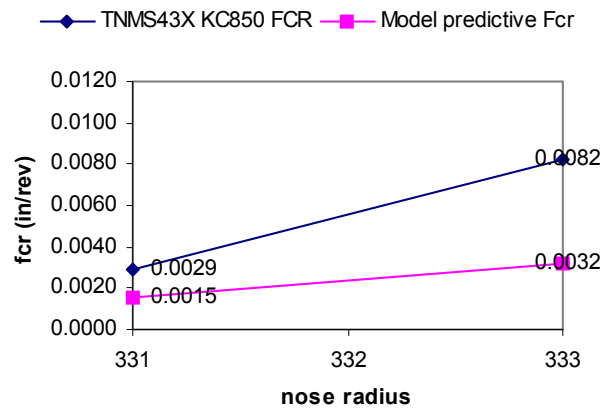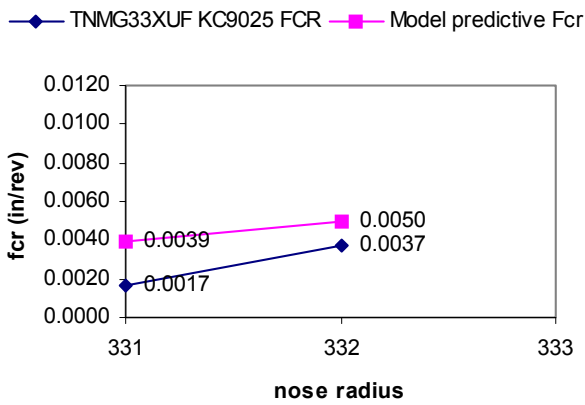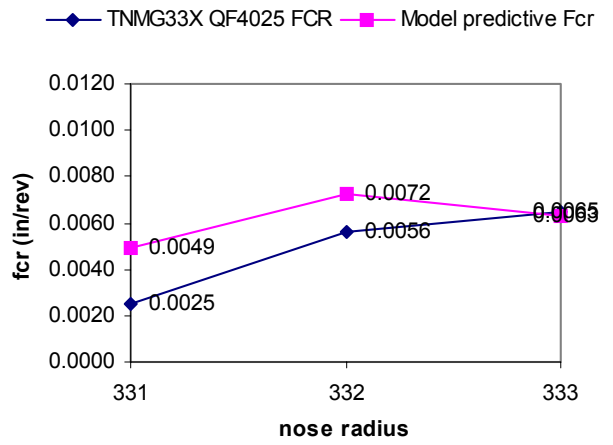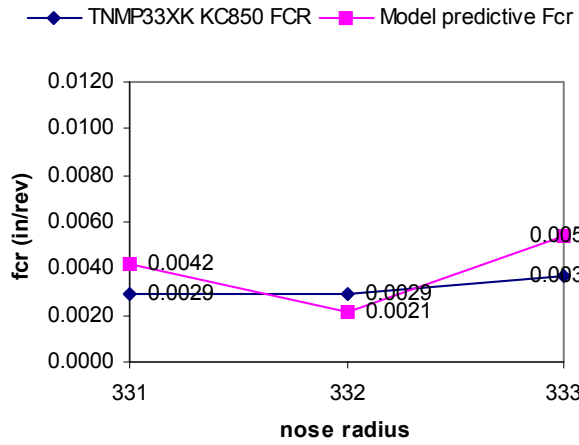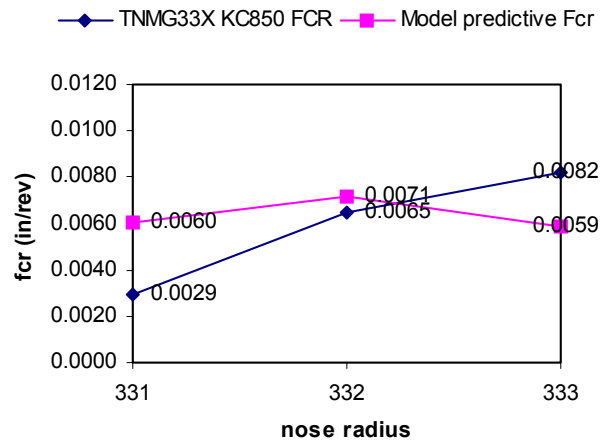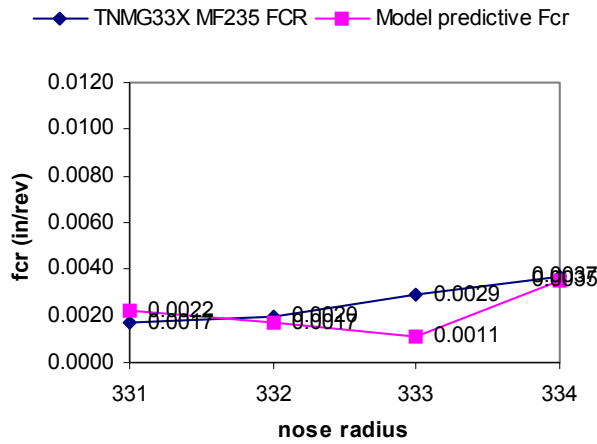**Figure 5-13** f_{cr}**: Experimental Results VS Model Predictive Results**

5.7 Experiment-based Predictive Model

of Chip-Breaking Limits

This section discuss another approach of studying chip-breaking limits for three-dimensional grooved inserts. Chip-breaking limits can be predicted by Equation 5-7, while there is another approach that can be used in the chip-breaking prediction in industry – an experiment-based approach. Compared with the feature-based approached presented in Equation 5-7, the experiment-based approach is easier to use in industry applications and to be integrated into the web-based chip-breaking predictive system developed in this research. It also has larger application range then the feature based approach – it can be used to predict chip-breaking for any kinds of insert in which chip-breaking limits exist.

The cutting tool modification coefficients K_{fT} and K_{dT} are empirical constants for every kind of insert in the   experiment-based approach. K_{fT} and K_{dT} can be gotten from cutting tests. A group of cutting tests is needed to get the empirical constants of K_{fT} and K_{dT} for each different type of inserts. When a new kind of insert is introduced, carry out cutting tests with the insert under predefined standard cutting conditions, to get a group of f_{cr} and d_{cr}. Then K_{fT} and K_{dT} can be calculated as:

$$\begin{cases} K_{fT} = f_{cr} / f_0 \\ K_{dT} = d_{cr} / d_0 \end{cases} \qquad (5\text{-}9)$$

f_0 and d_0 are the standard chip-breaking limits under the pre-defined standard cutting condition.

Putting the K_{fT} and K_{dT} into the database, next time we can use it to predict chip-breaking for this insert under any cutting condition, without the need for extra

cutting tests. A database of K_{fT} and K_{dT} has been set up for the inserts used in this research, which are shown in Table 5-3. Here the standard cutting condition are defined as:

- Work-piece material: 1010 steel

- Cutting speed: 523sfpm

- Main cutting edge angle: 90 degree

- Insert: TNMG332MF 235

The experiment-based approach has been applied in the development of the web-based chip-breaking predictive system in this research, and the K_{fT} and K_{dT} database has been included in the system. The system is discussed in the next chapter.

Table 5-3 K_{fT} and K_{dT} Results from Cutting Tests

No.	Insert Type	K_{fT}	K_{dT}
1	TNMG 331 KC850	1.000	1.667
2	TNMG 332 KC850	2.241	2.000
3	TNMG 333 KC850	2.828	2.333
4	TNMG 432 KC850	1.931	1.667
5	TNMG MF 331 235	0.586	0.667
6	TNMG MF 332 235	1.000	1.000
7	TNMG MF 333 235	1.000	1.333
8	TNMG MF 334 4025	1.276	1.333
9	TNMG QF 331 4025	0.862	1.000
10	TNMG QF 332 4025	1.931	1.667
11	TNMG QF 333 4025	2.241	2.000
12	TNMG UF 331 KC9025	0.586	0.333
13	TNMG UF 332 KC9025	1.276	1.667
14	TNMS 431 KC850	1.000	1.333
15	TNMS 433 KC850	2.828	1.667
16	TNMG 332 23	2.241	1.667
17	TNMG 332	2.241	1.333
18	TNMG 432	2.241	1.667
19	TNMS 332 KC850	1.000	1.667
20	TNMP 331K	1.000	0.667
21	TNMP 332K	1.000	1.000
22	TNMP 333K	1.276	1.667

5.8 Summary

Study of chip-breaking in steel cutting with three-dimensional grooved inserts is important for achieving the final goal of chip-breaking control due to the wide application of three-dimensional grooved inserts in industry. Three-dimensional grooved inserts are defined at the beginning of this chapter. The geometric features can be described by a few feature parameters. Chip-breaking limits can then be described as functions of a few key feature parameters of the inserts. Experiments have been designed to develop those functions. Special devices and software have been developed for insert geometry measurement. Through cutting tests, an empirical equation of chip-breaking limits has been developed as follows:

$$\begin{cases} f_{cr} = 0.010 + 0.099r_\varepsilon + 0.0474L - 0.009\alpha + 0.304b_{\gamma 0} - 0.014\gamma_n \\ d_{cr} = 0.064 + 1.17r_\varepsilon + 0.228L - 0.06\alpha + 0.753b_{\gamma 0} - 0.033\gamma_n \end{cases}$$

The semi-empirical chip-breaking predictive model for three-dimensional grooved inserts has been developed as:

$$f_{cr} = f_0 K_{fT} K_{fv} K_{fm}$$
$$d_{cr} = d_0 K_{dT} K_{dv} K_{dm}$$

where

$$\begin{cases} K_{fT} = 3.45 + 34.13r_\varepsilon + 16.35L - 3.10\alpha + 104.8b_{\gamma 0} - 4.82\gamma_n \\ K_{dT} = 2.13 + 39r_\varepsilon + 7.6L - 2\alpha + 25.1b_{\gamma 0} - 1.1\gamma_n \end{cases}$$

and

$$f_0 = 0.0029 in/rev$$
$$d_0 = 0.03 in$$

The predefined standard cutting condition is: insert TNMP332K KC850, cutting speed 523sfpm; workpiece material 1010 steel.

The equation discovers the relationship between the insert / groove geometry and chip-breaking. Once the insert feature parameters are known, chip-breaking limits can be predicted by this equation. The predictive values of the equation match the experimental results well. The equation is also useful for designing insert geometric features in order to achieve better chip breakability.

The experiment-based approach can also be used to develop a chip-breaking limits prediction model. Unlike Equation (5-7) and (5-8), which are developed through the feature-based approach, the experiment-based approach uses the empirical insert chip-breaking constants K_{fT} and K_{dT} to predict chip-breaking. This method is convenient for industry application. A database of K_{fT} and K_{dT} for different brands of industry inserts has been set up in this research.

6 Web-Based Machining Chip-Breaking Predictive System

In previous sections, chip-breaking prediction models have been developed for two-dimensional grooved inserts and three-dimensional grooved inserts. To use the models in real applications, a web-based semi-empirical chip-breaking prediction system is developed in this section. The system integrated the chip-breaking models presented in this research, and it is accessible through the Internet.

6.1 Introduction of the System

This system is designed to predict chip-breaking in the cutting process based on chip-breaking models of f_{cr} and d_{cr} presented before. The system functions include:

- Predict chip-breaking region (provide the chip-breaking chart) when tool/insert is selected

- Predict if chip will break or not when tool/insert is selected and cutting conditions (V, d, f, etc.) are given.

- Predict chip shapes with specified insert within insert cutting range

- Guide cutting condition design

- Guide cutting tool design / selection

The chip-breaking predictive models behind the system have been presented in

previous sections, which include:

- Semi-empirical chip-breaking predictive model for two-dimensional grooved inserts in steel cutting process

- Semi-empirical chip-breaking predictive model for three-dimensional grooved inserts in steel cutting process

   The system has many advantages, which include:

- Integrating the semi-empirical chip-breaking models for chip-breaking prediction.

   The semi-empirical chip-breaking predictive models provide the system a solid base for chip-breaking prediction.

- Availability through the Internet, a powerful online tool for industry use.

   Applying client/server technology, the system is accessible through the Internet or Intranet, so it could be a powerful online chip-breaking prediction tool in industry application. Multiple users can access it from anywhere on the Internet / Intranet at the same time without any installation requirement.

- Ease of setting up, maintaining, and expanding the databases.

   Compared with traditional machining databases, the semi-empirical chip-breaking predictive models only need a small number of cutting tests to setup the database and to expand the database for new cutting tools / new workpiece materials. Therefore, it provides an extraordinary saving of labor,

time and money.

6.2 System Structure

Figure 6-1 shows the system flow chart.

To predict chip-breaking, the first step is getting user input. The system will first check whether the input values are within allowed ranges or not. If not, a warning message will be shown to the user. According to the input, the system will also update the input and output screen.

After receiving all necessary input values, the system will predict chip-breaking by applying the semi-empirical chip-breaking models. First the system will look up the selected cutting tool and work-piece material from the system database. Then the system will decide which model should be applied, according to different types of cutting tools.

After the model is selected, the system will retrieve the relative empirical equations from the database to calculate chip-breaking limits and predict chip-breaking ranges under the current selected condition. The system will also retrieve the chip-breaking chart from the database to predict chip shape / length. Finally, the system will output the results to the user.

It is clear that the semi-empirical chip-breaking models are the basis of the system, and the chip-breaking predictive database, which includes the cutting-tools database and the workpiece material database, is the core of the system.
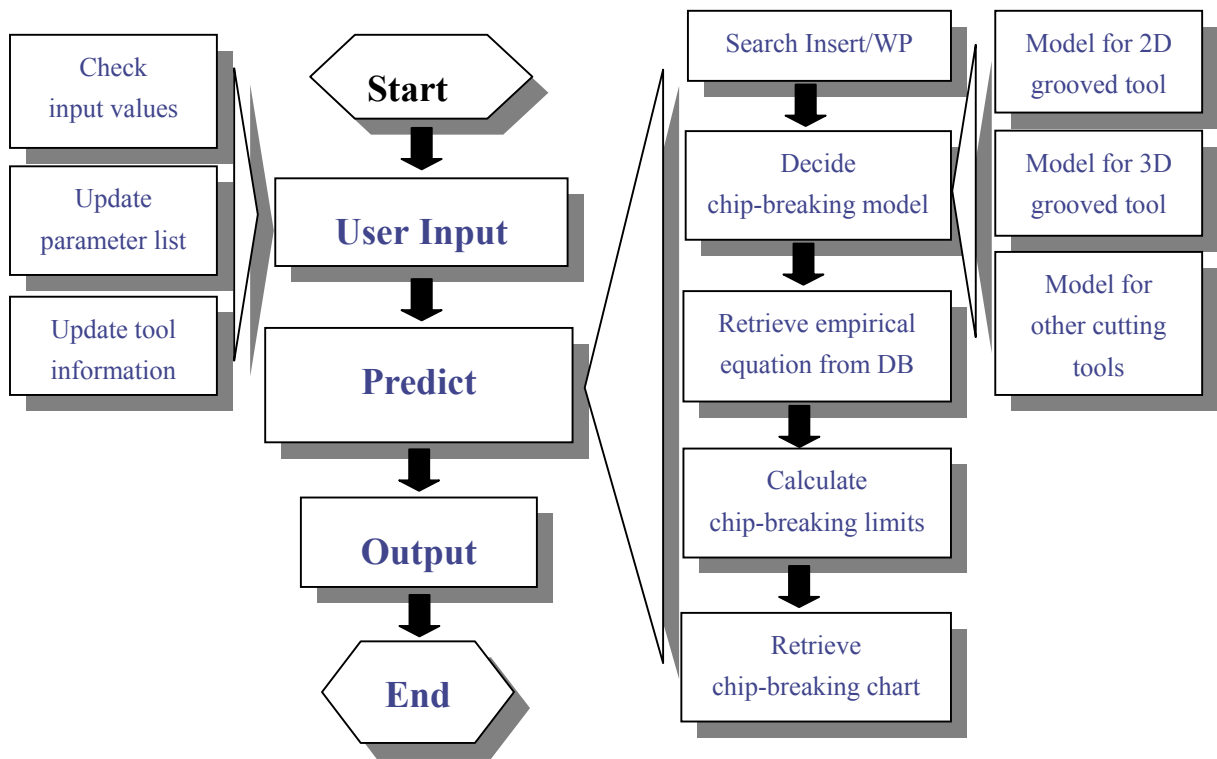
Figure 6-1 System Flow Chart

6.3 Chip Shape / Length Prediction

The chip shape and length could be predicted after the chip-breaking limits fcr and dcr have been figured out. The first step is to classify the chips.

6.3.1. Chip Classification

According to different chip shape / length, the chips will be classified according to six types in this system — two unbroken chip types, which have breakability rank number of 5 and 6 respectively; four broken chip types, which rank as 1 to 4 respectively. Table 6-1 gives the descriptions of each type.

Table 6-1 Chip Classification Used in the System

	Type 1 (Rank 1) C-type and/or e-type broken chips		Type 4 (Rank 4) Long helical broken chips (length 2.5-5.0 cm)
	Type 2 (Rank 2) Short helical broken chips (length less than 1.27 cm)		Type 5 (Rank 5) Long helical unbroken chips (length larger than 5 cm)
	Type 3 (Rank 3) Medium helical broken chips (length 1.27-2.5 cm)		Type 6 (Rank 6) Long and snarled unbroken chips

The above is not a very accurate classification, but is intended for industry application. Since presently there is no very reasonable chip shape/length predictive model, the empirical method is used in the system to predict chip shape/length. Therefore, the chip classification cannot be very accurate if we want to keep the number of required cutting tests within a reasonable range.

6.3.2. Chip-Breaking Chart and Chip-Breaking Matrix

To predict chip shape/length for a given insert under any cutting condition, first we need to carry out a group of cutting tests with the insert under pre-defined standard cutting conditions in order to get an overall chip-breaking chart sample, such as the chart shown in Figure 6-2. Later this chart sample will be stored in the system's database as the chip shape/length prediction basis of this insert under any cutting condition. That is, when the user selects this insert and specifies a cutting condition, the system will first

calculate the chip-breaking limits fcr and dcr; then the system will get the insert's chip-breaking sample chart, and find out the position of the chip-breaking limits. For example, for the following chip-breaking chart, it defined a 7 by 7 chip-breaking chart, and the position of the critical feed rate is 2, and the position of the critical depth of cut is 2.
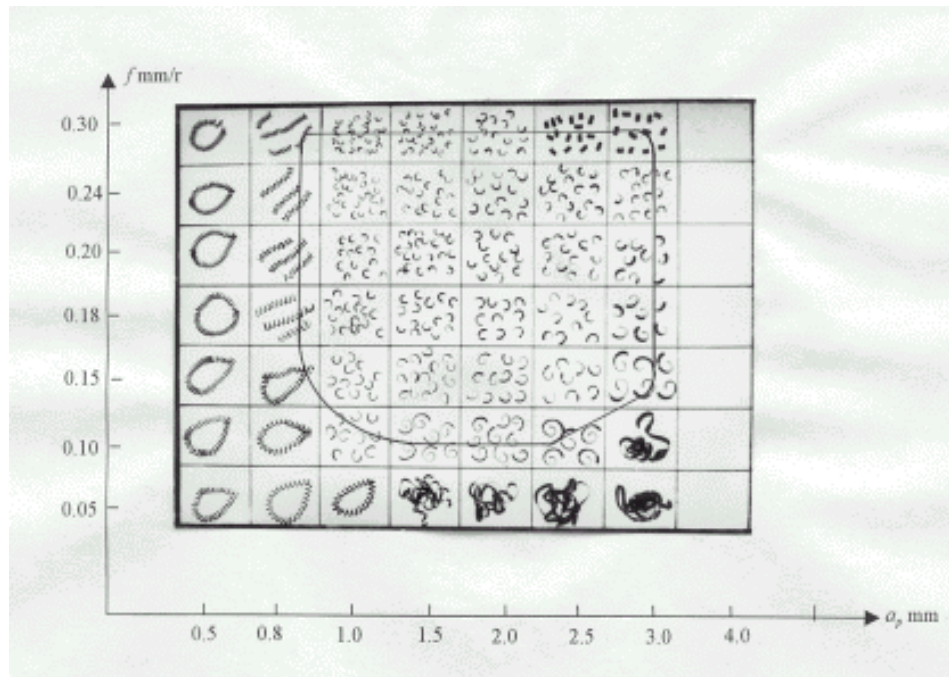
Figure 6-2 A Samples Chip-Breaking Chart

Next the system will calculate all other coordinators with Equation 6-1 and (6-2):

$$f_i = (f_{cr}/(position\ of\ f_{cr}))*i \qquad\qquad\qquad (6\text{-}1)$$

$$d_i = (d_{cr}/(position\ of\ d_{cr}))*i \qquad\qquad\qquad (6\text{-}2)$$

For example, if the system gets the critical depth of cut as 1.0mm for the insert, and the position of the critical depth of cut in the sample chart is 2, then 1.0mm is the coordinator value for the position 2; the value for position 1 will be 1.0/2=0.5mm, and

the value for position 4 will be (1.0/2)*4=2mm.

It is not necessary to store the whole picture of the chip-breaking chart sample into the database. Instead, to save storage and loading time, a chip-breaking matrix will be defined for each insert, which presents its chip-breaking chart sample. The matrix uses the chip classification rank number for its element value. For example, for the above chart, the chip-breaking matrix will be:

$$
\begin{bmatrix}
5 & 3 & 1 & 1 & 1 & 1 & 1 \\
5 & 4 & 1 & 1 & 1 & 1 & 1 \\
5 & 4 & 1 & 1 & 1 & 1 & 1 \\
5 & 4 & 1 & 1 & 1 & 1 & 1 \\
5 & 5 & 1 & 1 & 1 & 1 & 1 \\
5 & 5 & 1 & 1 & 1 & 1 & 6 \\
5 & 5 & 5 & 6 & 6 & 6 & 6
\end{bmatrix}
$$
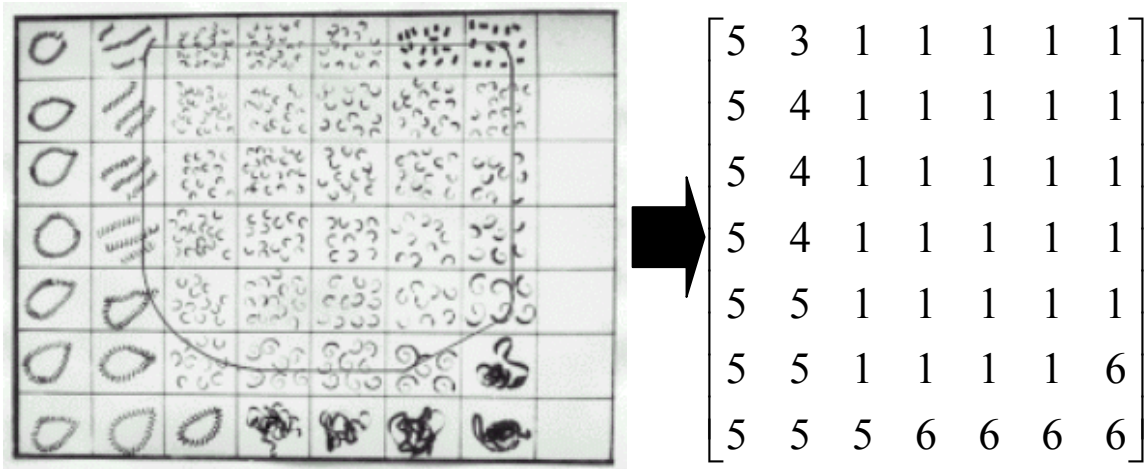
where 1 stands for chip type 1, 2 stands for chip type 2, and so on. When the system wants to get the overall chip-breaking chart, it first loads the matrix from the database, then replaces all element numbers with relative chip sample pictures, which are listed in Table 8.3-1; Then it gets the chip-breaking chart.

6.4 System Databases

The system is supported by two databases: an insert database, and a work-piece material database.

6.4.1. Insert Database

The insert database contains all inserts whose chip-breaking can be predicted by the system. The system will create a piece of record in the insert database for each different insert. The record contains all information that the system needs about the insert. Basically, a piece of record will contain the following information: insert name, insert manufacturer, insert cutting range, insert geometric parameters, insert chip-breaking chart matrix, insert picture filename/path, and all the empirical equations/constants that will be used to predict chip-breaking for this insert, which include the equations/constants of the K_{fT}, K_{fV}, K_{dT}, and K_{dV}.

6.4.2. Work-Piece Material Database

The work-piece material database contains all work-piece materials whose coefficients K_{fm} and K_{dm} have been established The system will create a piece of record in the insert database for each different kind of work-piece material. The record contains all information that the system needs about that kind of material. Basically, a piece of record will contain the following information: material name/brand, and the constants K_{fm} and K_{dm}.

6.4.3. Using the Two Databases

When the user selects an insert and a work-piece material, the system will check the work-piece material database to find out the relative record and retrieve the K_{fm} and K_{dm}. Next, the system will search the insert database to find the record of the insert and retrieve the insert name, manufacturer, cutting range, chip-breaking chart matrix,

equations, etc. Then the system can use the equations and the constants to predict

chip-breaking and predict the overall chip-breaking chart.

6.5 Updating / Extending the System

To update / extend the system, we need to update / extend the two databases. The

system maintenance work is very easy with the above databases structure.

6.5.1. Update / extend the insert Database

To update an insert, we only need to find out the record of the insert in the

database, and then update the record. It is that simple.

Since different models will be applied to different insert types, to add new inserts

to the system, the type of the new insert should be decided first. Then we need to do

cutting tests to set up the empirical constants/equations for that insert. Then we need to

create a new record for that insert and then add it to the database. The flow chart shown

in Figure 6-3 shows the process. The design of the cutting tests is described in section 3.

```
┌─────────────────────────────┐
│   User requires adding a new │
│   tool to the system DB      │
└─────────────────────────────┘
              ↓
┌─────────────────────────────┐
│  Decide new tool type:       │
│     ▪  2D grooved            │
│     ▪  3D grooved            │
│     ▪  Tool with block-type chip breaker │
└─────────────────────────────┘
              ↓
┌─────────────────────────────┐
│       Measure tool           │
│    geometric parameters      │
└─────────────────────────────┘
              ↓
┌─────────────────────────────────────────┐
│  Do a group of cutting tests under standard │
│              condition.                   │
│       Get chip-breaking chart             │
│  for 3D grooved tool, calculate $K_{fT}$ and $K_{dT}$ │
└─────────────────────────────────────────┘
              ↓
┌─────────────────────────────────────┐
│   Create a new tool record with its  │
│   information (names, manufacturers,  │
│   pictures, constants and equations etc.) │
└─────────────────────────────────────┘
              ↓
┌─────────────────────────────┐
│      Add the record to       │
│      tool database           │
└─────────────────────────────┘
```
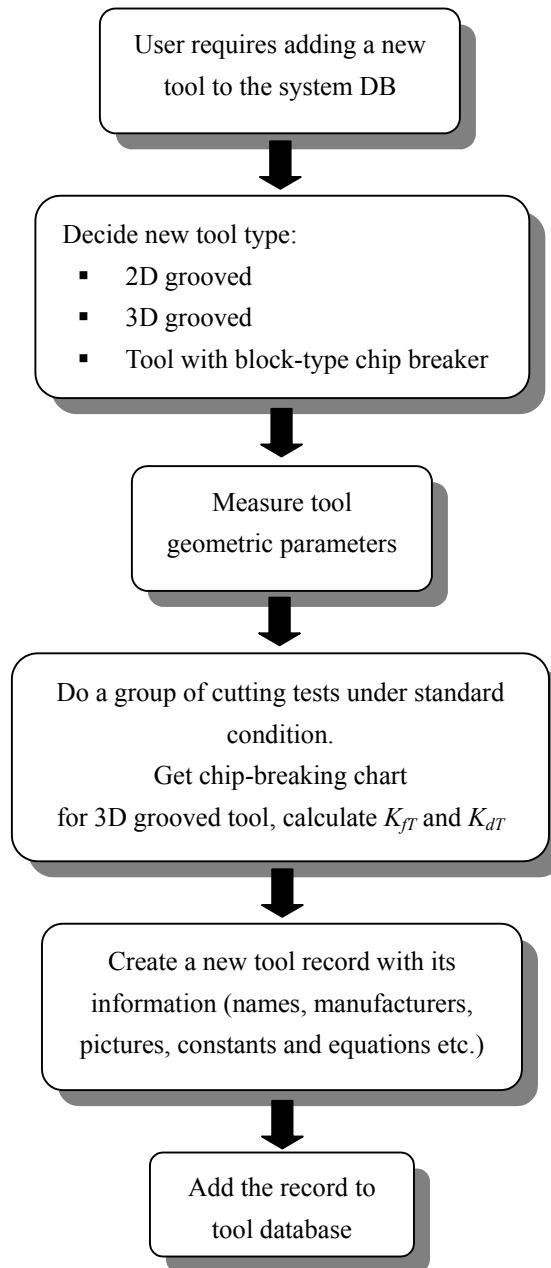
Figure 6-3 Adding a New Cutting Tools to the System

6.5.2. Update / Extend the Work-Piece Material Database

To update any kind of work-piece material, we only need to the record of the

material in the database and update the record.

To add new inserts to the system, we first need to conduct cutting tests to set up

the empirical constants K_{fm} and K_{dm} for that material. Then we need to create a new record for that material and add it to the database. The flow chart shown in Figure 6-4 shows the process. The design of the cutting tests is described in section 3 too.
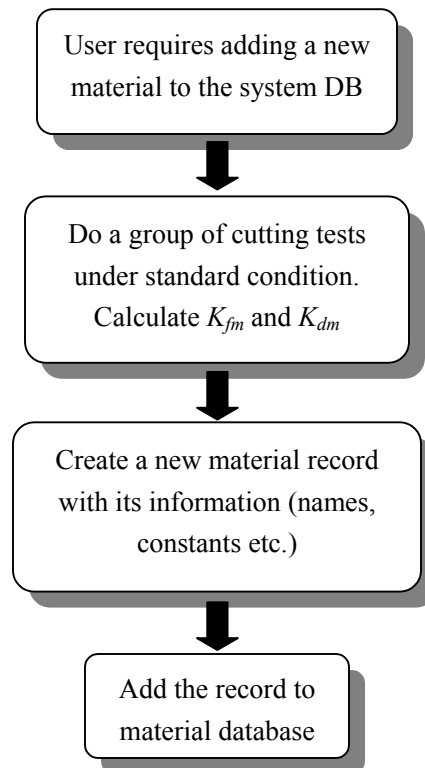
User requires adding a new material to the system DB

Do a group of cutting tests under standard condition. Calculate K_{fm} and K_{dm}

Create a new material record with its information (names, constants etc.)

Add the record to material database

Figure 6-4 Adding a New Cutting Tools to the System

6.6 Web-Based Client-server Programming Technology

The traditional expert systems are single-computer based application, so they are not accessible through the Internet/Intranet. Furthermore, most window-system based systems need manual installation. The system presented here is a web-based client-server application that is programmed by HTML and Java language. That is to say, the system has been accessible through any computer that is connected to the Internet and is issued

any required permission. The system can deal with multiple users at the same time, and no installation is needed. A common web-browser — IE or Netscape, version 3.0 or higher — is all the system needs on the client side.

6.6.1. Client-Server Technology

Security is a big problem in using the Internet. To ensure the security of the system and the valued databases, client-server technology is applied. The main part of the system and the databases is placed on the server side, and the client side is responsible for getting user input and displaying the results returned from the system.

The server side is programmed by Java language with Java Servlet technology. Therefore the server side application is a Java Servlet. Once registered with the Web-server, the Servlet will stay in the memory of the server, waiting for requests from users. Once a request is received from the client side (submitted by the web-browser), the Servlet will be noted by the Web-server and start to deal with the request. If the request needs the Servlet to deal with the databases, the Servlet will connect with the databases and retrieve data from them. After finishing all processes, the Servlet will create a web page with the results and send it back to the client side (the web-browser). For example, if a user selected an insert, a work-piece material, and input other parameters, and then clicked the "Predict Chip-breaking" button, a request with all the user input will be sent to the system on the server (the Servlet). The Servlet will first search the selected insert and material from the databases, and then retrieve equations, constants, matrices, pictures, etc., to calculate the chip-breaking limits and figure out the chip-breaking chart. After all

these steps are done, the Servlet will create a web page, which displays the predictive overall chip-breaking chart with other information, and send that back to the user's browser. The user can then see the results. Since the Servlet is able to deal with multiple users at the same time, users do not interfere with each other.

The client side is a computer that can access the server through the Internet or the company's Intranet and has a web-browser. First, the client side will display a user input interface in the browser to get the user input. Then it will submit the user input to the server. The Web-server running on the server side will get the request and transfer to the chip-breaking predictive system (the Servlet). The Servlet will deal with the request and send results back in the form of an HTML file; then the browser on the client side will display the file.

The Web-server on the server side is the bridge between the user and the system. It gets requests from users and passes them to the system; after system finishes its work, the Web-server gets the results and passes to the user.

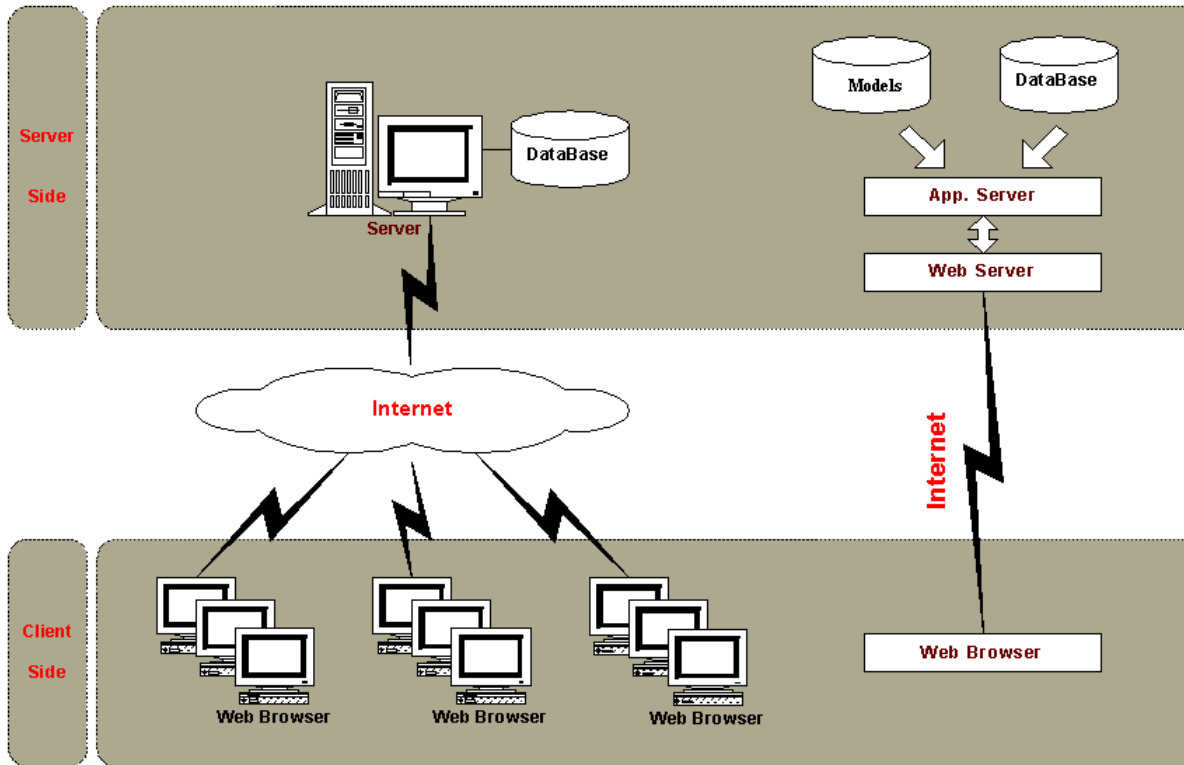Figure 6-5 shows the system structure in programming view.

Figure 6-5 Web-System Infrastructure

6.7 Introduction of the User Interface

Figure 6-6 shows the user interface. It includes two part. The left frame displays input and the right frame displays output part. The user should input parameters first and then press the button "Predict Chip-breaking", then the output will be shown in the right frame at once.
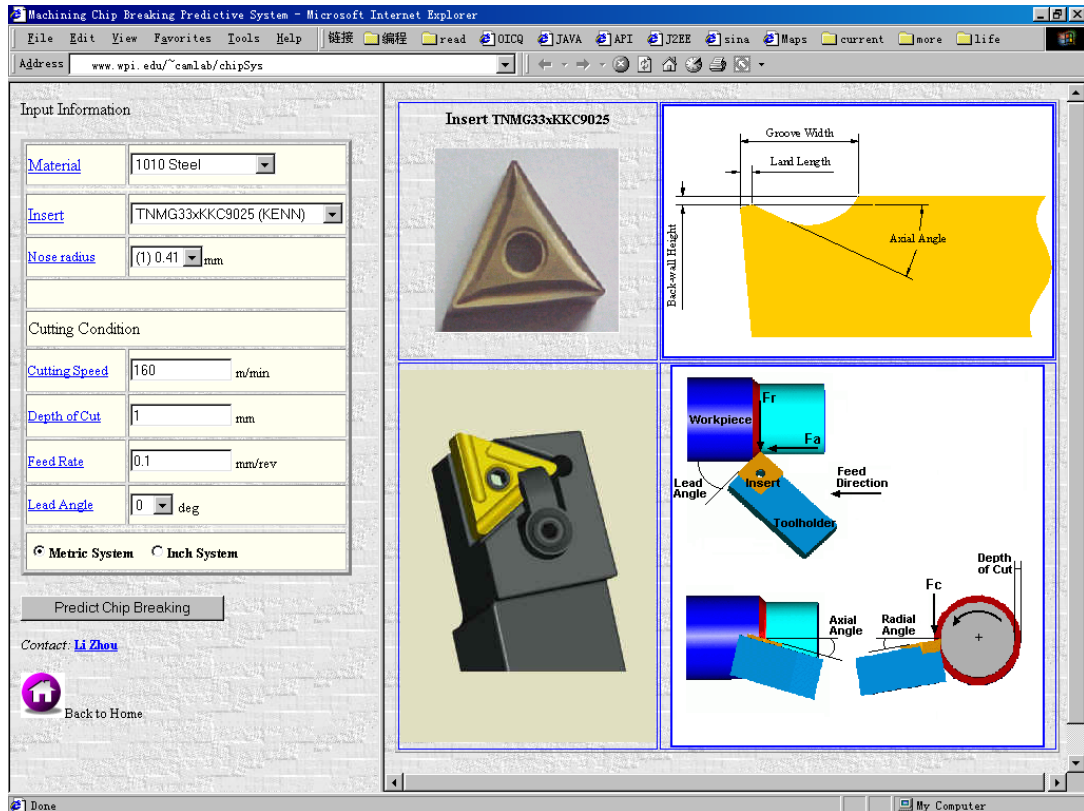
Figure 6-6 User Interface of the System

6.7.1. System Input

The left frame of the system is for user input. The user inputs machining conditions here first: the workpiece material, the insert used in the machining, the insert nose radius, cutting speed, feed rate, depth of cut, and lead angle. The user can also select from the Inch or Metric measurement option.

There is a pull-down list for material selection, which is shown below. It contains all workpiece materials in the database.
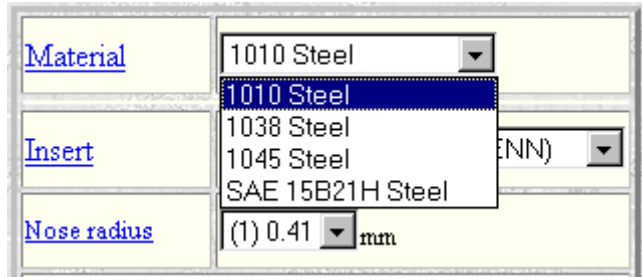
Figure 6-7 Work-Piece Material Menu

The insert selection list is similar to workpiece selection list, which is shown in
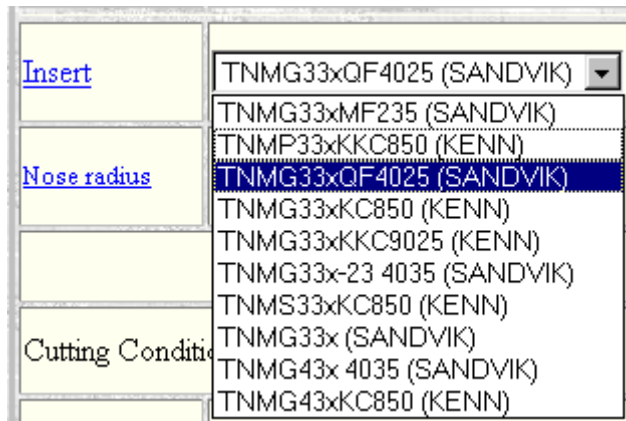
Figure 6-8.

Figure 6-8 Insert Menu

To specify the insert nose radius, the user needs to select a nose radius from the

list shown in Figure 6-9. The numbers (1), (2), … (6) stand for industry-standard levels

of insert nose radius.
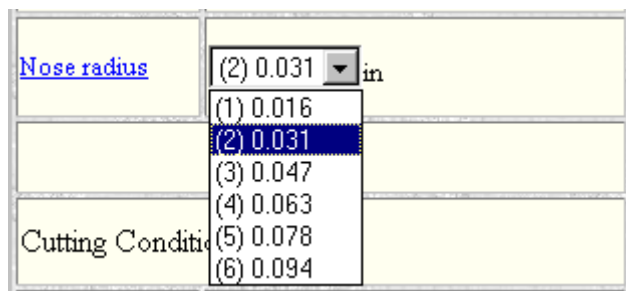
Figure 6-9 Nose Radius Menu

To specify cutting conditions, the user needs to type in values of cutting speed, feed rate, depth of cut, and select cutting edge angle from the list values. The cutting condition input interface is shown in Figure 6-10.

Figure 6-10 Cutting Condition Input

There will be a warning message shown in the screen if the user types in a value that is too large or too small, as shown below (Figure 6-11). The values will be reset to default values after the user press OK.

Figure 6-11 Warning Message When Input Is Not in Range

The user can select output unit measurement in metric or inches by choosing one of two radio buttons shown in Figure 6-12. The default system is the metric system. The relevant interface/output will then be updated immediately.

Figure 6-12 Unit Selection

The user can get online help from clicking on those items that have an underline (a hyperlink). Figure 6-13 is an example: when the user clicks the "Lead Angle" item, the definition of lead angle will be shown on the screen.

Figure 6-13 Help Information for User Input

6.7.2. System Output

After successfully inputting all parameters, the user can click the "Predict Chip-breaking" button to predict chip breakability. The user will get the overall chip-breaking chart on the right frame of the system.

The right frame of the interface will first show the picture of the currently selected insert and the insert geometry diagram. When the user changes the insert, the page will be updated at once. The user can also click the geometric feature names shown on the screen to get detailed descriptions (Figure 6-14).
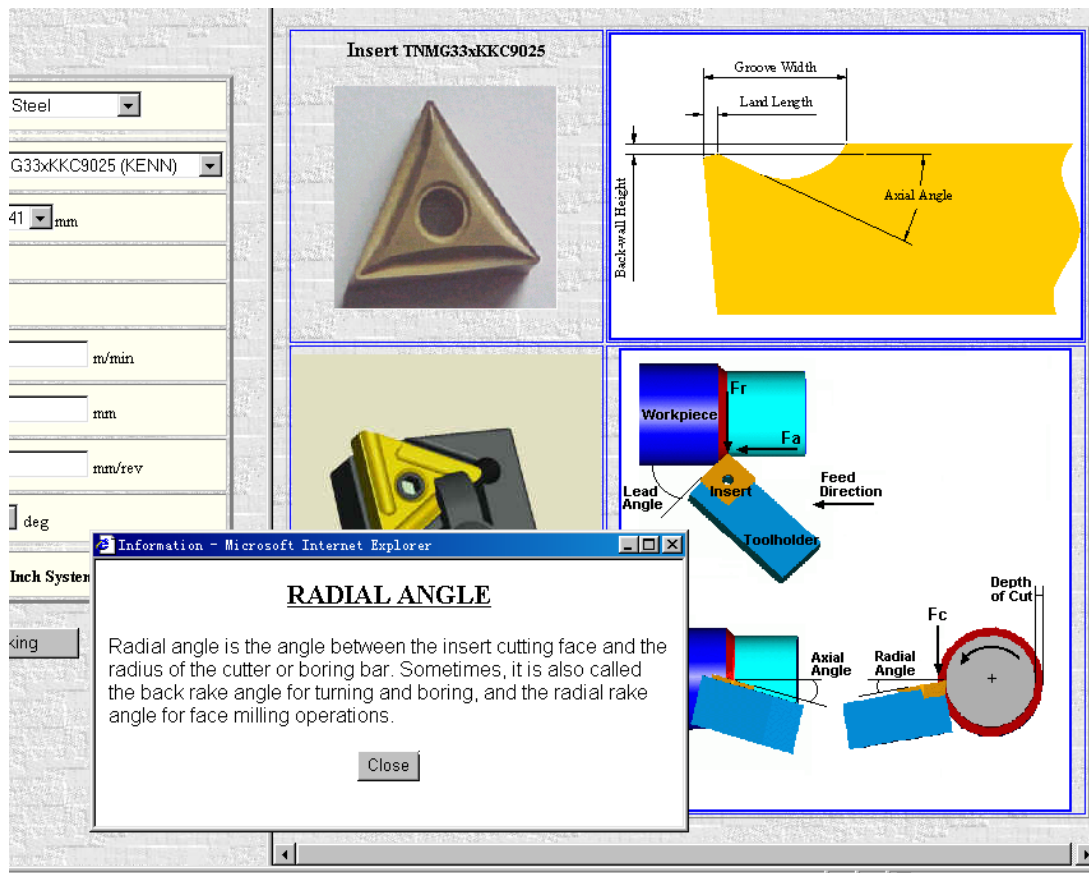

Figure 6-14 Insert Geometry Diagram Shown in the System

After the user clicks the "Predict Chip-breaking" button, the overall

chip-breaking chart and the critical depth of cut and the critical feed rate will be shown in the right frame. The overall chip-breaking chart tells user the chip-breaking region. The user can then use the chart as a guide to select applicable cutting conditions for chip-breaking.

As shown Figure 6-15, the chip shapes will appear the overall chip-breaking chart. The chip classification is based on chip length and chip shapes. The chips will be classified to six types — two unbroken chip types, which have breakability rank number of 5 and 6 respectively; four broken chip types, which rank as 1 to 4 respectively. Through clicking the "Help" button on the output screen, or clicking any of the chip pictures on the screen, the use can get a definition of a related chip type and an enlarged picture in a new window.

6.8 Summary

A web-based chip-breaking predictive system has been developed in this part. Based on the semi-empirical chip-breaking predictive models presented in this dissertation, the system developed here can be used to predicted chip-breaking and to guide cutting tool design and cutting condition design. The system can be accessed through the Internet, and is easy to maintain and expand.
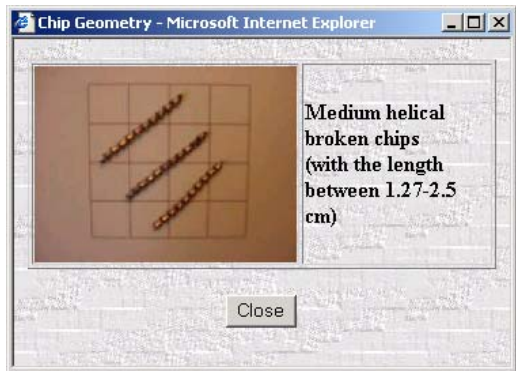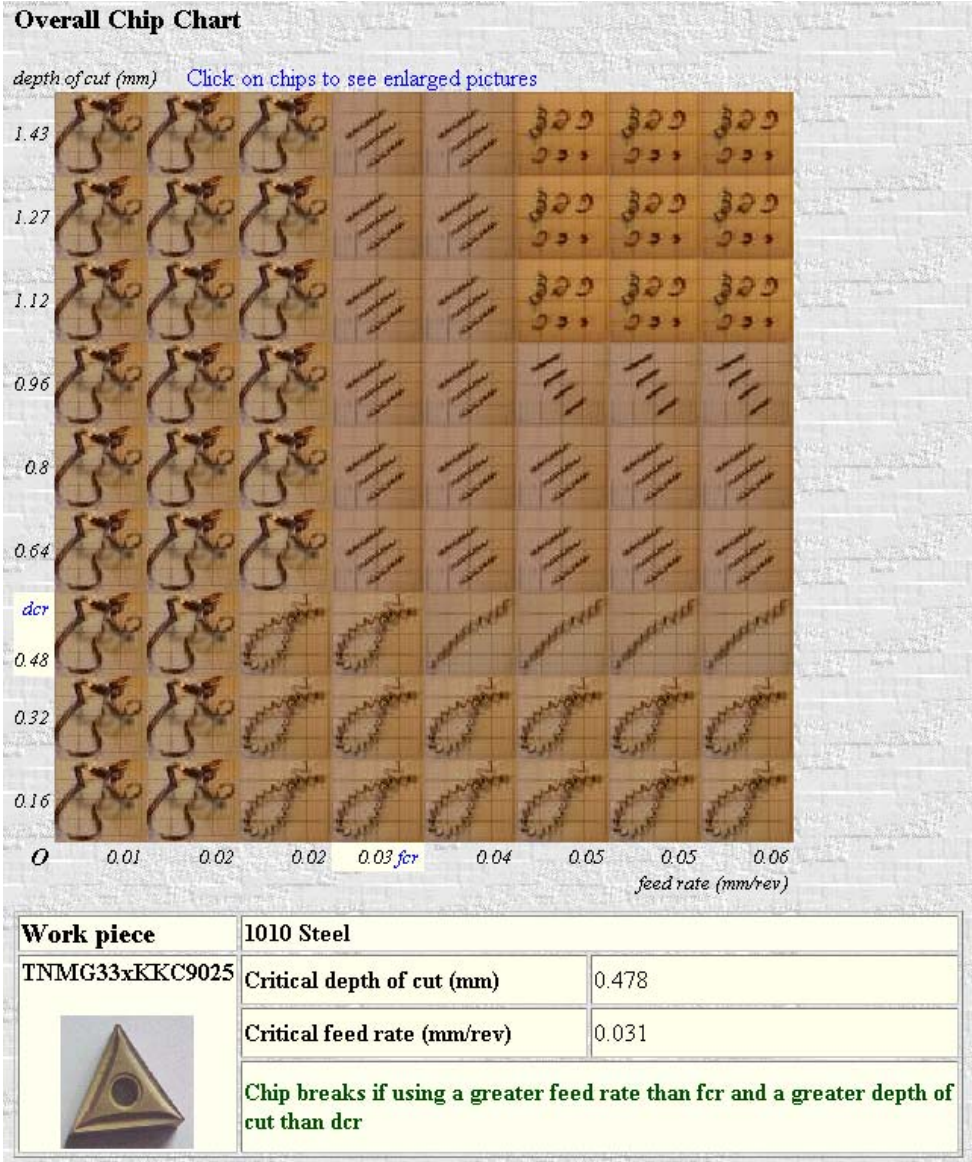
Figure 6-15 Screen Shot of the System Output and Help Window

7 Conclusions And Future Work

7.1 Summary of this Research

Quality, productivity, cost, and environment are four main concerns in manufacturing. Chip control is very important in optimizing the manufacturing process. To achieve the chip control goals in industry, chip-breaking predictive tool is crucial. The semi-empirical approach could be a powerful way to reach that goal. It bridges the existing gap between theoretical work on chip-breaking prediction and industry requirements. The chip-breaking limits theory is the basis of the semi-empirical approach. Once the predictive model of the chip-breaking limits is set up, chip-breaking can be predicted. In this research semi-empirical chip-breaking models are developed for two-dimensional grooved inserts and three-dimensional grooved inserts. The models are integrated into the web-based chip-breaking predictive system for online use in industry. The main contribution in this research includes:

1. The development of an extended semi-empirical chip-breaking predictive model for two-dimensional grooved inserts, which contains theoretical equations of chip-breaking limits and empirical equations of the modification coefficient for the cutting tool rake angle, land length, land rake angle, and backwall height.

2. The development of a feature-based semi-empirical chip-breaking predictive

model for three-dimensional grooved inserts. Empirical equations are developed, which describes the chip-breaking limits as functions of the cutting-tool feature parameters. The semi-empirical chip-breaking predictive model is then developed for three-dimensional grooved inserts. The empirical model approach is also applied for developing a chip-breaking predictive model for three-dimensional grooved inserts, which use empirical constants as the tool coefficients for each different tool type.

3. The final outcome of this research is an integrated web-based chip-breaking predictive system, which contains an extended chip-breaking predictive model for two-dimensional grooved inserts and a chip-breaking predictive model for three-dimensional grooved inserts. The system developed here is specially directed to model a grooved cutting tool for oblique cutting. The system provides a powerful online predictive tool for chip-breaking prediction and cutting-tool / cutting-condition design or selection.

The final web-based machining chip-breaking predictive system has been launched and is running on Ford Powertrain.

7.2 Future Work

The inserts can be classified into four categories: inserts with a two-dimensional chip-breaking groove, inserts with a three-dimensional chip-breaking groove, inserts with a block-type chip breaker, and inserts with complicated geometric modifications. The semi-empirical chip-breaking predictive models developed in this research cover inserts with two-dimensional chip-breaking groove and three-dimensional chip-breaking groove.

In the future research may be conducted to develop chip-breaking predictive models for the other two categories of inserts.

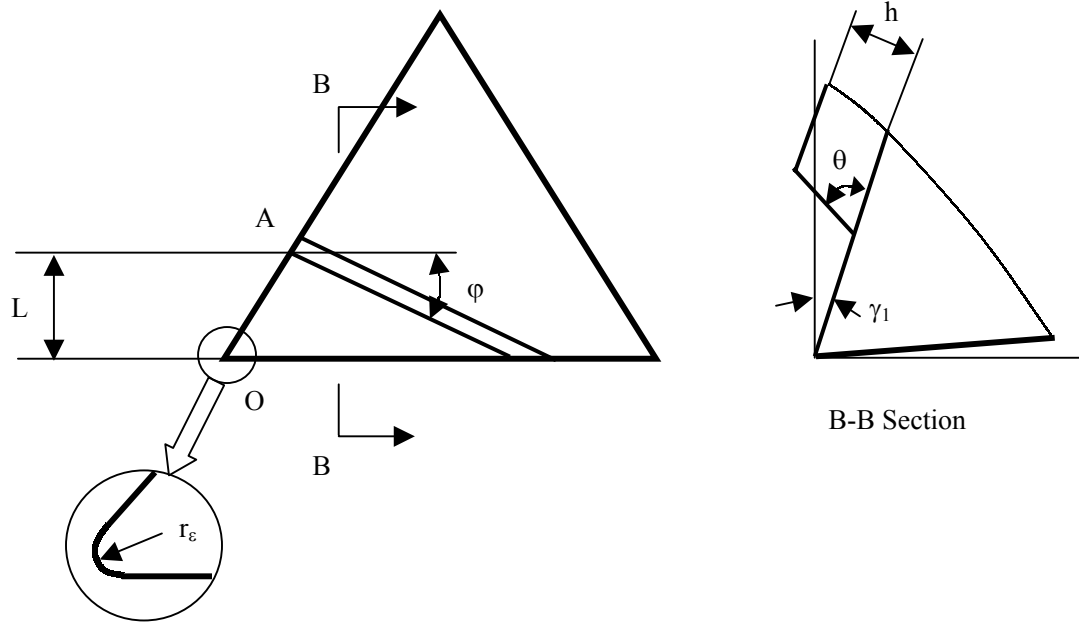## 7.2.1. Inserts with Block-type Chip Breaker

Inserts with block-type chip breaker, especially CBD inserts, are widely applied in soft-metal (e.g. copper, aluminum) cutting in industry. For the inserts with a block type chip breaker, the process of developing a semi-empirical chip-breaking predictive model could be similar to the process for modeling three-dimensional grooved inserts. The first step is definition and measurement of insert / breaker geometric features. The second step is carrying out cutting tests, followed by modeling work and model validation. Figure 7-1 shows the geometric features of inserts with a block-type chip breaker.

The semi-empirical chip-breaking predictive model for inserts shown in Figure 7-1 could still be in the form of Equation 7-1:

$$\begin{cases} f_{cr} = f_0 K_{fT} K_{fv} K_{fm} \\ d_{cr} = d_0 K_{dT} K_{dv} K_{dm} \end{cases} \tag{7-1}$$

To determine the K_{fT} and K_{dT} four geometry parameters (φ, L, h, θ) need to be taken into account. Equation 7-2 will be got as the chip-breaking model for all block-type chip breaker based on the experimental results.

$$\begin{aligned} K_{fT} &= F_f(L, \varphi, \theta, h) \\ K_{dT} &= F_d(L, \varphi, \theta, h) \end{aligned} \tag{7-2}$$

Geometric features

B-B Section
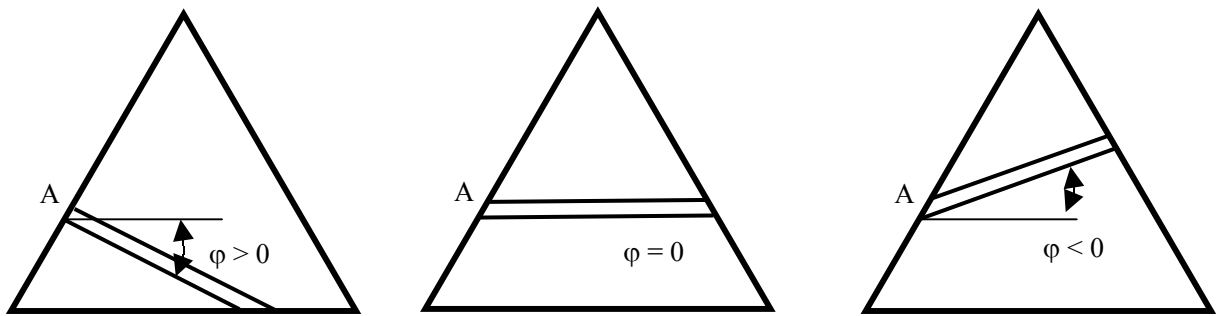
Sign conversion of the angle φ

Figure 7-1 Illustration of the Geometry of the Block-Type Chip Breaker

The development of the above equations could be similar to that for three-dimensional grooved inserts. This process is illustrated in the form of the flow chart shown in Figure 7-2.

```
┌─────────────────────────────┐          ┌┄┄┄┄┄┄┄┄┄┄┄┄┄┄┄┄┄┄┄┄┐
│ Define 3 levels of values for each │ ◄──────  ┊ Purpose:          ┊
│ chip breaker geometry parameters │          ┊ Design of experiments ┊
└─────────────────────────────┘          └┄┄┄┄┄┄┄┄┄┄┄┄┄┄┄┄┄┄┄┄┘
              │
              ▼
┌─────────────────────────────┐          ┌┄┄┄┄┄┄┄┄┄┄┄┄┄┄┄┄┄┄┄┄┐
│ Do cutting tests with chip breakers │ ◄──────  ┊ Purpose:          ┊
│ with different geometry parameters │          ┊ Get experimental data ┊
└─────────────────────────────┘          └┄┄┄┄┄┄┄┄┄┄┄┄┄┄┄┄┄┄┄┄┘
              │
              ▼
┌─────────────────────────────┐          ┌┄┄┄┄┄┄┄┄┄┄┄┄┄┄┄┄┄┄┄┄┐
│                             │          ┊ Purpose:          ┊
│ Establish models of $K_{fT}$ and $K_{dT}$ │ ◄──────  ┊ Establish semi-empirical ┊
│                             │          ┊ model for the insert   ┊
└─────────────────────────────┘          ┊ geometry parameters   ┊
              │                           └┄┄┄┄┄┄┄┄┄┄┄┄┄┄┄┄┄┄┄┄┘
              ▼
┌─────────────────────────────┐          ┌┄┄┄┄┄┄┄┄┄┄┄┄┄┄┄┄┄┄┄┄┐
│ Final Goal: Integrate the   │          ┊ User will be able to predict ┊
│ established model to the     │ ◄──────  ┊ chip-breaking with the    ┊
│ chip-breaking predictive system │          ┊ system for chip breakers   ┊
│                             │          ┊ with any geometry       ┊
└─────────────────────────────┘          ┊ parameters under any     ┊
                                         ┊ cutting conditions      ┊
                                         └┄┄┄┄┄┄┄┄┄┄┄┄┄┄┄┄┄┄┄┄┘
```
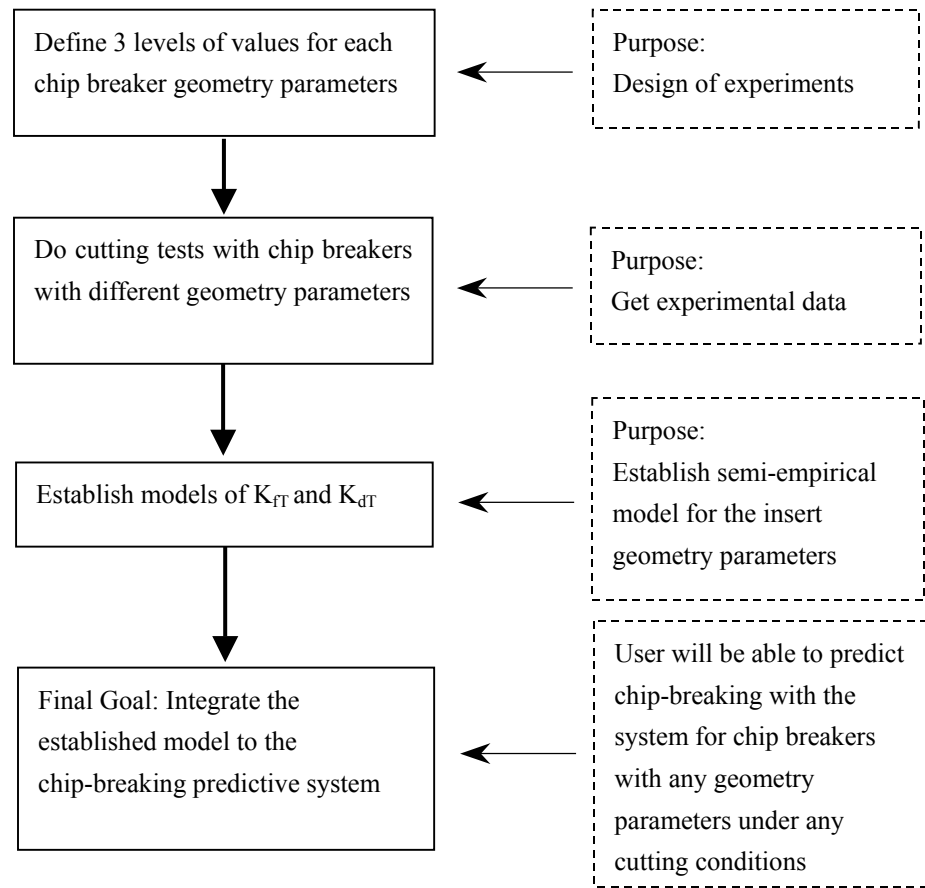
Figure 7-2 Modeling Process for Inserts with Block-Type Chip Breaker

Difficulty is expected when performing soft-metal cutting tests with inserts that have a block-type chip breaker. To get acceptable surface finish, the feed rate and the depth of cut need to be small. But the chip of the soft-metal is very hard to break under small feed rate and depth of cut. Therefore it is difficult to get chip-breaking limits from the cutting tests. Once this difficulty is overcome, it should be easy to develop the chip-breaking predictive model for inserts with a block-type chip breaker. Figure 7-3 shows a sample chip-breaking chart of copper cutting with insert of a block-type chip breaker. It is shown there is no chip-breaking limits in the cutting range (that is, no

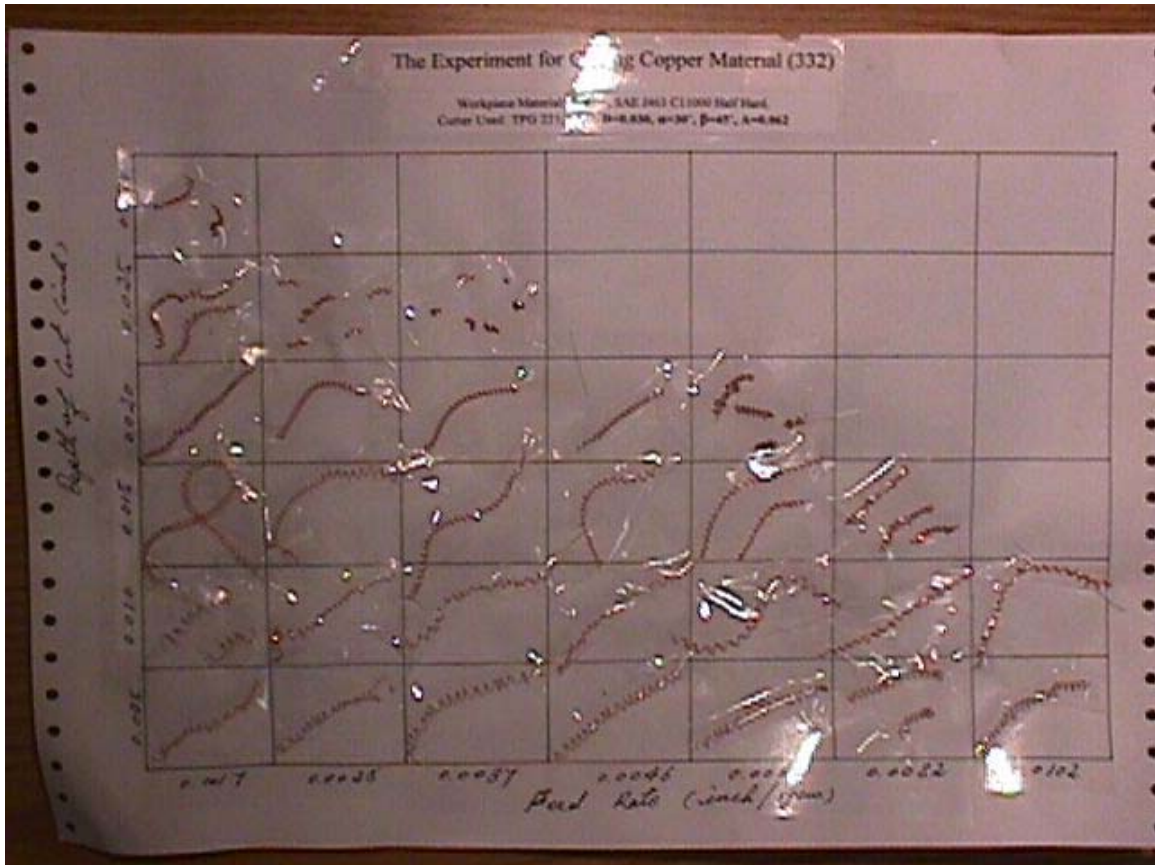broken chip if the user wants to keep a good surface finish).

Figure 7-3 A Sample Chip-Breaking Chart of Copper Cutting with Inserts having Block-Type Chip-Breaker

7.2.2. Inserts with Complicated Geometric Modifications

For inserts with complicated geometric modifications, the biggest problem is that there are no general chip-breaking limits at all. Therefore, the modeling process would be very different from approaches applied in this research. One possible approach is to separate the basic elements of the complicated three-dimensional chip-breaking groove, investigate each element's influence on chip-breaking, and then integrate the results into a general model. The elements may include pimples, dimples, and waviness, etc. Some work in this field has been done (Li, Z. 1995). Due the complexity of this kind of insert,

there is still a long way to go before we reach an applicable chip-breaking predictive model for complicated three-dimensional grooved inserts. Figure 7-4 shows a sample chip-breaking chart with inserts having complicated geometric modifications. The insert picture is also shown here.
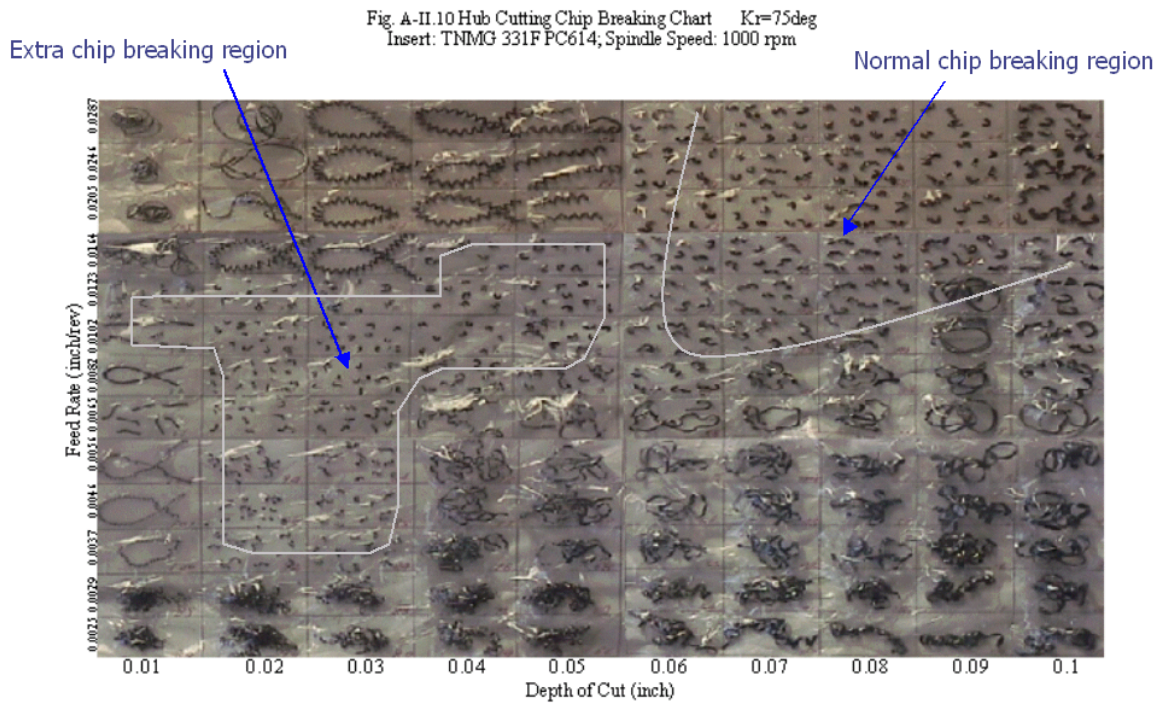

Insert: TNMG331F PC614

Figure 7-4 A Sample Chip-Breaking Chart with Inserts with Complicated Geometric Modifications

Bibliography

Brown 1983
C. A. Brown. "Material Behaviour During Chip Formation", Diss. Abstr. Int. 44(4), University of Vermont, October 1983, p.186.

Chen 1993
Y. Chen and H. Shi, "Curling and Flowing of 3D Chips", *Journal of Huazhong University of Science and Technology,* Vol.21, No.4, 1993, pp.1-6.

Cowell 1954
L. V. Cowell, "Predicting the Angle of Chip Flow for Single Point Cutting Tools", *Transactions of ASME,* Vol.76. No.2, 1954, pp.199-202.

Dewhurst 1979
P. Dewhurst. "The Effect of Chip Breaker Constraints on the Mechanics of the Machining Process", *Annals of the CIRP,* 1979, 28 (1), pp.1-5.

Fang, N. 1994
N. Fang. "The Study of New-type Chip-breaking Groove Geometry of Indexable Cemented Carbide Inserts and Related CAD Technology", PhD thesis, Huazhong University of Science and Technology, Wuhan, People's Republic of China, 1994.

Fang, N. 1997
N. Fang, M. Wang, and C. Nedess. "Development of the New-type Indexable Inserts with Helical Rake Faces." *Proc. Instn Mech. Engrs*, *Part B, Journal of Engineering Manufacture*, 1997, 211(Bl), pp.159—164.

Fang, N. 2000
N. Fang. "An Auxiliary Approach to the Experimental Study on Chip Control: a Kinematically Simulated Test", *Proc Inst. Mech Engrs*, 2000, Vol 212, pp.159-166

Fang, N. 2001
N. Fang. "Kinematic Characterization of Chip Lateral-Curl - The Third Pattern of Chip Curl in Machining. ASME Journal of Manufacturing Science and Technology, In press.

Fang, N. 2001
N. Fang, I. S. Jawahir, P. L. B. Oxley. "A Universal Slip-line Model with Non-unique Solutions for Machining with Curled Chip Formation and a Restricted Contact Tool", *International Journal of Mechanical Sciences*, 43, 2001, pp.570-580

Fang, X. 1990-a
X. D. Fang and I. S. Jawahir. "An Expert System Based on A Fuzzy Mathematical Model for Chip Breakability Assessments in Automated Machining", *ASME Proc. Int. Conf. MI'90,* Atlanta, Georgia, USA, Vol.4, March 1990, pp.31-37.

Fang, X. 1990-b
X. D. Fang and Y. Yao. "Expert System-Supported On-line Tool Wear Monitoring", *Proc. of International Conference on Artificial Intelligence in Engineering - AIE'90,* Sponsored by I.E.E. (UK), August 21-22, 1990, Kuala Lumpur, Malaysia, pp.77-84.

Fang, X. 1991
X. D. Fang and I. S. Jawahir, "On Predicting Chip Breakability in Machining of Steels with Carbide Tool Inserts Having Complex Chip Groove Geometries", *Journal of Materials Processing Technology (USA),* Vol.28(2), 1991, pp.37-48.

Fang, X. 1993
X. D. Fang and I. S. Jawahir, "The Effects of Progressive Tool-wear and Tool Restricted Contact on Chip Breakability in Machining", *Wear,* Vol.160, 1993, pp.243-252.

Fang, X. 1994-a
X. D. Fang and I. S. Jawahir, "Predicting Total Machining Performance in Finish Turning Using Integrated Fuzzy-Set Models of the Machinability Parameters", *International Journal of Production Research,* Vol.32(4), 1994, pp.833-849.

Fang, X. 1994-b
X. D. Fang, "Experimental Investigation of Overall Machining Performance with Overall Progressive Tool Wear at Different Tool Faces", *Wear,* Vol.173, 1994, pp.171-178.

Jawahir 1988-a
I. S. Jawahir and P. L. B. Oxley. "New Developments in Chip Control Research: Moving Towards Chip Breakability Predictions for Unmanned Manufacture", *Proc. Int Conf ASME,* MI'88, Atlanta, Georgia, USA, April 1988, pp.311-320.

Jawahir 1988-b
I. S. Jawahir and P.L.B. Oxley, "Efficient Chip Control at Reduced Power Consumption: An Experimental Analysis", *Proceedings of the 4th International Conference on Manufacturing Engineering,* Brisbane, Australia, May 1988.

Jawahir 1988-c
I. S. Jawahir, "A Survey and Future Predictions for the Use of Chip-breaking in Unmanned Systems", *International Journal of Advanced Manufacturing Technology*, 1988, 3(4), pp.87-104.

Jawahir 1988-d
I. S. Jawahir, "The Chip Control Factor in Machinability Assessments: Recent Trends", *Journal of Mechanical Working Technology,* Vol.17, 1988, pp.213-224.

Jawahir 1988-e
I. S. Jawahir, "The Tool Restricted Contact Effect as a Major Influencing Factor in Chip-breaking", *Annals of the CIRP,* Vol.37, 1988, pp.121-126.

Jawahir 1989
I. S. Jawahir and X D. Fang. "A Knowledge-based Approach for Improved Performance with Grooved Chip Breakers in Metal Machining", *Proc. 3rd International Conference on Advances in Manufacturing Technology,* Organized by *IProdE,* Singapore, August 14-16, 1989, pp.130-144.

Jawahir 1990-a
I. S. Jawahir and X. D. Fang. "Some Guidelines on the Use of a Predictive Expert System for Chip Control in Automated Process Planning", *Proc. Fifth International Conference on Manufacturing Engineering,* Vol.1, Wollongong, Australia, July 11-13, 1990, pp.288-292.

Jawahir 1990-b
I. S. Jawahir, "On the Controllability of Chip-breaking Cycles and Modes of Chip-breaking in Metal Machining", *Annals of the CIRP,* Vol.39, 1990, pp.47-51.

Jawahir 1991
I. S. Jawahir, "An Investigation of Three-dimensional Chip Flow in Machining of Steels with Grooved Chip Forming Tool Insert", *Transactions of NAMRC*, 1991*,* 19, pp.222-231.

Jawahir 1993-a
I. S. Jawahir and C. A. van Luttervelt, "Recent Developments in Chip Control Research and Applications", *Annals of the CIRP,* 42(2)*,* 1993, pp.659-685.

Jawahir 1993-b
I. S. Jawahir, "Chip Control Literature Database", Technical Report, *Annals of the CIRP,* 42(2), 1993, pp.686-693.

Jiang 1984
C. Y. Jiang, Y. Z. Zhang and Z. J. Chi, "Experimental Research of the Chip Flow Direction and its Application to the Chip Control", *Annals of the CIRP,* Vol.33, 1984, pp.81-84.

Johnson 1970
W. Johnson, R. Sowerby and J. B. Haddow, *Plane - Strain Slip-line Fields: Theory and Bibliography.* Edward Arnold (Publishers) Ltd., London, 1970.

Kiamecki 1973
B. E. Kiamecki, "Incipient Chip Formation in Metal Cutting - A Three Dimension Finite Element Analysis", Ph.D. Dissertation, University of Illinois at Urbana-Champaign, 1973.

Kluft 1979
W. Kluft, W. Konig, C.A. van Luttervelt, K. Nakayama and A.J. Pekeiharing, "Present knowledge of chip control", *Annals of the CIRP,* Keynote Paper, 28(2), 1979, pp.441-455.

Klushin 1960

M. I. Klushin. "Determination of the Contact Zone between Chip and Rake Face and the Pressure in this Zone", *Stanki i Instrument* 31, 1960, pp.22-23.

Lajczok 1980

M. R. Lajczok, "A study of Some Aspects of Metal Machining Using Finite Element Method", Ph.D. Dissertation, N.C. State University, 1980.

Lee 1951

E. H. Lee and B.W. Shaffer, "The Theory of Plasticity Applied to a Problem of Machining", *Journal of Applied Mechanics,* Vol.73, 1951, pp.405.

Li, Z. 1990

Z. Li, *Machining Chip-breaking Mechanism with Applications,* Dalian University press, Dalian, China, 1990 (in Chinese).

Li, Z. 1995

Z. Li and Y. Rong, "Analysis on Formation and Breaking of C-type Side-curling chips", *Computer-aided Tooling,* ASME IMECE, San Francisco, CA, Nov. 12-I 7, 1995, MED-Vol. 2-1, pp.715-722.

Li, Z. 1996

Z. Li, *Machining Chip-breaking Process Analysis,* Mechanical Industry Press, Beijing, China, 1996 (in Chinese).

Li, Z. 1997

Z. Li andY. Rong, "Study on Formation and Breaking of Side-curl Screw Chips", ASME IMECE, Dallas, TX, Nov. 16-21, 1997.

Li, Z. 1999

Z. Li andY. Rong, "A Study on Chip-breaking Limits in Machining", *Machining Science and Technology,* 3(1), 1999, pp.25-48

Lo 1966

Y. Lo, U. Lode and E. J. A. Armarego. "Experiments with Controlled Contact Tools", *Int, J. MTDR 6,* 1966, pp.115-127

Lutov 1962

V. M. Lutov. "Selecting the Optimum Size of Chip-breaking Grooves", *Machines and Tooling* 33 (7),1962, pp.27-30.

Merchant 1944

M. E. Merchant. "Basic Mechanics of the Metal Cutting Process", *Journal of Applied Mechanics,* Vol.11, 1944, p. A-168.

Merchant 1945

M. E. Merchant. "Mechanics of the Metal Cutting Process", *Journal of Applied* Physics, Vol.16, No.5, 1945, p.267.

Nakamura 1982
S. Nakamura, G. I. Wuebbling and J. D. Christopher. "Chip Control in Turning", *Proc. Int. Tool and Manuf Eng. Conf* , SME. USA, May 1982, pp.159-177.

Nakayama 1958
K. Nakayama, "Studies of the Mechanism in Metal Cutting", *Bulletin of Faculty of Engineering,* Yokohama National University, Vol.7, 1958, p.1.

Nakayama 1962-a
K. Nakayama, "A Study on Chip-breaker", *Bulletin of Japanese Society of Mechanical Engineers,* Vol.5, No.17, 1962, pp.142-150.

Nakayama 1962-b
K. Nakayama. "Chip Curl in Metal Cutting Process", *Bulletin of the Faculty of Engineering; Yokohanta National Univ.,* 1962, 11, pp.1-13.

Nakayama 1963
K. Nakayama. "Pure Bending Test of Chip - An Approach to the Prediction of Cutting Force", *Bulletin of the Faculty of Engineering. Yokohama National Univ.,* 1963, 12, pp.l-14.

Nakayama 1972-a
K. Nakayama, "Origins of Side-curl in Metal Cutting", *Bulletin of Japanese Society of Precision Engineer)zg,* Vol.6, No.3, 1972, pp.99-101.

Nakayama 1972-b
K. Nakayama. "Origins of Side-curl of Chip in Metal Cutting", *Bull. Japan Soc. Of Prec. Engg.,* 1972, 6(3), pp.99-101.

Nakayama 1977
K. Nakayama and M. Arai. "Roles of Brittleness of Work Material in Metal Cutting", *Proc. Int. Symposium on Influence of Metallurgy on Machinability" of Steel.,* Sept. 1977, Tokyo. Japan. pp.421-432.

Nakayama 1978
K. Nakayama and M. Ogawa. "Basic Rules on the Form of Chip in Metal Cutting", *Annals of the CIRP*, 27(1), 1978, pp.17-21.

Nakayama 1979
K. Nakayama, "Basic Rules on The Form of Chip in Metal Cutting", *Annals of CIRP,* Vol.28, 1979, p.17.

Nakayama 1981
K. Nakayama, "Cutting Tool with Curved Rake Face - A Means for Breaking Thin Chips", *Annals of CIRP,* Vol.30, 1981, pp.5-8.

Nakayama 1984
K. Nakayama, "Chip Control in Metal Cutting", *Bulletin of Japanese Society of Precision Engineering,* Vol.18, No.2, 1984, pp.97-103.

Nakayama 1986
K. Nakayama, Z. Li, and M. Arai, "Performance of the Chip breaker of Cutting Tool (1st report): Range of Cutting Conditions for Chip-breaking", *Journal of JAPE,* Vol.52, No.12, 1986, pp.126-131.

Nakayama 1990
K. Nakayama and M. Arai, "The Breakability of Chip in Metal Cutting", *Proc. Int. Conf. On Manufacturing Engineering,* Melbourne, Australia, 1990, pp.6-10.

Okoshi 1967
M. Okoshi and K. Kawata. "Effects of the Curvature on Work Surface on Metal Cutting", *Annals of the CIRP 15,* 1967, pp.393-403

Okushima 1959
K. Okushima, and K. Minato, "On the Behaviors of Chips in Steel Cutting", *Bulletin JSME, 2(5),* 1959

Okushima 1960
K. Okushima, T. Hoshi, and T. Fujinawa, "On the Behaviors of Chips in Steel Cutting", *Bulletin JSME, 3(10),* May, 1960

Oxley 1962
P. L. B. Oxley. "An Analysis for Orthogonal Cutting with Restricted Tool-Chip Contact", *Int. J. Mech. Sci.,* 1962, 4, pp.129-135.

Oxley 1963-a
P. L. B. Oxley and M.J.M. Welsh, "Calculating the Shear Angle in Orthogonal Metal Cutting from Fundamental Stress, Strain, Strain-Rate Properties of the Work Material", *Proceedings 4th International Machine Tool Design and Research Conference,* Pergamon, Oxford, 1963, pp.73-86.

Oxley 1963-b
P. L. B. Oxley, "Mechanics of Metal Cutting", Proceedings of International Production Engineering Research Conference, Pittsburgh, 1963, p.50.

Palmer 1959
W. B. Palmer, and P.L.B. Oxley, "Mechanics of Metal Cutting", *Proceedings of the Institution of Mechanical Engineers,* Vol.173, 1959, p.623.

Ramalingam 1980
S. Ramalingam and P. V. Desai. "Tool-Chip Length in Orthogonal Machining", *ASME* Paper 80, WA/Prod. 23, 1980.

Shaw 1953
M. C. Shaw, N.H. Cook, and I. Finnie, "The Shear-Angle Relationship in Metal Cutting", *Transaction ASME,* Vol.75, 1953, pp.273-283.

Shaw 1963
M. C. Shaw. "Resume and Critique of Papers in Part One", *Proc. Int. Prod. Eng. Res. Conf. ASME.* Pittsburgh, September 1963, pp.3-17.

Shaw 1984
M. C. Shaw, *Metal Cutting Principles,* Oxford Series on Advanced Manufacturing, 1984.

Shivathaya 1993
S. Shivathaya and X. D. Fang. "Hybrid Knowledge-Based Tool Room Scheduling", *Proc. Australian Conference on Manufacturing Engineering,* Adelaide, Australia, Nov., 1993, pp.215-222.

Shivathaya 1994
S. Shivathaya, X. D. Fang and J.G. Williams. "Knowledge Elicitation for Material Design Expert System", *9th International Conf. of AIENG'94 (Application of Artificial Intelligence in Engineering),* 19-21 July 1994, Philadelphia, U.S.A., pp.117-124.

Spaans 1970-a
C. Spaans and P. F. H. J. van Geel, "Breaking Mechanisms in Cutting with a Chip Breaker", *Annals of the CIRP,* Vol. 18, 1970, pp.87-92.

Spaans 1970-b
C. Spaans. "A Systematic Approach to Three Dimensional Chip Curl, Chip-breaking and Chip Control", SME Paper 7-241, 1970.

Spaans 1971-a
C. Spaans. "A Comparison of an Ultrasonic Method to Determine the Chip/Tool Contact Length with Some Other Methods", *Annals of the CIRP* 19, 1971, pp.485-490.

Spaans 1971-b
C. Spaans. "The Fundamentals of Three-Dimensional Chip Curl, Chip-breaking and Chip Control", Doctoral Thesis, TH Delft, 1971.

Stabler 1951
V. G. Stabler, "The Fundamental Geometry of Cutting Tool", *Proc. Inst. Mech. Engg.,* 165, 1951.

Stabler 1964
V. G. Stabler, "The Chip Flow Law and its Consequence", *Proc.* 5th *International Machine Tool Design and Research Conference,* Birmingham, UK, 1964, pp.243-251.

Strenkowski 1985
J. S. Strenkowski and J.T. Carroll, "A Finite Element Model of Orthogonal Metal Cutting", *Journal of Engineering for Industry,* Vol.107, 1985, p.346.

Strenkowski 1990
J. S. Strenkowski and K.J. Moon, "Finite Element Prediction of Chip Geometry and Tool/Workpiece Temperature Distribution in Orthogonal Cutting", *Journal of Engineering for Industry,* Vol.112, 1990, pp.313-318.

Tolouei 1993-a
M. Tolouei Rad and X.D. Fang. "Application of Expert Systems in Design of Deep-Drawing Dies for Circular Shells", *Proc. Production and Manufacturing Engineering Conference (PMEC),* Tehran, fran, Oct., 1993, pp.143-151.

Tolouei 1993-b
M. Tolouei Rad and X.D. Fang. "Artificial Intelligence-based Design of Deep-Drawing Pressing Dies", *Proc. Australian Conference on Manufacturing Engineering,* Adelaide, Australia, Nov., 1993, pp.267-272.

Trent 2000
E. M. Trent and P.K. Wright, *Metal Cutting, 4th Edition,* Butterworth, London, 2000.

Trim 1968
A. R. Trim and G. Boothroyd, "Action of the Obstruction-Type Chip Former", *International Journal of Production Research,* Vol.6, 1968, p.227.

Usui 1962
E. Usui and M.C. Shaw, "Free Machining Steel-IV, Tool with Reduced Contact Length", *Journal of Engineering for Industry,* Vol.84, 1962, p.89.

Usui 1963
E. Usui and K. Roshi, "Slip-line fields in metal machining which involve centered fans", *Proceedings of International Production Engineering Research* (ASME Conference), Pittsburgh, September 1963, pp.61-71.

Usui 1964
E. Usui, K. Kikuchi and R. Hoshi, "The theory of plasticity applied to machining with cut-away tools", *Transactions ASME, Journal of the Engineering Industry*, May 1964*, pp.95-104.

van Luttervelt 1976
C. A. van Luttervelt. "Chip Formation in Machining Operation at Small Diameter", *Annals of the CIRP 25(I),* 1976, pp.7l-76

van Luttervelt 1989
C. A. van Luttervelt, "Evaluation of present possibilities of chip control", *VDI Berichte* 762, 1989, pp.181-200.

von Turkovich 1967
B. F. von Turkovich, "Dislocation Theory of Shear Stress and Strain Rate in Metal Cutting", *Proc. Of the 8th Int. Machine Tool Design and Research Conf.*, Manchester, United Kingdom, 1967, pp.531-542.

von Turkovich 1972
B. F. von Turkovich and M. E. Merchant, "On a Class of Thermo-Mechanical Processes During Rapid Plastic Deformation", *Annals of the CIRP*, 1972, p.15.

von Turkovich 1981
B. F. von Turkovich, "Metallurgy – A Foundation for Understanding the Art of Machining", *Proc. Winter Annual Meeting of ASME*, Washington D. C., 1981, PED-Vol .3.

Wallace 1968
P. W. Wallace and G. Boothroyd, "Tool Forces and Tool-Chip Friction in Orthogonal Cutting", *Journal of Engineering for Industry,* Vol.90, 1968, pp.54-62.

Worthington 1979
B. Worthington and M. H. Rahman, "Prediction Breaking with Groove type Breakers", *International Journal of Machine Tool Design and Research,* Vol. 19, 1979, pp.121-132.

Wright 1977
P. K. Wright. "Applications of the Experimental Methods used to Determine Temperature Gradients in Cutting Tools", *Proc. Australian Conf. on Manuf. Engineering.,* Aug. 1977, pp.145-149.

Young 1987
H. T. Young, P. Mathew and P.L.B. Oxley, "Allowing for nose radius effects in predicting the chip flow direction and cutting forces in bar turning", *Proceedings of the Institute of Mechanical Engineers* 201(C3), 1987, pp.213-226.

Zhang 1980
Y. Z. Zhang, "Chip Curl, Chip-breaking, and Chip Control of the Difficult-to-cut Materials", *Annals of the CIRP,* Vol.29, 1980, pp.79-83.

Zhang 1993-a
Y. Zhang and X. D. Fang. "Minimizing the Number of Surplus Components in Selective Assembly via a Fuzzy-set Model", *Proc. 12th International Conf on Assembly Automation,* Adelalde, Australia, Nov.1993, pp.61-67.

Zhang 1993-b
Y. Zhang and X.D. Fang. "A New Method for Sampling Inspection by Variables under Undesired Measurement Conditions", *Proc. 2nd International Symposium on Measurement Technology and Intelligent Instrument,* Wuhan, China, Oct., 1993, pp.74-83.

Zhou 2001
L. Zhou, H. Guo and Y. Rong, "Machining Chip Breaking Prediction", *4th Inernational Machining & Grinding Conference, of SME,* SME paper 601, Troy, Michigan, May 7-10, 2001.

Appendix A.   Sample Chip-breaking Charts

of Two-Dimensional Grooved Inserts

The following part shows the sample chip-breaking charts of the extended study on chip-breaking limits of two-dimensional grooved inserts. The workpiece material used in the tests is 1045 steel. The surface feeding speed V_C = 100 m/min. The geometric parameters of the insert 1 to insert 18 used in the experiments are listed in Table 4-1.
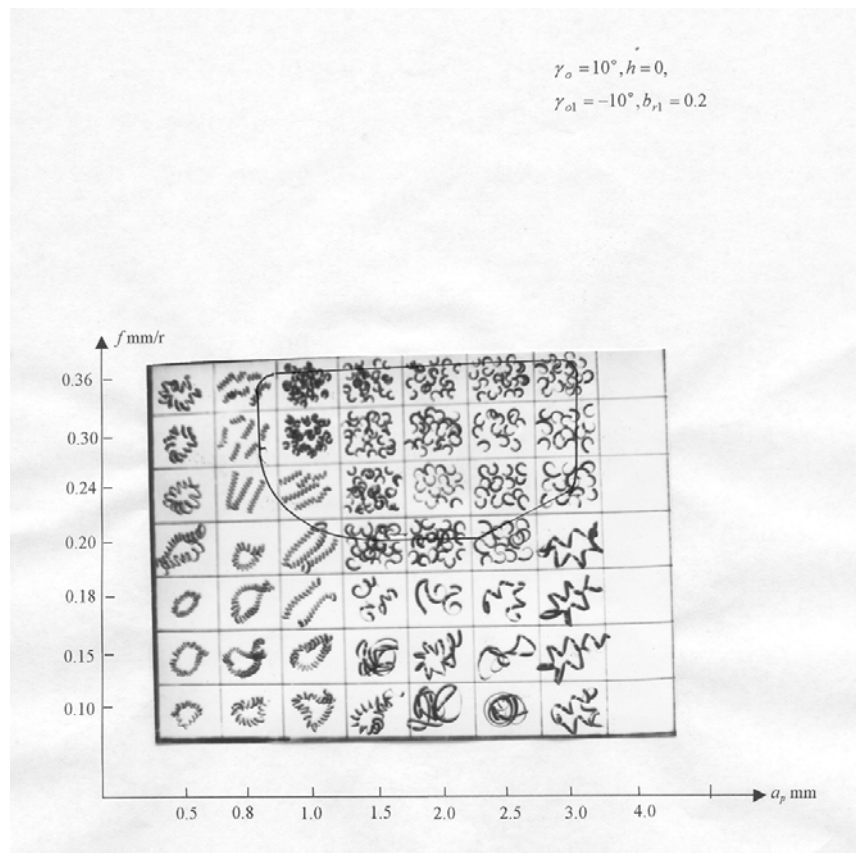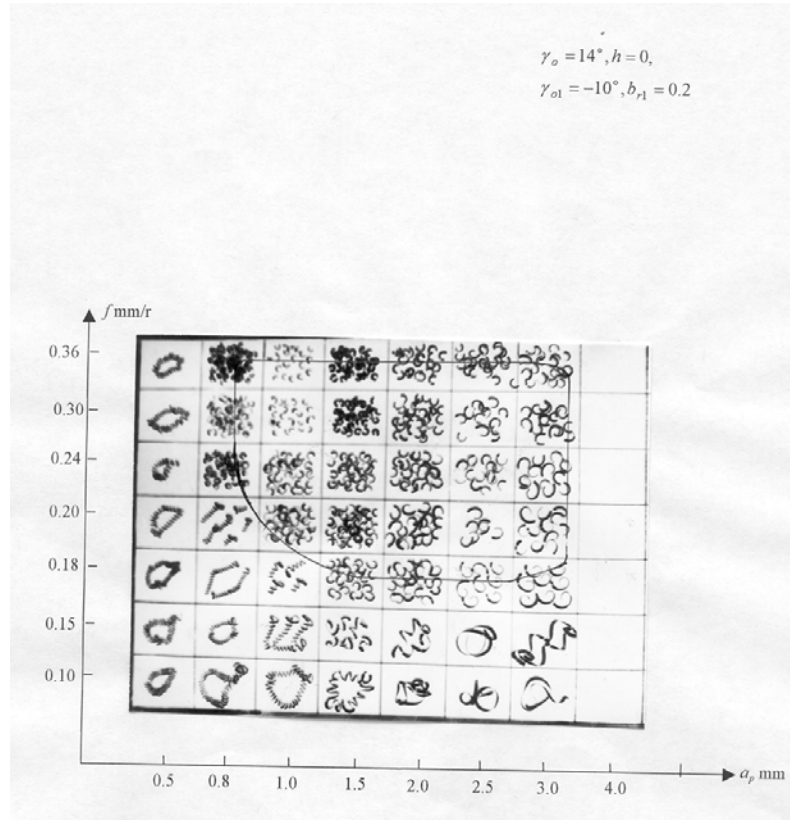

Figure A-1 The Chip-Breaking Chart Got from Insert 1

Figure A-2 The Chip-Breaking Chart Got from Insert 2

$$\gamma_o = 18°, h = 0,$$
$$\gamma_{o1} = -10°, b_{r1} = 0.05$$
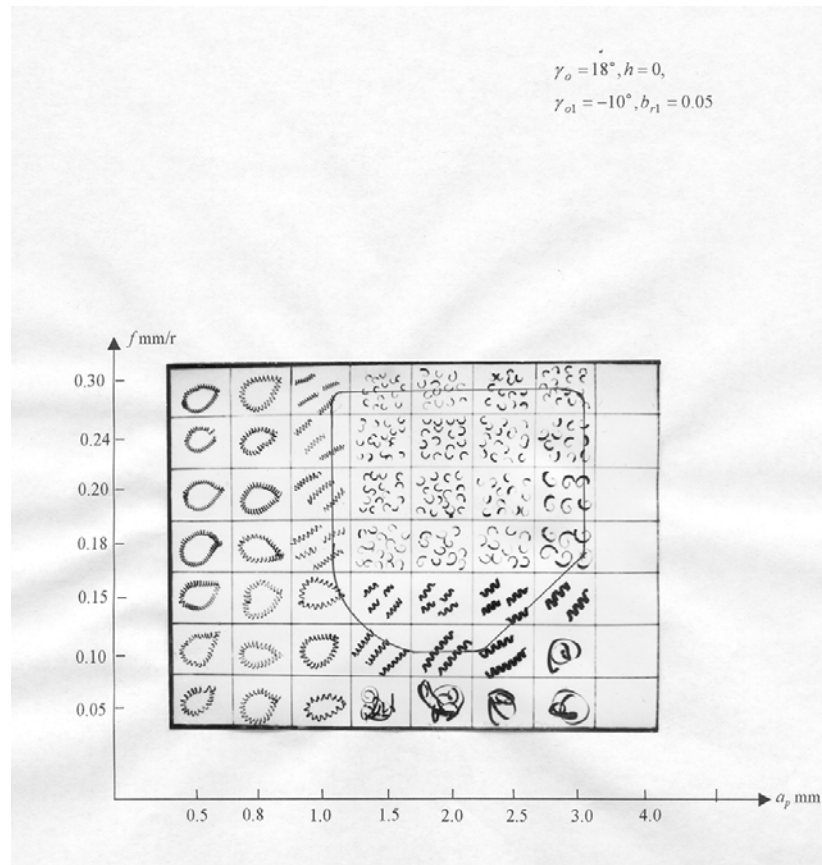
Figure A-3 The Chip-Breaking Chart Got from Insert 5
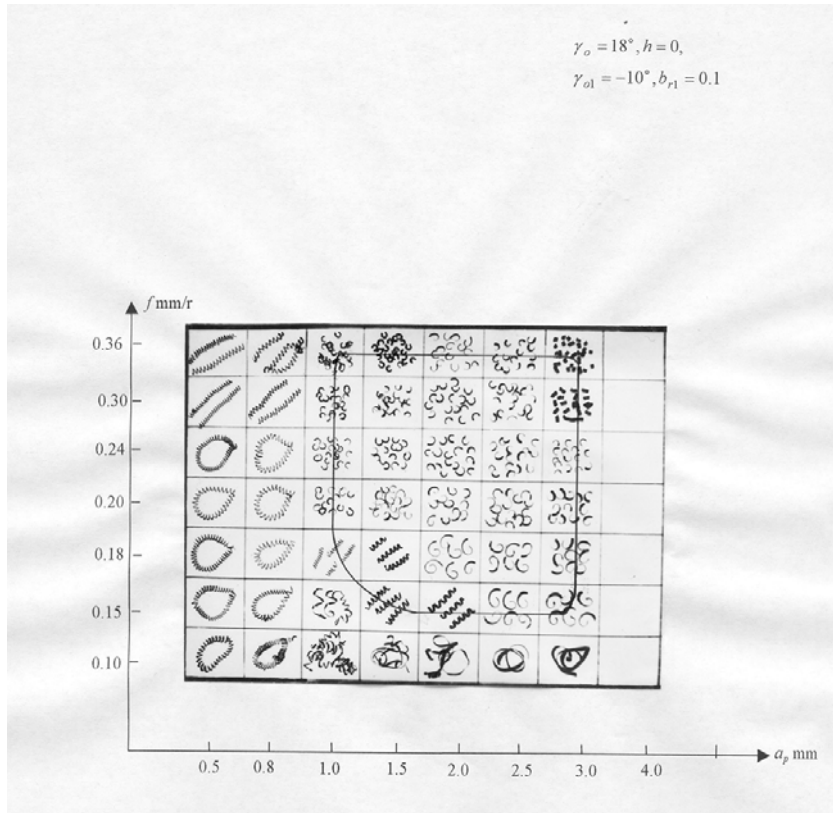
Figure A-4 The Chip-Breaking Chart Got from Insert 6

$$\gamma_o = 18°, h = 0,$$
$$\gamma_{o1} = 0°, b_{r1} = 0.2$$
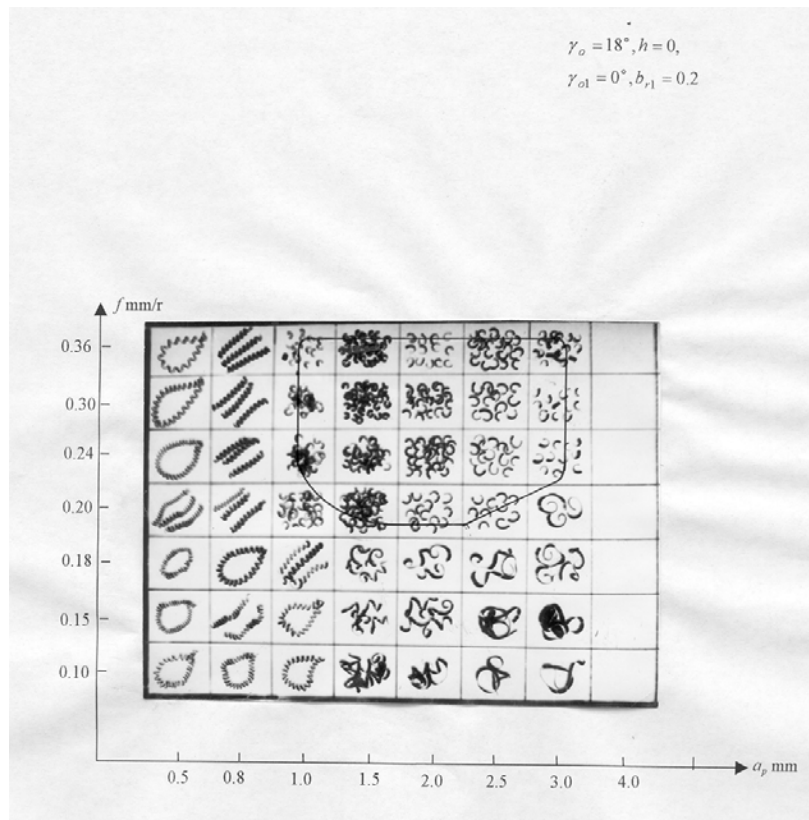
Figure A-5 The Chip-Breaking Chart Got from Insert 10

$$\gamma_o = \hat{1}8°, h = 0,$$
$$\gamma_{o1} = -5°, b_{r1} = 0.2$$
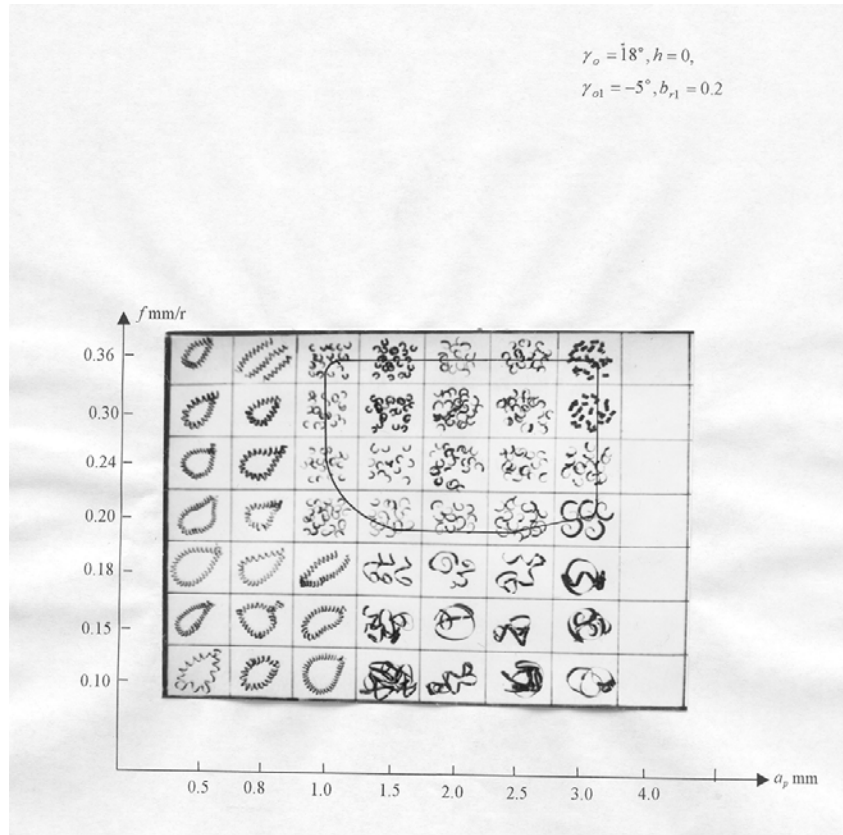
Figure A-6 The Chip-Breaking Chart Got from Insert 11
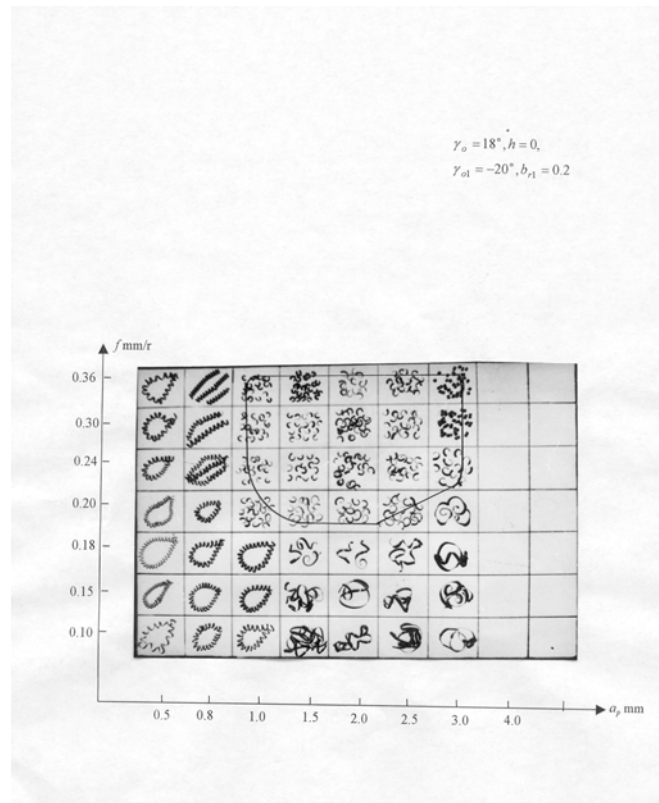
Figure A-7 The Chip-Breaking Chart Got from Insert 14

$$\gamma_o = 18°, h = 0,$$
$$\gamma_{o1} = -10°, b_{r1} = 0.2$$
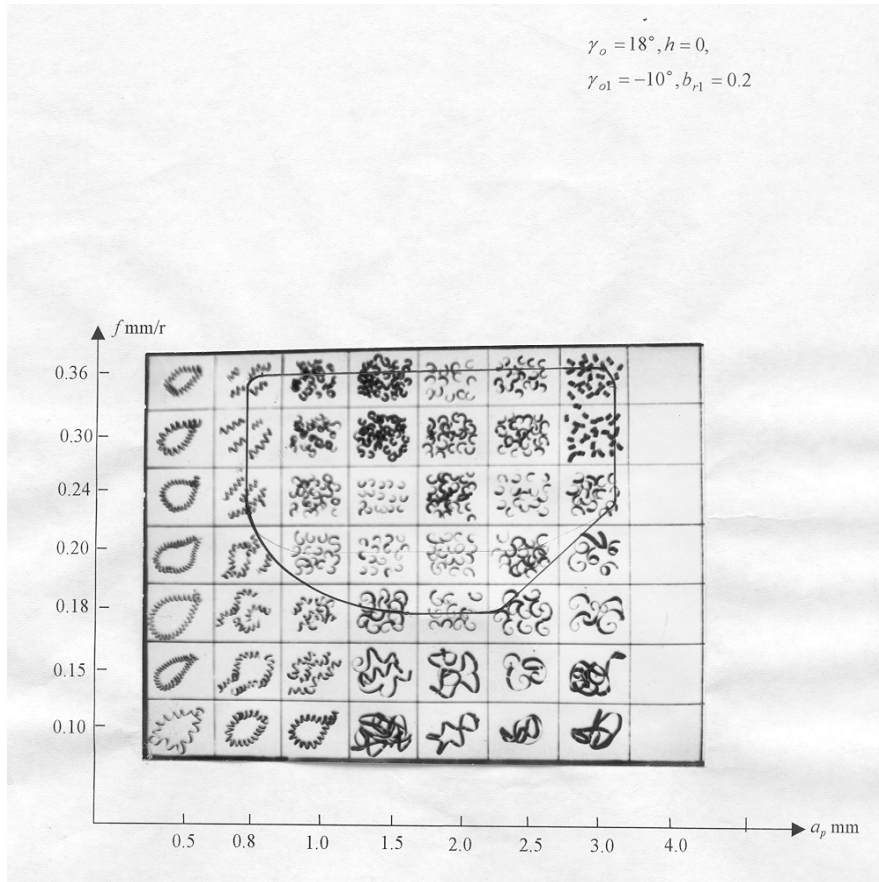
Figure A-8 The Chip-Breaking Chart Got from Insert 15
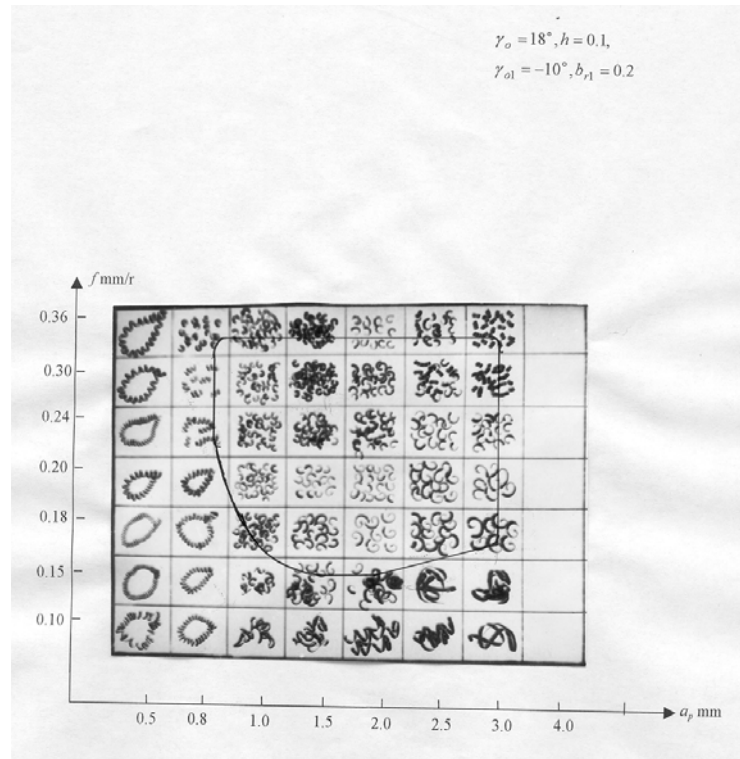
Figure A-9 The Chip-Breaking Chart Got from Insert 16

Appendix B. Sample Chip-breaking Charts

of Three-dimensional Grooved Inserts

The sample chip-breaking charts shown next are got from the study on chip-breaking limits of three-dimensional grooved inserts. The workpiece material used in the tests is 1010 steel. The surface feeding speed V_C = 523 sfpm.

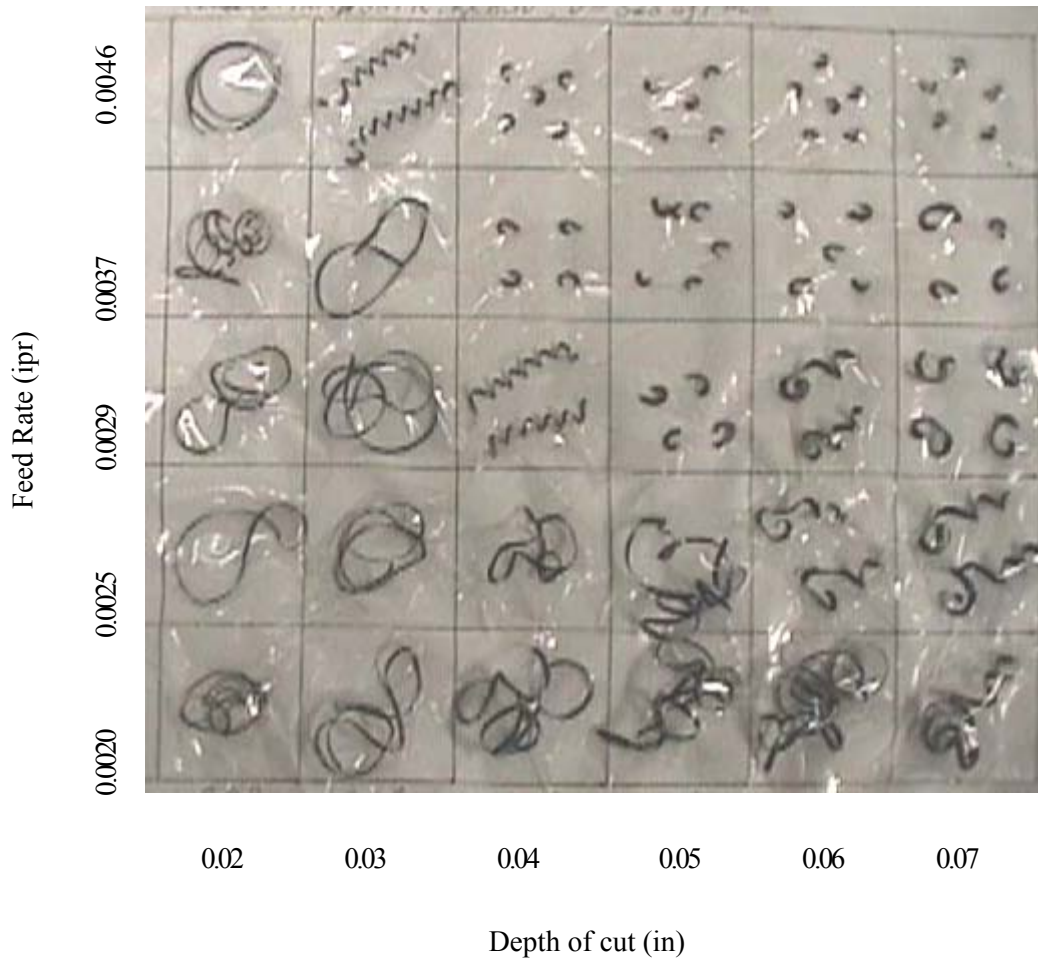**Figure B-1 Sample Chip-Breaking Chart; Insert: TNMG 331 QF4025**

Cutting Speed: 523 sfpm;   WP 1010 steel
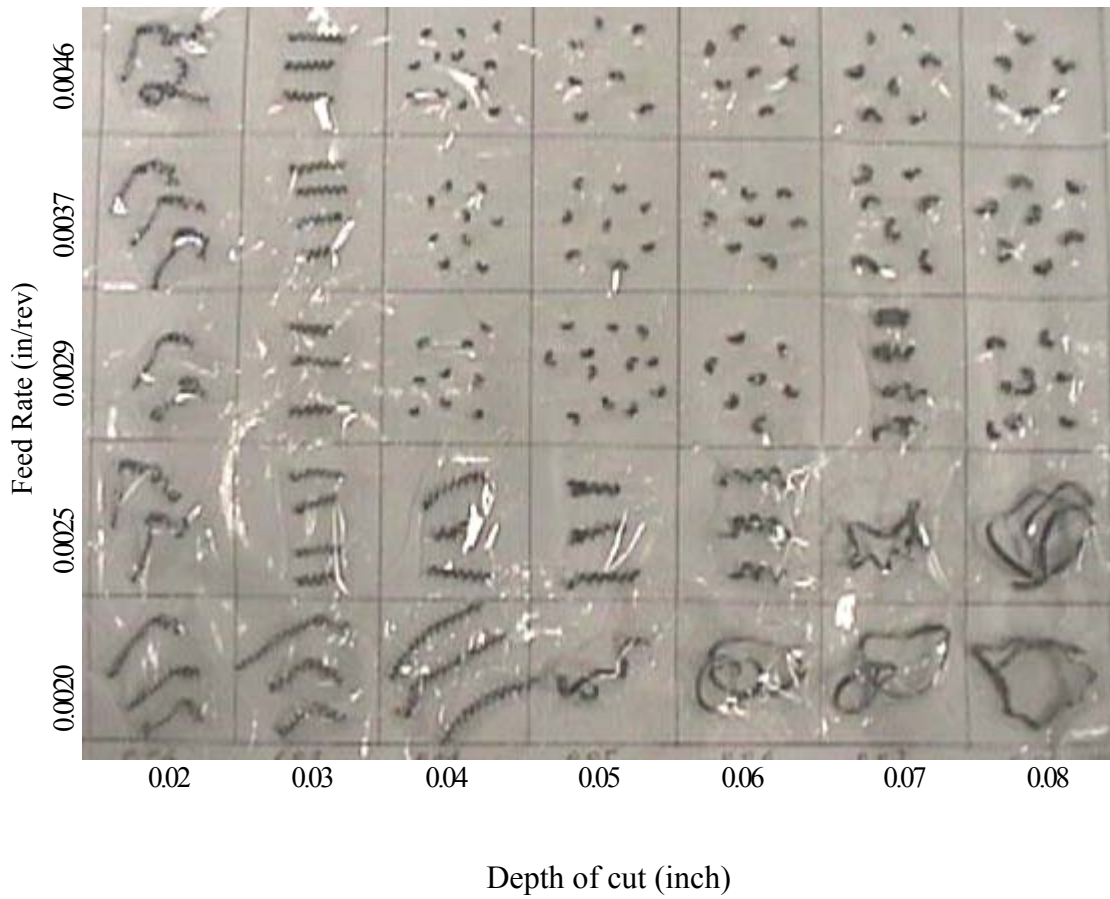
Figure B-2 Sample Chip-Breaking Chart; Insert: TNMG 332 QF 4025
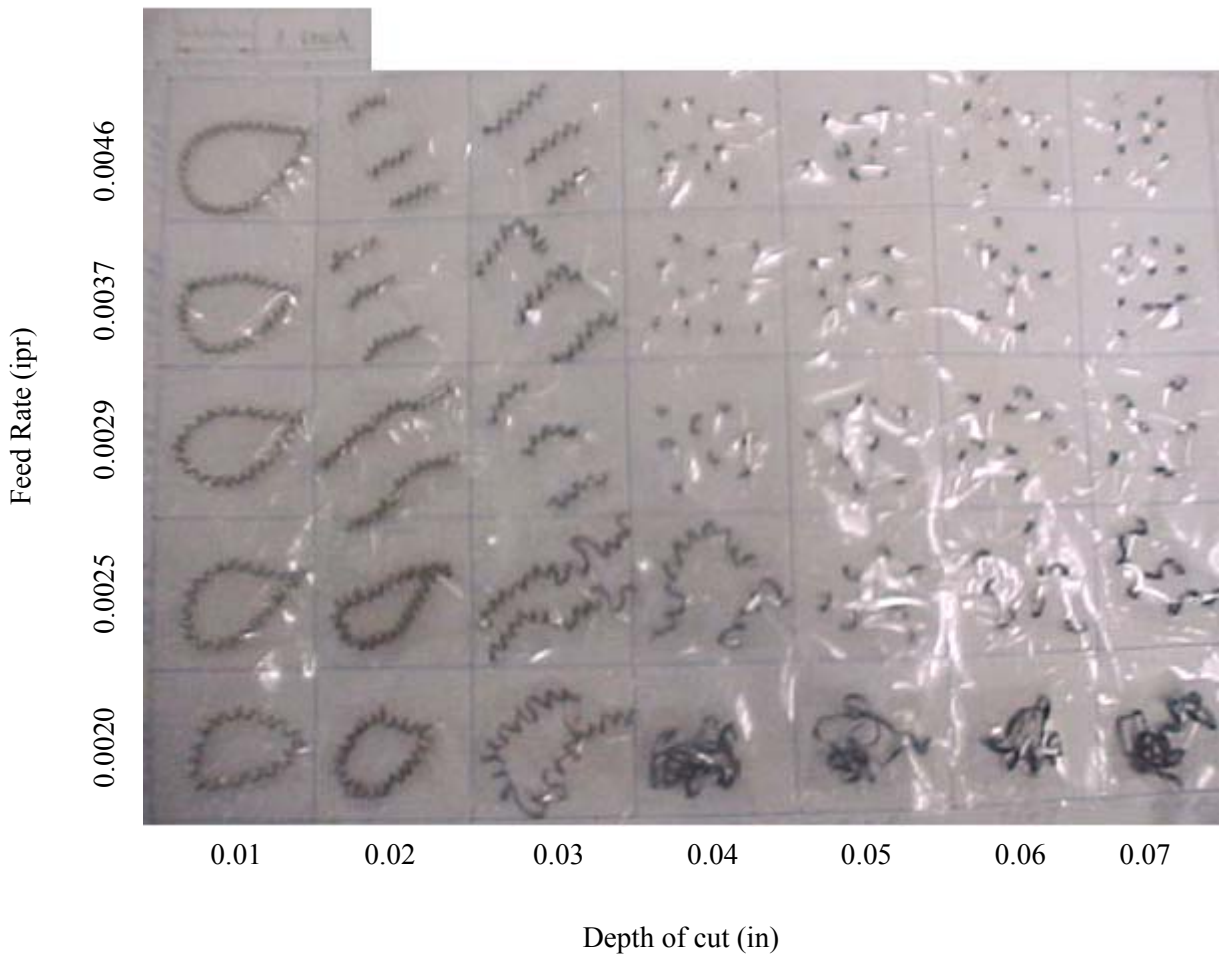
Cutting Speed: 523 sfpm;   WP 1010 steel
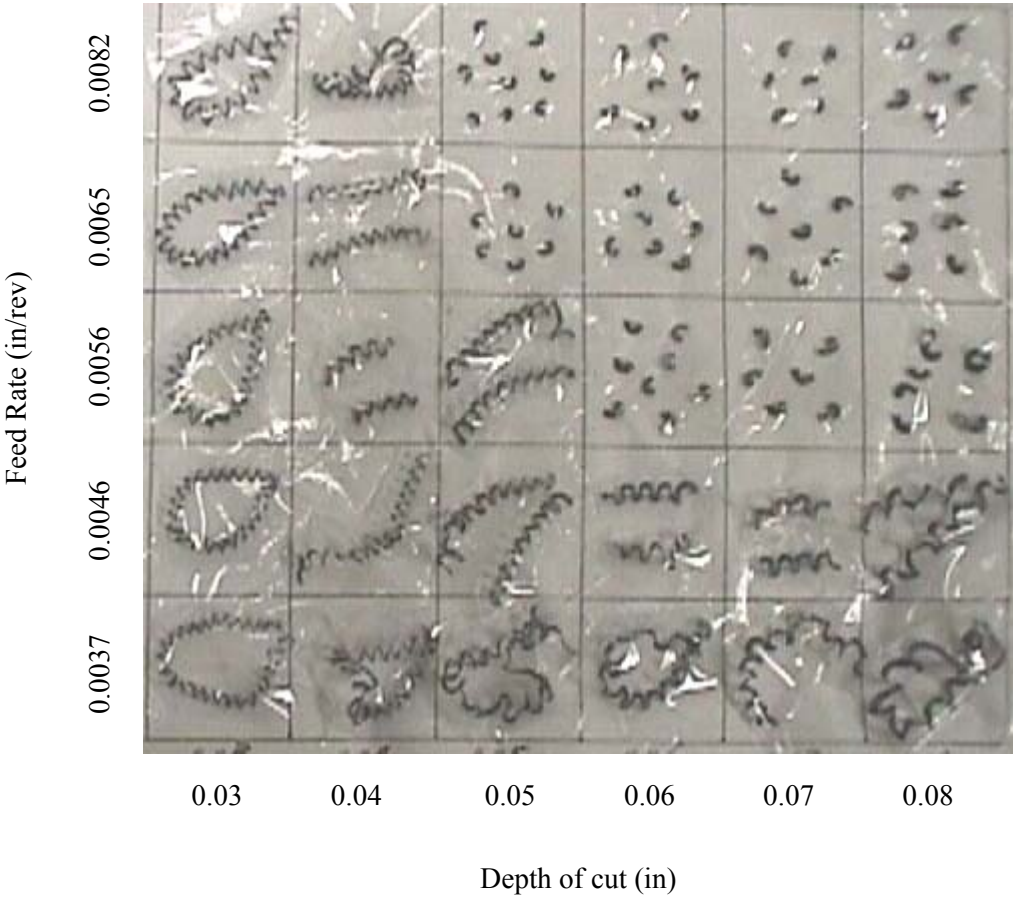
Figure B-3 Sample Chip-Breaking Chart; Insert: TNMG 333 QF 4025

Cutting Speed: 523 sfpm;   WP 1010 steel

0.02	0.03	0.04	0.05	0.06	0.07	0.08	0.09

Depth of cut (in)
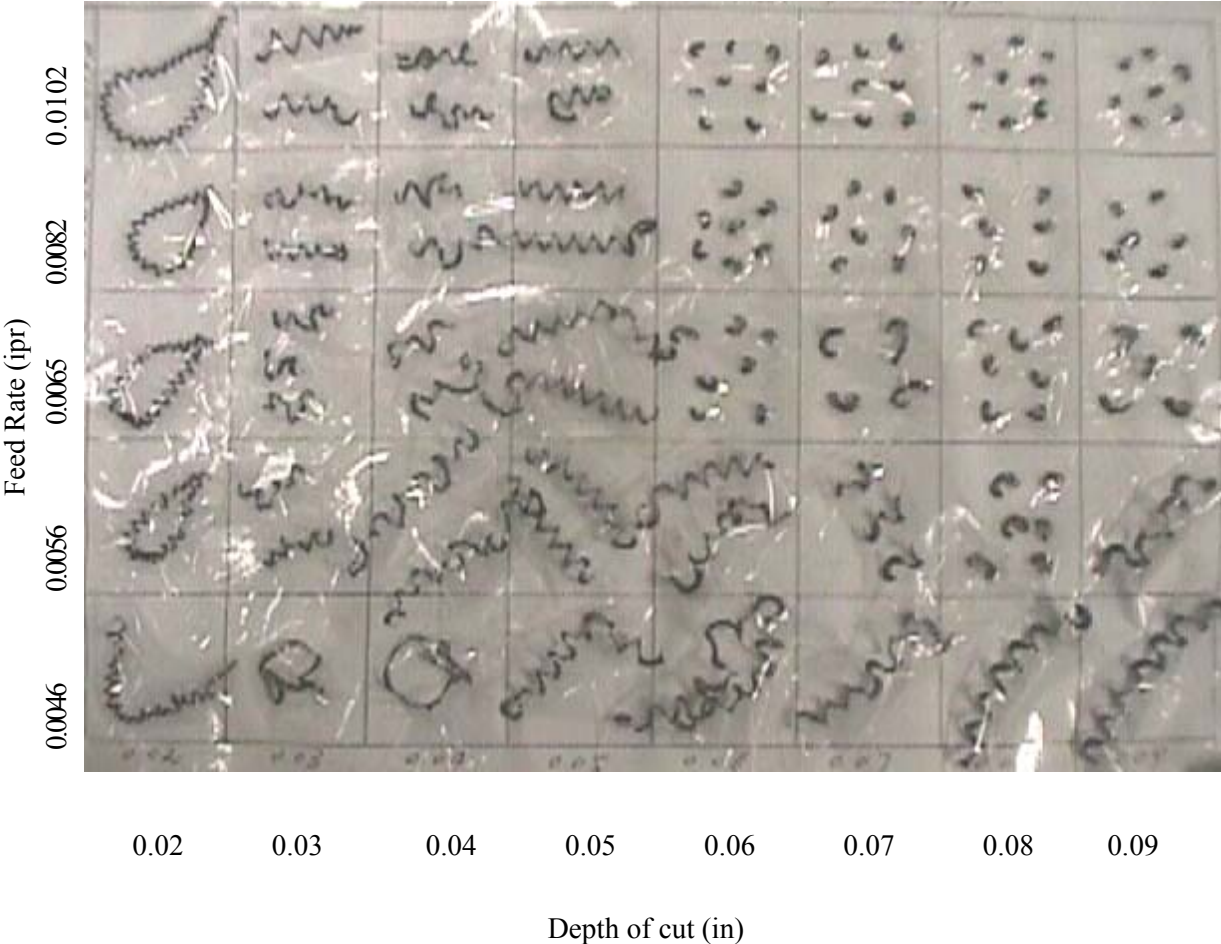
Figure B-4 Sample Chip-Breaking Chart; Insert: TNMP 331K KC850

Cutting Speed: 523 sfpm;   WP 1010 steel

Figure B-5 Sample Chip-Breaking Chart; Insert: TNMP 332K KC850

Cutting Speed: 523 sfpm;   WP 1010 steel

Figure B-6 Sample Chip-Breaking Chart; Insert: TNMP 333K KC850
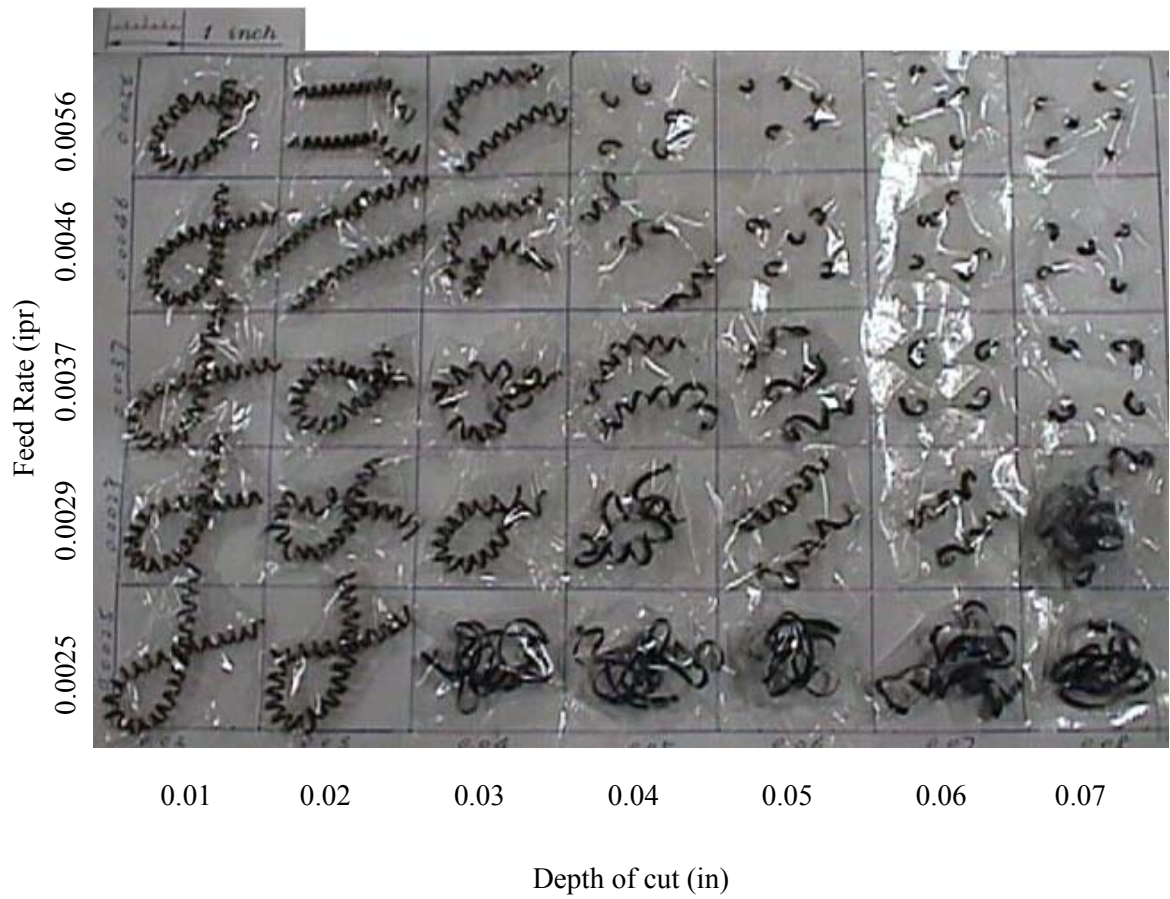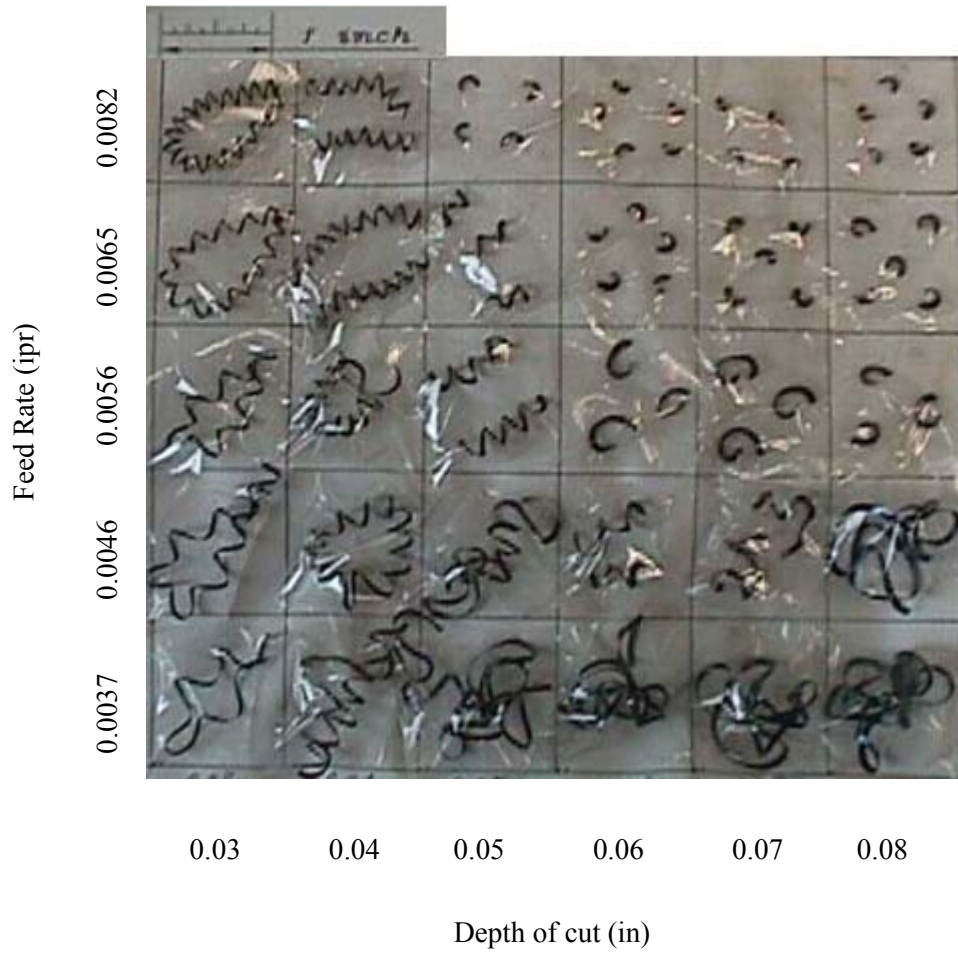
Cutting Speed: 523 sfpm;   WP 1010 steel

Feed Rate (ipr)

0.0056 0.0046 0.0037 0.0029 0.0025

0.01   0.02   0.03   0.04   0.05   0.06   0.07

Depth of cut (in)

Figure B-7 Sample Chip-Breaking Chart: TNMG 432 KC850

Cutting Speed: 523 sfpm;   WP 1010 steel

Figure B-8 Sample Chip-Breaking Chart; Insert: TNMG 332-23 4035
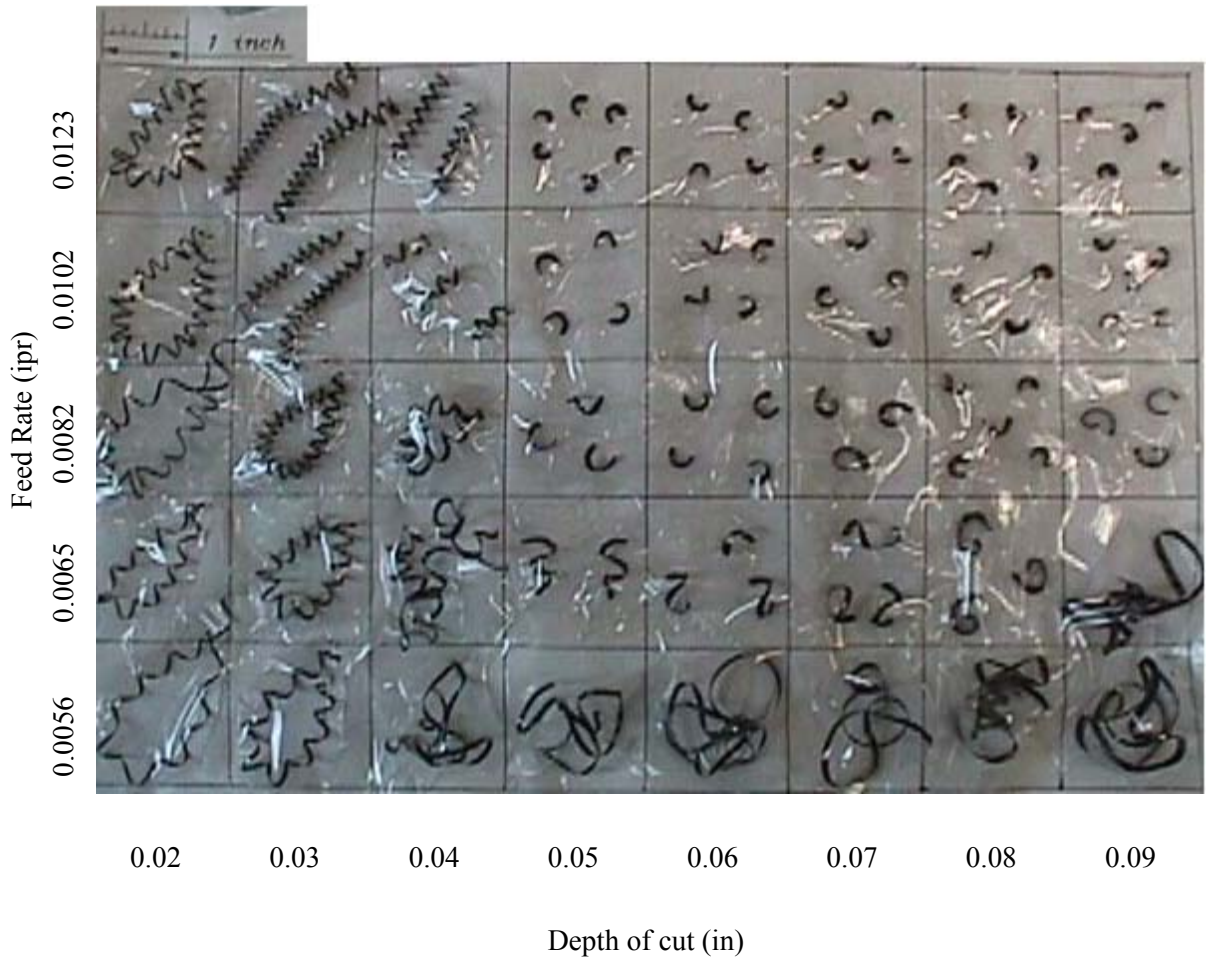
Cutting Speed: 523 sfpm;   WP 1010 steel

Figure B-9 Sample Chip-Breaking Chart; Insert: TNMG 332 4025

Cutting Speed: 523 sfpm;   WP 1010 steel

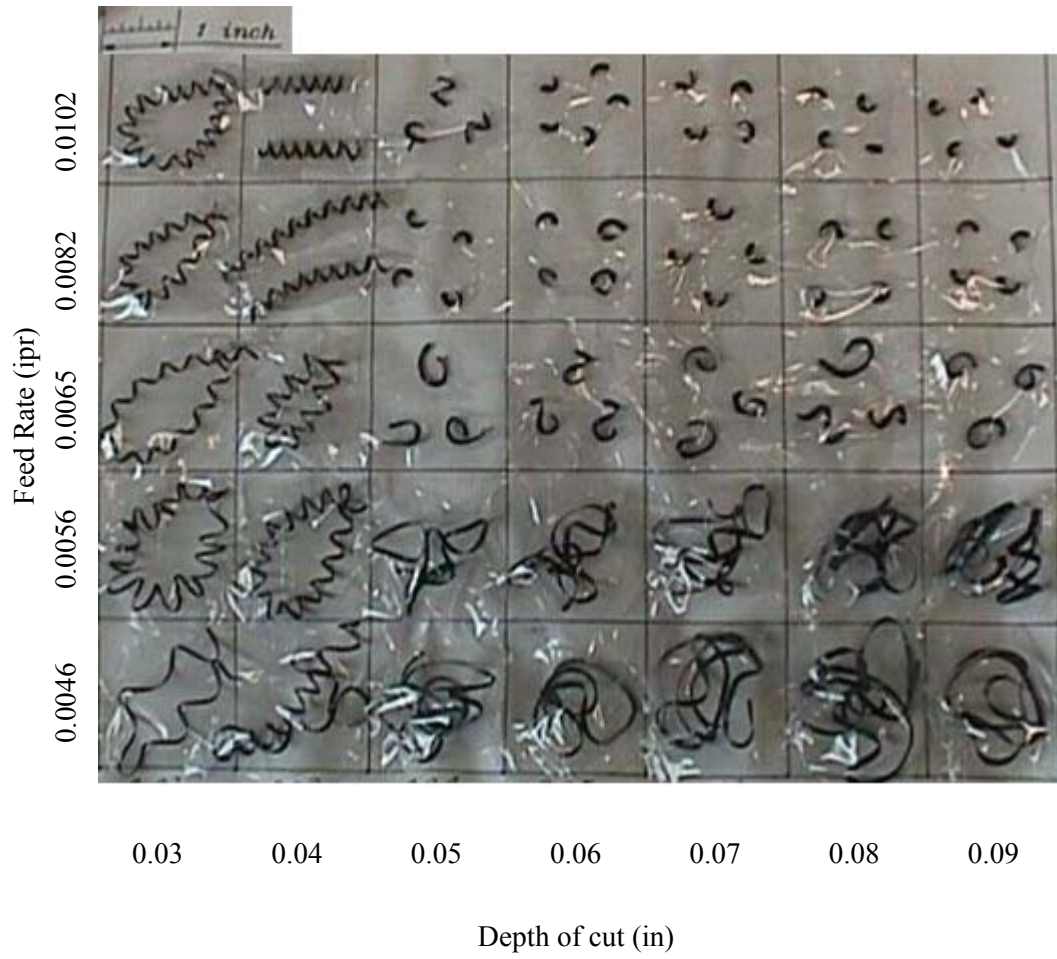**Figure B-10 Sample Chip-Breaking Chart; Insert: TNMG 332MF 235**

Cutting Speed: 523 sfpm;   WP 1010 steel